ADSORPTION OF HEXENE ISOMERS IN ZEOLITES X AND Y FROM LIQUID PHASE SOLUTIONS

BY

ASHOK K.MEHTA B.Sc.

A thesis submitted for the degree of Doctor of Philosophy of the University of London and for the Diploma of Membership of the Imperial College.

Physical Chemistry Department
Imperial College
London SW7 2AZ

September, 1982

"ADSORPTION OF HEXENE ISOMERS IN ZEOLITES X AND Y FROM LIQUID PHASE SOLUTIONS"

by ASHOK K. MEHTA

ABSTRACT

Adsorption of hexene isomers dissolved in heptane on zeolites X and Y and their ion-exchanged forms was studied at 25-26°C. The effect on the adsorption of the number of water molecules/unit cell in the zeolite was also determined.

Selectivity for each isomer was found to vary indicating that separation is likely to be dependent on different interaction energies between the zeolite and the isomer configuration. These interaction energies are dependent upon (a) cation-sorbate interactions (b) lattice-sorbate interactions (c) steric hindrances and (d) differences in polarizability between chemically similar molecules. From differences in sorption capacities of the hexene isomers when loaded individually in heptane on zeolites NaX, NaY and KY an insight of the competition of respective isomer for the sorption sites can be obtained.

Isomerization of 1-hexene to cis-and trans-2-hexene was observed on divalent or hydrogen forms of X and Y zeolites. Kinetics of this reaction on HY zeolite was established at three reaction temperatures, to evaluate the relevant rate constants and activation energies. Data showed that the double-bond shift from 1 to 2 position was stereoselective and much more strongly favoured compared to cis-trans isomerization. Brönsted acid sites were ascertained to be responsible for the isomerization. A secondary carbonium ion mechanism was proposed and evidence to support the mechanism was obtained from the studies of 3,3, -Dimethyl-1-butene isomerization.

ACKNOWLEDGEMENTS

I would like to express my appreciation to Dr. L.V.C. Rees for his expert guidance, encouragement and support throughout the course of this work.

Thanks are also due to my colleagues in the zeolite group, Mr. I.E.G. Morrison and Dr. W.A. McCann for many useful discussions. My thanks also to the Workshops for their help, and to Mr. R.V. Carter for his invaluable technical assistance. A special thank you to my family for all their support.

I am very grateful to SERC and Laporte Industries Limited for financial support in the form of a SERC-CASE studentship.

Finally, I am greatly indebted to Miss R. Carpenter for her expert typing of this thesis.

ERRATA

P60, eqn (3.10) D_s= Diffusion Coefficient in the liquid phase.

p63, line 2 : should read "The basic.....

p64, replace first six lines with: "The RI is determined on squalane (20%) and on D.E.G.S. (20%), under constant conditions. The difference is a measure of the polarity of D.E.G.S".
($\Delta I = I_{polar} - I_{non-polar} = ax$)

p86, line 1 : should read "The synthetic powder zeolites...

p112, line 8 : should read "Similarly from fig 6.4.....

p162, line 34 : should read "relative to other normal paraffins.....

p163, line 26 : should read "Complete dehydration showed preference for 1-hexene, i.e., for NaX, KX CsX(49), K = 2.0(2), 1.6(2) and 1.0(9) respectively."

p164, line 10 : should read "whereas complete dehydration showed preference for 1-hexene, i.e., K = 3.3(5), 1.3(2) and 1.7 for Na^+, K^+ and Cs^+ forms respectively"

p188, ref 179 : B. Imelik et al (Editors)
1980. Elsevier Scientific Publishing Company, Amsterdam - Printed in Netherlands. p55.

Page

INTRODUCTION

Zeolites play a very important role in the chemical and petrochemical industry as both adsorbents and catalysts. These uses of zeolites have made the investigation of sorption equilibrium and molecular transport phenomena of great theoretical and practical importance (1).

Zeolite adsorbents are probably the most important adsorbents of today, and their importance is increasing, mainly because of the following unique adsorptive properties:-

(a) selective adsorption of molecules based on molecular dimensions,

(b) highly preferential adsorption of polar or polarizable molecules,

(c) highly hydrophilic surfaces, and

(d) variation of properties by ion-exchange.

The typical molecular sieve effects of zeolites as studied by adsorption from the gas phase have also been observed on adsorption studies from solutions (2). It is well known that the Molex, Parex, and Olex processes use adsorption from the liquid phase (3) to produce n-paraffins, p-xylene, and n-olefins respectively. The use of n-paraffins recovered include octane value enhancement of gasoline, solvents and raw materials for biodegradable detergents, fire retardants, plasticizers, alcohols, fatty acids, synthetic proteins, lube oil additives, and α-olefins. A detailed discussion on n-paraffin separation processes is available (4). The continued rapid increase in demand for p-xylene as a raw material for polyester products in recent years necessitated the development of a new xylene separation process. Universal Oil Product (U.O.P.) developed a new adsorption process for separating p-xylene from a C_8 aromatics mixture containing

xylenes and ethylbenzene (5, 6). Patents (7, 8, 9) issued to U.O.P. in regard to aromatic separations suggest that the adsorbent used is a synthetic faujasite containing cations from groups 1 or 2 of the Periodic Table or both. Recent patent literature (10, 11) also claims that sodium mordenite and modified type Y zeolite containing predominantly potassium ions can separate p-xylene from a xylene mixture and a C_8 aromatic mixture respectively. The Olex process is used to separate olefins from a feedstock containing olefins and paraffins. The zeolite adsorbent used, according to patent literature (12, 13) is a synthetic faujasite with 1-40 wt % of at least one cation selected from groups IA, IIA, IB and IIB.

Other major commercial processes in n-paraffin separation include, B.P.'s process (14-16), Exxon's Ensorb process (17, 18), Union Carbide's Isosiv process (19-21), Texaco's T.S.F. process (22, 23), Shell's process (24) and Leuna Werke's process (25). These operate in the vapour phase and use fixed-bed cyclic adsorption technology.

The aim of this project was to investigate the adsorption properties of industrially important X and Y zeolites, from liquid phase solutions. Adsorption experiments with hexene isomers were carried out. Selectivity was found to depend on the different interaction energies between the zeolite and the adsorbate(s). The nature and importance of these interactions are variable but depend on charges on the zeolitic framework, nature and location of cations, hydration degree, and effects arising from polarizability and steric hindrance differences between similar molecules. Moreover, these different factors are not independent. Therefore, the location of cations depends on both their nature and the hydration degree. Setting up general rules to such a complex relationship between selectivity and these factors is difficult, but an attempt has been made to explain their relative importance to the adsorption processes involved.

CHAPTER I

ZEOLITE MOLECULAR SIEVES

1.1 Introduction to Zeolite Technology

In 1932 J.W. McBain (26), introduced the term 'molecular sieve" to define porous solid materials which exhibit the property of acting as sieves on a molecular scale. He used the term to describe the selective sorption properties of the natural zeolite mineral chabazite. Zeolite minerals were used to observe experimentally the adsorption of gases and to study their behaviour as molecular sieves. Further work, was carried out by R.M. Barrer from 1945 onwards. He achieved the separation of gaseous mixtures using dehydrated chabazite. A paper on the "Separation of mixtures using zeolites as molecular sieves' (27), describes three classes of molecular-sieve zeolites and their use to resolve hydrocarbon mixtures and to separate polar molecules from mixtures, e.g. acetone from methanol, water and ethanol from ether, primary, secondary and tertiary amines, a number of azeotropes, etc. As a result of later work (28, 29), Barrer added a fourth class based on the approximate minimum diameter of the channels or pores, viz: Table 1.1.

No other absorbent could match the distinctive properties of zeolites and this resulted in an increasing industrial use. D.W. Breck (1), has reported that from 1948-1972 over 7,000 papers and 2,000 U.S. patents have been published dealing with zeolite science and technology and that this interest still increasingly continues today.

There are over thirty naturally occurring zeolites. They are found in basaltic rocks rich in alkalis, such as occur in Northern Ireland and Iceland. Zeolite minerals known to occur in sedimentary rocks are analcime, clinoptilolite, mordenite, phillipsite, erionite, laumontite, chabazite, wairakite and ferrierite. A complete summary of zeolites in sedimentary rocks is given in the excellent review by Hay (30). Another recent detailed review by Sheppard deals with zeolites in sedimentary deposits in the United States (31).

Table 1.1 Classification of Zeolites

CLASS	ZEOLITE	APPROXIMATE MINIMUM DIAMETER OF THE PORES (nm)	TYPES OF COMPOUNDS ADSORBED
A	Faujasite	0.9-1.0	Readily takes up isoparaffins such as neopentane
B	Chabazite and synthetic Zeolites of the composition $BaO \cdot Al_2O_3 \cdot 4\ SiO_2 \times H_2O$ Gmelinite	0.49	Do not take up isoparaffins or aromatics. Rapidly adsorb CH_4 and C_2H_6 and slowly take up higher n-paraffins up to C_7H_{16}, also molecules with smaller dimensions.
C	Na Mordenite	0.40	Iso- and n-paraffins are not adsorbed. CH_4 and C_2H_6 are slowly occluded as well as N_2 and molecules with smaller dimensions.
D	K Mordenite Levynite	0.38	N_2 and molecules of smaller dimensions are occluded.

Synthetic zeolites are easy to manufacture and can be obtained in pure forms for use as drying agents, catalysts and separation of gas and liquid mixtures. Other applications are separation of air components, carrying catalysts in the curing of plastics and rubber, removing CO_2 and sulphur compounds from natural gas. Many of the properties of zeolites depend on their structure and growth of interest in their chemistry has stimulated investigations that have revealed much of their remarkable architecture. Their ion-exchange behaviour in certain cases has shown that they can scavenge cations from radio-active effluents and hence remove dangerously radioactive constitutents.

Lately geologists, have reported massive zeolite deposits which may compete in certain respects with the synthetic materials. Because of their comparative abundance in basic rocks and in certain sediments it has recently been suggested that zeolites can play a significant role in geological processes of mineral growth and transformations.

The growth of molecular sieve applications seems likely to continue. Porous crystals provide new kinds of sorbent materials with capacities as good as those of amorphous and non-porous crystalline sorbents hitherto employed industrially or in the laboratory, but with the additional molecular sieve function, which introduces a new order of selectivity into sorption process. New sorbents can be found in a range of classes each with a different molecular sieve character. For an appropriately chosen sieve sorbent quantitative separation can often be achieved in a single act of sorption. This opens up new possibilities for selective sorption by molecular sieve action as a unit engineering process.

1.2 Advantages of Molecular Sieve Zeolites in Separation over Other Adsorbents

For practical separations of gases or liquid mixtures, the adsorbents which are available fall into several categories: activated carbons, inorganic gels such as silica gel and activated alumina, and the new molecular sieve selective adsorbents. These materials are characterised by high internal surface areas available for adsorption, through channels or pores

penetrating the entire volume of the solid material. The external surface making only a very small contribution (~1%)to the overall available surface area.

Adsorbents such as activated carbon, activated alumina and silica gel have an amorphous structure with a distribution of pore sizes. The pore diameter distribution within these adsorbents may be fairly narrow such as from 2-5 nm for a high-grade silica gel, or may range from 2 to 1000 nm for some activated carbons. The internal surface area is therefore, available to all adsorbate molecules, since essentially all molecules except the higher polymeric materials have molecular diameters considerably smaller than these values. The new molecular sieve adsorbents are crystalline and have pores of uniform size. These pores have diameters of molecular dimension and are capable of preventing molecules of greater than a certain critical diameter from entering the adsorbent and being adsorbed within the internal structure. Fig. 1.1 shows the pore size distribution of an activated carbon and a silica gel and also shows the effective* pore size of molecular sieve types 4A, 5A, 10X and 13X.

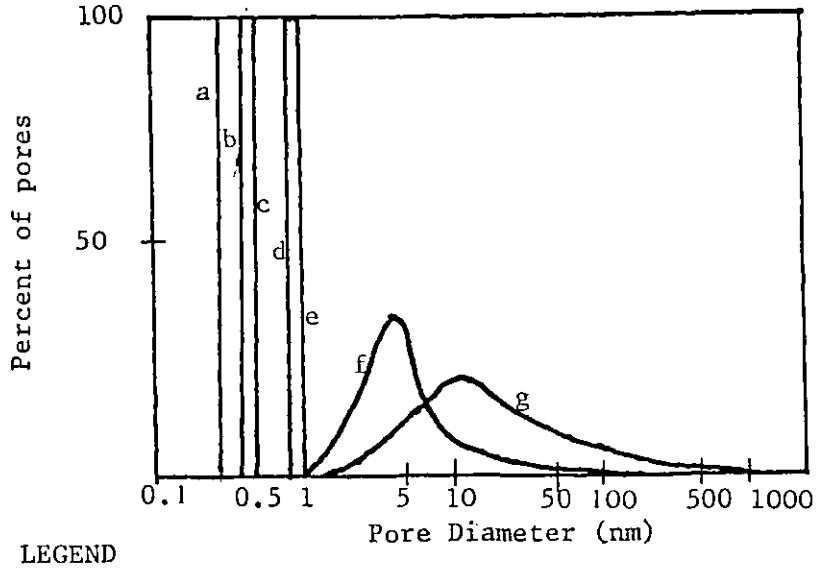

LEGEND

(a) Linde Molecular Sieve Type 3A
(b) Linde Molecular Sieve Type 4A
(c) Linde Molecular Sieve Type 5A
(d) Linde Molecular Sieve Type 10X
(e) Linde Molecular Sieve Type 13X
(f) Typical Silica Gel
(g) Typical Activiated Carbon

FIG 1.1 Schematic Description of Pore Size Distribution

* Effective pore size is defined as the critical diameter of the largest molecule which can enter the uniform pore system.

The chemical and physical nature of the surface of the adsorbent determines how strongly a given molecule is adsorbed compared to another of a different chemical character as manifested by the selective separations that can be made of two molecules both of which are small enough to enter the pore system and compete for adsorption on the surface. The adsorption on activated carbon is governed almost entirely by Van der Waals or condensation forces, since the amount of any compound adsorbed is governed principally by its volatility or boiling point. The higher the boiling point the more strongly it is adsorbed. For example, activated carbon readily separates C_2, C_3 and C_4 hydrocarbons from each other, but cannot effectively separate olefins from the paraffins with the same number of carbon atoms. The inorganic gel adsorbents, particularly silica-gel, also adsorb materials based upon their relative boiling points but superimpose upon this a selectivity for the more polar or more polarizable molecules. Silica gel, for example, will remove selectively aromatic compounds from paraffinic and naphthenic materials. The molecular sieve zeolite adsorbents due to their crystalline structure and cation content, adsorb polar or polarizable compounds very strongly, such that in many instances this effect completely outweighs the selectivity based on the relative boiling points of the materials. Molecular sieves, for example, will separate water from ethanol, ethylene from ethane and aromatics from paraffins.

1.3 Crystalline Zeolites, Classification and Basic Structure

Zeolites are crystalline, hydrated aluminosilicates of Group I and II elements. Structurally, they comprise a framework based on an infinitely extending three-dimensional network of SiO_4^{4-} and $A\ell O_4^{5-}$ tetrahedra linked together through common oxygen atoms. The isomorphic substitution of Si^{4+} by $A\ell^{3+}$ gives rise to a net negative charge compensated by cations. The maximum extent to which $A\ell^{3+}$ can replace Si^{4+} is governed by Lowenstein's rule (32), which states that two aluminium atoms cannot be linked with the same oxygen atom. Zeolites may be represented by the empirical formula $M_{2/n}O \cdot A\ell_2O_3 \cdot d\ SiO_2 \cdot y\ H_2O$. In this oxide formula, d is generally greater than 2, since $A\ell O_4^{5-}$ tetrahedra are joined only to SiO_4^{4-} tetrahedra; n is the cation valency. The structural formula of a zeolite can be expressed in terms of crystallographic unit cell as:

$$M_{x/n}\left[(A\ell O_2)_x(SiO_2)_y\right] \cdot wH_2O$$

where M is the cation of valency n, w is the number of water molecules and the ratio $y/_x$ usually lies between values of 1-5, depending upon the structure. The sum (x + y) is the total number of tetrahedra in the unit cell and the portion within the square brackets represents the framework composition. There are 30 known natural zeolites and about 120 structures which are entirely synthetic. An excellent review of structural and chemical data was given by Breck (1), and covers the literature up to 1973.

Zeolites have been classified into seven groups (1). Within each group there is a common subunit of structure which is a specific array of $(A\ell,Si)O_4$ tetrahedra. The classification neglects the Si-Aℓ distribution. In many framework aluminosilicates, two simple units are found i.e. the ring of four tetrahedra (4-ring) and six tetrahedra (6-ring). These subunits are called secondary building

units (SBU), (the primary units being SiO_4^{4-} and $A\ell O_4^{5-}$ tetrahedra). Also, polyhedral truncated octahedrons are frequently involved in zeolite structures, and these can be stacked in various ways to form large intracrystalline cavities and channels. Water molecules and cations are located in these channels and cavities.

Zeolites A, X and Y consist of linked cubooctahedral arrangements of 24 silica or alumina tetrahedra known as the sodalite unit, as illustrated in Fig.1.2. Such a polyhedron, has a central cage of free diameter 0.65 nm, accessible through 6-membered rings of oxygen atoms with a free diameter of 0.22 nm. Zeolite A consists of cubooctahedra linked together with bridging oxygen atoms along the 4-membered rings following a cubic symmetry. This arrangement creates a central cage of free diameter 1.15 nm, accessible through six 8-membered rings with free diameter of 0.42 nm. In the mineral faujasite and the synthetic faujasites (zeolites X and Y), the cubooctahedra are linked with bridging oxygen atoms but in a tetrahedral symmetry. The sodalite units connected along two 6-membered rings gives rise to hexagonal prism. In this way, the polyhedra enclose a supercage with an internal free diameter of 1.25 nm accessible through four 12-membered rings of oxygen atoms with free apertures 0.75 nm.

Each of the zeolite structures mentioned above has a three dimensional network of channels, or linked cavities, which are of molecular dimensions and can thus adsorb species which are small enough to have access to the internal surface of the zeolite. Some zeolites, however, may have channel systems running in one direction only, like a bundle of pipes (e.g. mordenite), while others may have two-dimensional nets of channels which may be interconnected via channels with dimensions different from those of the main network. Table 1.2, summarizes the common materials which are adsorbed by each type of molecular sieve and includes in the case of Types 10X and 13X those molecules which have been used to determine the effective pore size of these materials.

Table 1.2 Selective Adsorption by Molecular Sieve Adsorbents

Adsorbed on 4A, 5A, 10X, and 13X.	Adsorbed on 5A, 10X, and 13X, but not on 4A.	Adsorbed on 10X and 13X, but not on 4A or 5A.
Water Methanol Ammonia Hydrogen sulphide Sulphur dioxide Carbon dioxide Propylene Ethylene Ethane	n-Butanol and higher n-alcohols n-Butene and higher n-olefins. Propane and higher n-paraffins up to at least C_{14}. Cyclopropane "Freon"-12 refrigerant	i-Butane and all i-paraffins. Benzene and all aromatics. Cyclohexane and all cyclics with at least 4-membered rings. Molecules larger then 0.5 but less than 0.9 nm $(C_2F_5)_2NC_3H_7$.
Adsorbed on 13X but not on 4A, 5A, 10X		Not adsorbed on 4A, 5A, 10X, or 13X
Di-n-propylamine Di-n-butylamine Molecules larger than 0.9 but less than 1 nm.		$(C_4F_9)_3N$ Molecules larger than 1 nm.

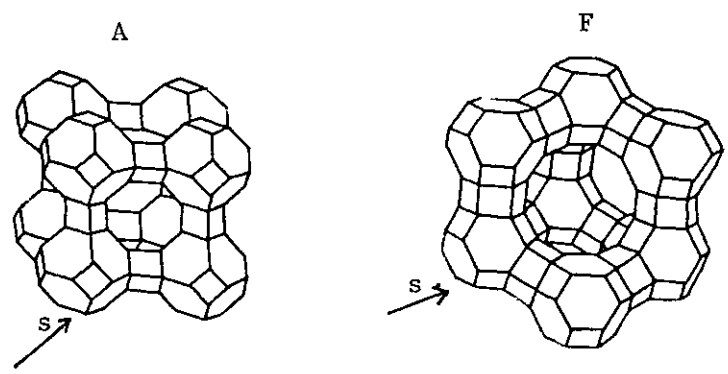

Fig. 1.2 Schematic representation of the arrangement of sodalite units (s) in the structure of zeolite A and of the mineral faujasite, zeolites X and Y (F).

Molecular sieve action may be total or partial. If total, the diffusion of one species into the solid may be wholly prevented while the diffusion of the second species occurs. If partial, the components of a binary mixture diffuse into the solid at different rates depending upon the conditions. In some cases, the activated diffusion of the species in the solid is of particular interest. As the size of the diffusing molecule approaches the size of the pores in the zeolite, the interaction energy between the species and the aperture increases in importance. If the aperture is sufficiently small relative to the size of the diffusing species, the repulsive interaction becomes dominant and the diffusing species needs a specific activation energy to pass through the aperture. Selectivity can then be a function of temperature, dependent on activated diffusion of molecules as given by the Arrhenius Equation for the diffusion coefficient $D = D_o e^{-E/RT}$. This has formed the basis for a commercial separation of permanent and inert gases at cryogenic temperatures.

Many measurements on dehydrated zeolites e.g. A, X, Y, etc. ... have been made. An example of this is chabazite. It was found that the minimum and maximum free dimensions of the 8-ring vary from 0.37 x 0.41 nm to 0.31 x 0.44 nm on dehydration. Such changes will differ for the different zeolites and must help to determine the gauge of the mesh and introduce variety into this gauge. Moreover, if the windows do change dimensionally in this way on dehydration, they may also change dimensionally when a guest molecule is pushing its way through them. Further, neither the oxygen atoms that form the inner rim of the windows nor the guest molecules are incompressible.

1.4 Zeolites X and Y - available sites and cation distribution

Zeolites X and Y belong to Group 4, and the framework structures of these zeolites are based on the double-six-ring (D6R) as the secondary building unit (SBU). The aluminosilicate framework consists of a diamond-like array of linked octahedra which are joined tetrahedrally through

the 6-rings (see Fig. 1.2). The linkage between the adjoining truncated octahedra has already been discussed.

Zeolites are distinguished on the basis of chemical composition, structure, and their related physical and chemical properties. Differences are found in their Si/Aℓ ratio, with zeolite Y for example having a higher ratio than X. Since one equivalent of cation is needed per mole of Aℓ, X possesses a higher cation density than Y. The number of tetrahedral Aℓ atoms in Y ranges from 48 to about 76 per unit cell, whereas, it is about 77-96 per unit cell in X. The unit cells are cubic with a very large cell dimension of nearly 2.5 nm, and contain 192 $(Si\ Aℓ)O_4$ tetrahedra. There are eight supercages, eight sodalite cages, and sixteen hexagonal prisms in one unit cell of these zeolites. The space group assigned to this structure is Fd3m(33). However, it was demonstrated from (3D) single crystal X-ray analysis that hydrated NaX zeolite has a symmetry Fd3, for the ideal faujasite framework (34). The unusually stable and rigid framework structure involves the largest void space of any known zeolite and amounts to about 50 volume % of the crystal when dehydrated. It is difficult to conceive of materials which, when formed, are so highly hydrated and yet after dehydration exhibit the high degree of stability shown by these zeolites.

The sites available for cations are well defined in these structures. Thus, 16 of the cations are considered to be located within the hexagonal prism connecting the truncated octahedra, and in these positions designated site I, the cations are isolated from the adsorption surface. The site II positions, of which there are 32 per unit cell are located in the centre of the exposed six member oxygen rings in the large adsorption cavity. The third cation position, which decreases in number with decreasing Aℓ in the framework is also within the large adsorption cavity. Cation occupancy in this position has never been observed directly by X-ray methods, but the most favoured position is that at the centre of a 4-membered oxygen ring, in the group of three such rings (35). The third position is referred to as site III. There are 48 of these per unit cell, and the remaining Na^+ ions are assumed to be accommodated in these positions. Sites I' and II' lie on the other sides of the respective 6-rings of the unprimed sites, within the

sodalite cages. With the exception of the I sites, the sites are not defined by unique coordinates.

The framework oxygen atoms are numbered as follows: O1 is the bridging oxygen atom of the double 6-membered ring (hexagonal prism), O2 is the oxygen atom that is in both the hexagonal prism 6-ring and the supercage 6-ring, O3 is the second oxygen atom of the hexagonal prism 6-ring and O4 is the second oxygen atom of the supercage 6-ring.

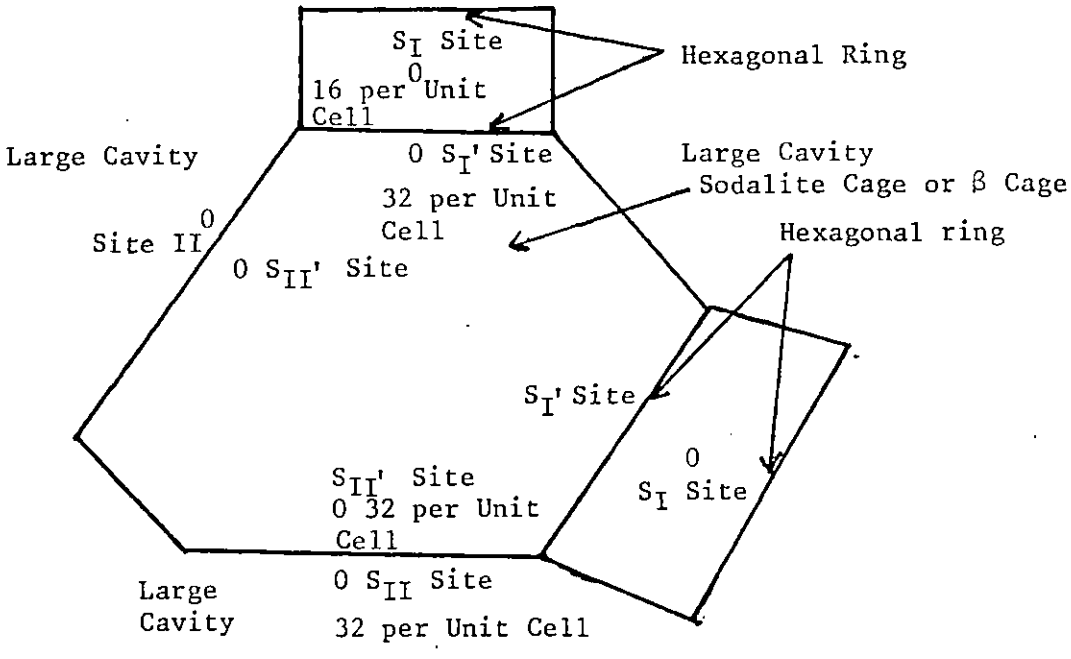

FIG 1.3 Cation locations in X and Y Zeolites

The distribution of cations in the various sites depends on a number of factors, for example, size and charge of cation, $Si/_{A\ell}$ ratio (36), and the process of hydration and dehydration of the zeolite. It is also found that the cations seek out positions of minimum coulombic potential energy, and consequently of zero electric field (37). Dempsey (38) formed an approximate relation for the occupancy of site I and I' by uni and divalent cations in zeolite X. The population N_I' of site I' is given by the relation,

$$N_I' = 2(16 - N_I)$$

where N_I is the number of cations at site I. This relation implies that it is very unlikely on electrostatic and symmetry grounds that the site I and I' are occupied simultaneously. Similarly, it is found that the sites II and II' are also not occupied simultaneously. This occupancy depends on the number of residual water molecules, since the polarizing power of the cation determines the amount of water retained. Smaller cations retain more water molecules than larger ions. At zero water content sites I' and II' should be empty (39).

Also on dehydration, cations move from their original sites to other sites. The exact positions which the cations occupy have been ascertained by Rees and Lai (40, 41, 42). Their work on Szilard Chalmers cation recoil on ion-exchanged forms of zeolites X and Y showed that divalent cations exhibit high affinity for the locked in sites (hexagonal prisms), and that they start migrating into these sites in appreciable amounts at as low a temperature as 40°C. This result agreed with Madelung potentials calculated for divalent cations (41), where the cations at site I are more strongly held than the cations at site II, and the stability of site I cations relative to that of site II cations increases as the size of the cation increases.

The electrostatic field for ionic fully exchanged ideal models of zeolites X and Y was calculated by Rabo et al. (44). The fields

were obtained as a function of the distance from the site II cation along the 3-fold axis. These calculations revealed that the fields were larger in zeolite Y than in zeolite X, with divalent cations than with univalent cations, near site III than near site II provided that both of these sites are occupied. The structure and the electrostatic field calculations reveal the order of preference for alkali and alkaline earth cations as, site I > site II > site III. This also suggests that divalent cations will replace univalent cations at the most preferred sites.

A knowledge of the distribution of cations relevant to this work is presented in Table 1.3.

A recent review of cation locations in extra framework sites in zeolites has been compiled by Mortier (51).

Table 1.3 Distribution of Cations

AVAILABLE SITES	I	I'	II'	II	II*	III	IV	U	Ref
MAXIMUM CAPACITY	16	32	32	32	32	48	16	8	
De-NaX[a]	4	32	-	32	-	4	-	-	44, 47 49
Hy-NaX[a]	9	8 12 H_2O	26 H_2O	24 8 H_2O	-	-	-	-	34
De-KX [b]	8	-	-	-	-	-	-	-	-
Hy-KX [b]	8.9	7.2	-	23.2	-	-	-	-	35
De-NaY[c]	7.5	19.5	-	30	-	-	-	-	48
Hy-NaY[c]	3.3	12	-	1.2	-	34.5	-	-	
De-KY [d]	12	14.2	-	30	-	-	-	-	35, 48, 49
Hy-KY [d]	-	13.6	-	17.8	-	-	-	-	35, 48

a) Composition of NaX is $Na_{80}[(A\ell O_2)_{80}(SiO_2)_{112}] \cdot xH_2O$

b) Composition of KX is $K_{84.5}Na_2[(A\ell O_2)_{86.5}(SiO_2)_{105.5}]$
It is activated by heating in vacuum at 500°C.

c) Composition of NaY is $Na_{57}[(A\ell O_2)_{57}(SiO_2)_{135}]$

d) Composition of KY is $K_{47.5}\ Na_{0.7}[(A\ell O_2)_{48.2}(SiO_2)_{143.8}]$

Site II* is situated on the triad axis but considerably displaced from the unshared 6-ring into the supercage. Sites IV and U, are displaced slightly from the centre of the 12-membered ring separating the supercages, and at the centre of sodalite cage respectively.

1.5 Zeolitic Water

Water is an essential component of all zeolites, but it can be removed continuously and reversibly. The water content in a zeolite depends on the type of zeolite, the cations present, and the humidity conditions. In a fully hydrated faujasite-type zeolite, water constitutes approximately 26% of its total weight. This is approximately equal to 260 water molecules per unit cell.

Water molecules form hydration complexes by coordinating with the exchangeable cations and interact electrostatically with the framework oxygen atoms. The hydration complexes associated with monovalent exchanged cations are weakly bonded, whilst those associated with polyvalent exchanged cations are strongly bonded. The cation may polarize the water molecule sufficiently to split it into a hydroxyl group which bonds to the cation and a proton which attaches itself to a negatively charged framework oxygen.

N.M.R. provides information on the state of the water molecules in hydrated zeolites. In zeolites X and Y, water molecules are distributed in both the supercages and the small sodalite cages. Water molecules in

the larger zeolite cavities exhibit the same pattern as in the isolated liquid indicating that molecules in the centres of the large cavities do not occupy definite lattice sites. In zeolites with smaller cavities, the molecules of water appear to cluster around the cations. During dehydration, it appears that the water molecules line the inside of the zeolite structural cage (45). Cation-dipole interactions play an important role in the nature and structure of the zeolitic water. Water molecules are observed to be mobile down to about 200 K. Below this temperature there is an increase in the line width of the nmr spectrum. At 77 K, the spectrum becomes wide, indicating an ice-like structure (43).

The proposal has been made that the non-framework water and cations in zeolites behave as a concentrated electrolyte (46). In zeolite X, for example, the intracrystalline phase (86 Na^+ ions and 264 H_2O molecules) correspond to an 18 molal NaOH solution of 42% NaOH by weight which would have a density of 1.45 g/cc. The nmr measurements show that this water acts as a liquid with a long relaxation time, similar to a viscous liquid. The width of the line for zeolite X at room temperature indicates a very sharp single line suggesting highly mobile water molecules (46).

For hydrated zeolites with small and narrow cavities, the positions of the water molecules appear well-defined and coordination occurs with the cations in the cavities. The cations in the hydrated zeolites seem to be surrounded by as many water molecules as is spatially possible, as long as they do not lie too far away from the aluminosilicate framework and the negative charge distribution. The water content per unit cell of alkali metal cation exchanged forms of faujasite type zeolites have been studied by TGA and DTA, and has been found to decrease as the alkali metal series $Li^+ > Na^+ > K^+ > Rb^+ > Cs^+$ is descended (47).

CHAPTER II

CHEMICAL PROPERTIES AND REACTIONS

2.1 Phenomenon of Ion-Exhange

The phenomenon of ion-exchange was first discovered in 1845 by H.S. Thompson (52), who showed that certain soils have the power of "decomposing" and retaining ammonium salts. He found that when a solution of ammonium sulphate was filtered through the soil, the filtrate contained calcium sulphate and the ammonium salt was retained in the soil. Later Way (53) showed that the hydrated silicates in the soil produced this phenomenon. He was able to show that only the ammonium or the potassium ion was exchanged for the calcium in the soil. Subsequently, Way prepared an artifical base exchanger consisting of a sodium aluminosilicate. The first synthetic ion-exchanger was prepared by Harm and Rümpler in the year 1903 (54).

The ease of cation exchange in zeolites and other minerals led to an early interest in ion-exchange materials for use as water softening agents. Because of their three dimensional framework structure, most zeolites do not undergo any appreciable dimensional change with ion-exchange, and this has been confirmed by X-ray diffraction studies (55). The phenomenon of cation exchange in zeolites depends upon several factors,: (1) the nature of the cation, its size, charge and its anhydrous and hydrated properties, (2) temperature at which the exchange is carried out, (3) the concentration of the cations in solution, (4) the solvent used, (5) the framework structure of the zeolites, (6) the anion associated with the cation in the solution.

Ion-exchange studies in zeolites X and Y have been extensively studied by Barrer and Rees (56, 57, 58) and Sherry (36). An important feature of ion exchange in these zeolites is that in order for an entering ion to replace the Na^+ ions in the sodalite cages or hexagonal prisms it must diffuse through the ring of six tetrahedra that is the window between the supercage and sodalite cage. It is clear that the presence of two independent 3-D networks of cavities with cations located in both networks

causes double sieving effects. One network is dense and contains little water (the network of sodalite cages and hexagonal prisms) and the other network is open and highly hydrated. These two networks exhibit differing thermodynamic ion-exchange properties. The sites in the network of large cages exhibit a thermodynamic preference for higher charged ions over lower charged ones and among univalent ions, the thermodynamic preference depends on the Aℓ content, or framework charge. The thermodynamic preference of the sites in the large cages of the more aluminous zeolite X with the exception of Li^+ decreases with increasing ionic hydration energy. In the small cages of X and Y, the sites exhibit a preference for the ion with the smaller ionic radius and lowest charge - as is true of small-pore, dense zeolites. The rejection of ions on the basis of both size and charge in the small cages is more marked in Y.

The study of ion-exchange in zeolites X and Y affords an opportunity to study alkali metal ion exchange selectivity as a function of negative charge density in the aluminosilicate framework; because zeolites X and Y are isostructural, differing only in aluminium content.

2.2 Uni-Univalent Ion Exchange

Silver and Potassium are the largest univalent metal ions that can completely replace all of the sodium ions in zeolite X at 25°C. This indicates that the free diameter of the six membered ring is about 0.25 to 0.26 nm. Alkali metal cations with large crystal radii such as Rb^+ (0.298 nm) and Cs^+ (0.338 nm) cannot replace all of the Na^+ ions in X or Y at 25°C. It was concluded by Sherry (36) that the Na^+ ions that could not be replaced by Rb^+ and Cs^+ were located in the small cavities and that the exchangeable cations were located in the large cavities or supercages. This would limit exchange to 80% for zeolite X and 70% for zeolite Y. For Rb^+ and Cs^+ ions, the observed limit in zeolite X is about 65%. This has been attributed to "crowding" by Rb^+ and Cs^+ ions exchanged into site III or IV within the supercages. This forces about 14 Na^+ cations from site II into site I' in the β-cages. In zeolite Y, with low cation population in site III this crowding does not occur.

Focusing attention on ion exchange in the large cages of X and Y, we find the selectivity series Cs > Rb > K > Na > Li is observed in both zeolites (36) at low exchange levels. The thermodynamic selectivity of the negatively charged framework for alkali metal ions decreases in the order in which the ionic hydration energies increase. This selectivity series is the one that should be observed if the first ions to exchange are the mobile hydrated ones. At 50 % exchange levels, the selectivity series observed in X is Na > K > Rb > Cs > Li and in Y is Cs > Rb > K > Na > Li. The selectivity series for zeolite X at 50% loading can be best accounted for by assuming that the ions in or near site II are undergoing exchange. It has been found by Barrer, Rees and Davies (56, 58) that the isotherm for K^+ in Y does not vary much on replacing the water in the channels by methanol but that the exchange in methanol proceeds slower, this indicates stronger association of cations with the lattice sites when methanol fills the channels rather than water.

Tl^+ cations replace all of the cations in zeolite X, but they do not exchange the 16 site I cations in zeolite Y at 25°C. Sherry (36) explained this fact on the basis of lattice contraction as SiO_2/Al_2O_3 ratio increases from NaX to NaY. Another explanation was offered by Barrer, Rees and Davies (58). They concluded that zeolite X enhanced the polarization energy with Tl^+ so that the free-energy of the small-cage sites changes from a positive quantity in Y to a negative quantity in X, because of the stronger polarization effect of Tl^+ in X than in Y. Following this explanation, Ag^+ another polarizable ion also shows greater preference for zeolite X than Y.

Some disagreement exists in the maximum level of ammonium ion exchange in X. Sherry (59) has reported complete exchange of Na^+ by NH_4^+ in X, while Theng et al (60) could not replace 16 Na^+ by NH_4^+ in this zeolite. Barrer et al (61) found the maximum level of exchange to be 92%. Lai(62) found a complete exchange of Na^+ with NH_4^+ in zeolite Y containing 68 Na^+ cations per unit cell.

Alkyl ammonium ion exchange in X and Y zeolites have also been studied by Theng et al (60). The maximum degree of exchange was found to decrease with increasing molecular weight, and polarizability of the cation but was always below the limits imposed by the space requirements of the cations. The fraction of Na^+ ion replaced has been found to be lower for X than Y; and to be dependent on the inorganic ion which the alkyl ammonium ion replaces from the zeolite. This indicates the relative affinity of cations for the zeolite when determining the maximum degree of exchange.

2.3 Uni-divalent Ion Exchange

At room temperature, ion exchange with divalent cations is generally incomplete; however at higher temperatures the exchange level increases. Moreover, on dehydration of the zeolite containing divalent cations redistribution of the cations among the small cavities (sites I and I') occur. In zeolite X, complete ion-exchange for Na^+ with Ca^{2+} takes about four days at 25°C. The exchange has a fast and a slow step. The fast step involves exchange with Na^+ cations in the large cages (corresponding to 82% exchange), whilst the slow step involves the exchange in the small cages. Calcium ions with ionic radii of 0.096 nm should be able to pass through the rings of six tetrahedra, that are the entrances to the network of sodalite cages and hexagonal prisms. The equilibrium isotherm is sigmoidal, because of an early Ca^{2+} ion selectivity for supercage sites followed by a later Na^+ ion selectivity for small cage sites.

X-ray analysis of Ca^{2+} exchanged Y zeolite (33) indicates that after dehydration the Ca^{2+} ions are preferentially localized in the small cavities at the sites I and I' positions. The first Ca^{2+} ions to be exchanged occupy inaccessible sites inside the small cavities. This is achieved by a migration, during the dehydration process, of Ca^{2+} ions towards the small cavities. A possible replacement of Na^+ ions to supercage positions can be a stoichiometric migration (i.e. 1 Ca^{2+} for 2 Na^+). Since X-ray studies of CaY zeolites have demonstrated absolute preference of

Ca^{2+} ions for the sites I and II'; it can be suggested that in partially Ca^{2+} exchanged NaY zeolites, up to a Ca^{2+} content of 35%, the Na^{+} and Ca^{2+} ions prefer the exchange positions site I' and I respectively.

A different picture is presented in the case of Ba^{2+} exchange in zeolite X. Sherry (63) reported only 82% of the ions were replaced by Ba^{2+} ions at room temperature. This corresponds to the "magic number" of 16 Na^{+} ions per unit cell which were not replaced by Ba^{2+} ions. It has been reported (57) that only about 74% Ba^{2+} ion exchange could be achieved in X at equilibrium. The inability of Ba^{2+} ions to diffuse into the sodalite cages of zeolite X can be attributed in part to the ionic radius of the bare ion being 0.135 nm. However, K^{+} ion with an ionic radius of 0.133 nm diffuses rapidly into the small cages so not only cation size, but the size of the hydration shell associated with the cation is also important. Sherry (64) has obtained Ba-Na-X isotherms at 5, 25 and 50°C, and found that at 50°C, Ba^{2+} ions could completely replace all of the Na^{+} cations. The isotherm is sigmoidal, indicating as in the case of complete Ca^{2+} ion exchange; that at equilibrium the sites in the small cages prefer Na^{+} ions to Ba^{2+} ions. After calculating ΔG and subsequently the equilibrium constants for small (K = 0.037), and large (K = 72.5) cages; it was ascertained that divalent ion exchange of the small cages in X was very unfavourable; and was even more unfavourable in Y.

It has been reported (56, 65) that at 25°C, Ca^{2+}, Sr^{2+} and Ba^{2+} ions cannot replace 16 of the Na^{+} ions per unit cell of NaY. Sherry (65) suggested that the inability of these cations to replace the last 16 Na^{+} ions in NaY is kinetic in origin, whereas it has been suggested that there is no slow step in Y and that the lack of small cage ion exchange is caused by a positive free energy of exchange of these sites resulting from the low framework charge of this zeolite compared with X. Sherry (65) also studied alkaline earth ion-exchange in zeolite Y at 5, 25 and 50°C; and found that at the highest temperature 16 Na^{+} ions per unit cell were not replaced, but isotherms at 50°C did not cover the last 20% of the solution composition range. However, even if free energy is positive one would expect complete exchange to occur if one passed sufficient

large quantities of the pure electrolyte of the ingoing ion.

Transition metal ion exchange in zeolites X and Y have been studied by Maes and Cremers (66). The ionic diameters of Co^{2+}, Cu^{2+} and Zn^{2+} are much smaller than the six-ring free diameter; so one would expect complete exchange to take place. But these cations exist as aquo complexes in the supercages of these zeolites. Cu^{2+} and Zn^{2+} aquo complexes cannot replace 16 Na^{+} ions at site I in both zeolites; whilst Co^{2+} aquo complex cannot replace 26 Na^{+} ions per unit cell in X and 20 Na^{+} ions per unit cell in Y. The reason for this can be explained by the fact that, in the case of $Cu(H_2O)_6^{2+}$, two of the six water molecules are furthest away from the central ion and are loosely held. These two water molecules can be shaken off easily, making the cation volume of Cu^{2+} smaller than Co^{2+}, hence accounting for the higher level of Na-Cu exchange. The hydration state of Zn^{2+} is thought to exist as $Zn(H_2O)_6^{2+}$. The low level of Na-Co exchange may possibly be due to the $Co(H_2O)_6^{2+}$ complex being very strong and the crowding effect as found with Rb^{+} and Cs^{+} ions to apply. At 90°C, Na-Co exchange show the usual magic limits of 16 Na^{+} ions per unit cell not replaced in both zeolites.

2.4 Ion-Exchange Isotherms

An ion-exchange reaction can be represented by the following equation:

$$Z_A B_{(z)}^{z_B+} + Z_B\ A_{(s)}^{z_A+} \rightleftarrows Z_A B_{(s)}^{z_B+} + Z_B A_{(z)}^{z_A+} \qquad \ldots (2.1)$$

where Z_A, Z_B denote the charges of the exchange cations A and B and the subscripts z and s refer to the zeolite and solution phase respectively. The equivalent fractions of the exchanging cation in the solution and the zeolite phase are defined by:

$$A_s = \frac{Z_A m_{AY_{Z_A}}}{Z_A m_{AY_{Z_A}} + Z_B m_{BY_{Z_B}}} = \frac{Z_A m_s^A}{Z_A m_s^A + Z_B m_s^B} \qquad \ldots (2.2)$$

$$A_z = \frac{\text{number of equivalents of exchanging cation A}}{\text{total equivalents of cations in the zeolite}} \quad \ldots \quad (2.3)$$

where m_s^A and m_s^B are the molalities of the ions A and B, respectively, in the equilibrium solution, also $(A_z + B_z) = 1$ and $(A_s + B_s) = 1$. The ion exchange isotherm is represented by a plot of A_z versus A_s at a given total concentration in the equilibrium solution and at constant temperature. The preference for one of the two ions by the zeolite is expressed by the separation factor , α_B^A , and defined by:

$$\alpha_B^A = \frac{A_z\ B_s}{A_s\ B_z} \quad \ldots \quad (2.4)$$

If α_B^A is > 1.0, ion A is selectivity preferred over ion B, and vice-versa.

The exchange isotherms for exchange of cations in zeolites have been classified into five types (Fig. 2.1).

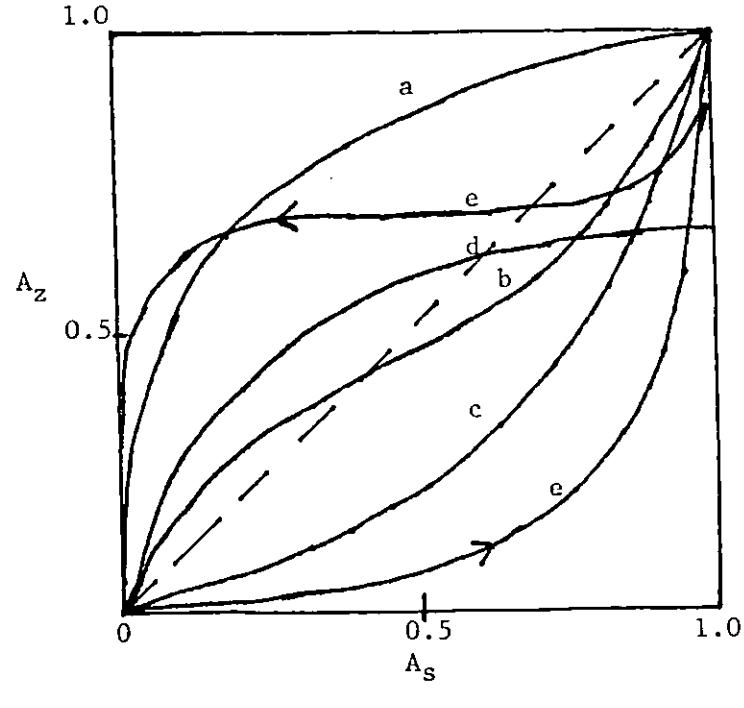

FIG. 2.1 Exchange Isotherm Classification

(a) Lies above the diagonal, the entering cation is selectively preferred by the zeolite.

(b) A sigmoidal isotherm indicating selectivity reversal of the entering cation.

(c) Lies below the diagonal, the outgoing cation is selectively preferred by the zeolite.

(d) Exchange does not go to completion although the entering cation is initially preferred.

(e) Two zeolite phases, exhibits a hysteresis loop.

The rational selectivity coefficient, K_B^A , includes the charge of the ions, z_A and z_B

$$K_B^A = \frac{A_z^{z_B} \; B_s^{z_A}}{B_z^{z_A} \; A_s^{z_B}} \qquad \ldots \quad (2.5)$$

If $Z_A = Z_B$, then $K_B^A = (\alpha_B^A)^{Z_A}$ ... (2.6)

If $Z_A \neq Z_B$, then

$$\{\alpha_B^A\}^{Z_A} = K_B^A \left(\frac{A_z}{A_s}\right)^{Z_A - Z_B} \qquad \ldots \quad (2.7)$$

The corrected selectivity coefficient, K'^A_B includes a correction for the activity coefficients of the ions in the equilibrium solution:

$$K'^A_B = K_B^A \; \frac{\gamma_B^{z_A}}{\gamma_A^{z_B}} \qquad \ldots \quad (2.8)$$

where γ_B, γ_A are the ionic activity coefficients of the cations in the equilibrium solution. In terms of the dissolved electrolytes:

$$K'^A_B = K_B^A \; \frac{\left[\gamma_{\pm BY_{z_B}}^{(Z+1)}\right]^{z_A}}{\left[\gamma_{\pm AY_{z_A}}^{(Z+1)}\right]^{z_B}} \qquad \ldots \quad (2.9)$$

where $\gamma_{\pm AY_{z_A}}$ and $\gamma_{\pm BY_{z_B}}$ are the mean molal activity coefficients of the electrolytes in solution (67).

The thermodynamic equilibrium constant K_a for the ion exchange reaction can be expressed as:

$$K_a = K'^{A}_{B} \frac{f_A^{z_B}(z)}{f_B^{z_A}(z)} \qquad \ldots \quad (2.10)$$

where $f_{A(z)}$ and $f_{B(z)}$ are the activity coefficients of A and B in the zeolite.

K_a is evaluated from the relation (56, 57):

$$\ell n\ K_a = (z_B - z_A) + \int_0^1 \ell n\ K'^{A}_{B}\ d\ A_z \qquad \ldots \quad (2.11)$$

assuming that changes in the activity of water in the zeolite and solution phases can be neglected. To obtain K_a, $\log K'^{A}_{B}$ is plotted against A_z which is referred to as the Kielland plot (68). The second term is then evaluated graphically from the area under the curve.

f_A^{zB} and f_B^{zA} in the zeolite are given by:

$$\ell n\ f_A^{zB}(z) = -(z_A - z_B)B_z - \int_{K^o}^{K} B_z\ d\ \ell n\ K'^{A}_{B} \qquad \ldots \quad (2.12)$$

$$\ell n\ f_B^{zA}(z) = -(z_A - z_B)A_z + \int_{K'}^{K} A_z\ d\ \ell n\ K'^{A}_{B} \qquad \ldots \quad (2.13)$$

where $K^0 = K'^{A}_{B}$ when $B_z = 0$ and $K' = K'^{A}_{B}$ when $B_z = 1$.

For uni-univalent exchanges (56)

$$K'^{A}_{B} = \alpha^{A}_{B} \cdot \frac{\gamma^{2}_{\pm BY}}{\gamma^{2}_{\pm AY}} = \text{constant at constant } A_z \qquad \ldots \quad (2.14)$$

For dilute solutions, the ratio of activities $\simeq 1$, so

$$K'^{A}_{B} = \alpha^{A}_{B} \qquad \ldots \quad (2.15)$$

For uni-divalent exchanges

$$K'^{A}_{B} = \frac{A_z \, B_s^2}{A_s \, B_z^2} \cdot \frac{\gamma^{4}_{\pm BY}}{\gamma^{3}_{\pm AY_2}} \qquad \ldots \quad (2.16)$$

$$\text{and} \quad K_a = K'^{A}_{B} \frac{f_{A(z)}}{f^{2}_{B\,(z)}} \qquad \ldots \quad (2.17)$$

K'^{A}_{B} has a unique value for a given A_z; so the ratio $\dfrac{B_s^2 \, \gamma^{4}_{\pm\, BY}}{A_s \, \gamma^{3}_{\pm\, AY_2}}$ must remain constant. If this ratio approaches unity, then $\dfrac{m^2_{BY}}{m_{AY_2}}$ is constant and $\dfrac{B_s^2}{A_s}$ is constant. The exchange isotherms however, are related to $\dfrac{B_s}{A_s}$ and depend on the total amounts of cations in the solution. Hence for uni-divalent exchanges, isotherms are dependent on the concentration of the solution phase.

2.5 Cation Hydrolysis and Structural Hydroxyl Groups

A complete description of the surface acid properties of a solid with a relatively high surface area must involve the determination of the acid strength, the density and the nature of the sites. The concept of surface acidity was originally introduced in order to explain the presence of intermediates (e.g. carbonium-ions) in chemical reactions catalysed by these solids such as cracking, polymerization, isomerization and alkylation. The mechanism of these reactions can be understood if intermediate substances are formed by interaction of the reactant molecule with an acid centre.

A solid is capable of converting an adsorbed basic molecule into its conjugated acid form. The acid site is able to transfer a proton from the solid to the adsorbed molecule (Brönsted acid site) or an electron pair from the adsorbed molecule to the solid surface (Lewis acid site).

Zeolites X and Y have been the centre of most of the attention. Hydroxyl groups, cations and Lewis acid sites seem to function as adsorption sites. The nature and population of hydroxyl groups depends on the type of cation involved, crystal size and the calcination temperature. This information has been obtained from spectroscopic techniques such as IR, NMR, UV and EPR.

Three infra red bands in the hydroxyl stretching region have been observed in X and Y zeolites. The 3740 cm^{-1} band is observed in all cases after dehydration and is generally attributed to the terminal hydroxyl groups, or associated with amorphous silica impurity. The other two bands; one a sharp band at a higher frequency (HF) of 3650 cm^{-1} and a broader band at lower frequency (LF) of 3550 cm^{-1} are attributed to protons bonded to framework oxygen atoms. The HF band results from an O-H group on O_1 of the lattice which has a normal O-H bond distance and extends into the large cavity. The LF band is assigned to an O-H group on O_3, with possibly smaller contribution from O_2 and O_4, and this is not directly accessible from the large cavity.

It has been reported by Angell and Schaffer (69) that some univalent cationic forms of zeolites have been found to contain a deficiency in the

metal ion content. This deficiency has been attributed to partial hydrolysis of the cation and replacement by H_3O^+. Ward (70) however found no absorption bands due to hydroxyl groups for the alkali cation forms of the zeolite. The alkaline earth forms of the zeolite exhibited distinct hydroxyl absorption frequencies, which depended markedly on the cation. The catalytically active sites are thought to be located either at the cation sites or at sites formerly satisfied by the cation. There is considerable evidence that in divalent exchanged X and Y zeolites, the cations have a strong preference for site I where they have six fold coordination with the surrounding lattice oxygens. On the other hand, divalent cations in site II have only three fold coordination with the lattice oxygens. The electropositive charges on these cations are only partially neutralised by the $A\ell O_4^-$ but are balanced by the negative charges existing at the unoccupied site II. The degree of exchange of the site II with divalent cations has been found to correlate directly with the catalytic activity of the type Y and probably also type X.

Thus, for a divalent ion (M^{2+}) zeolite the following reactions occur:

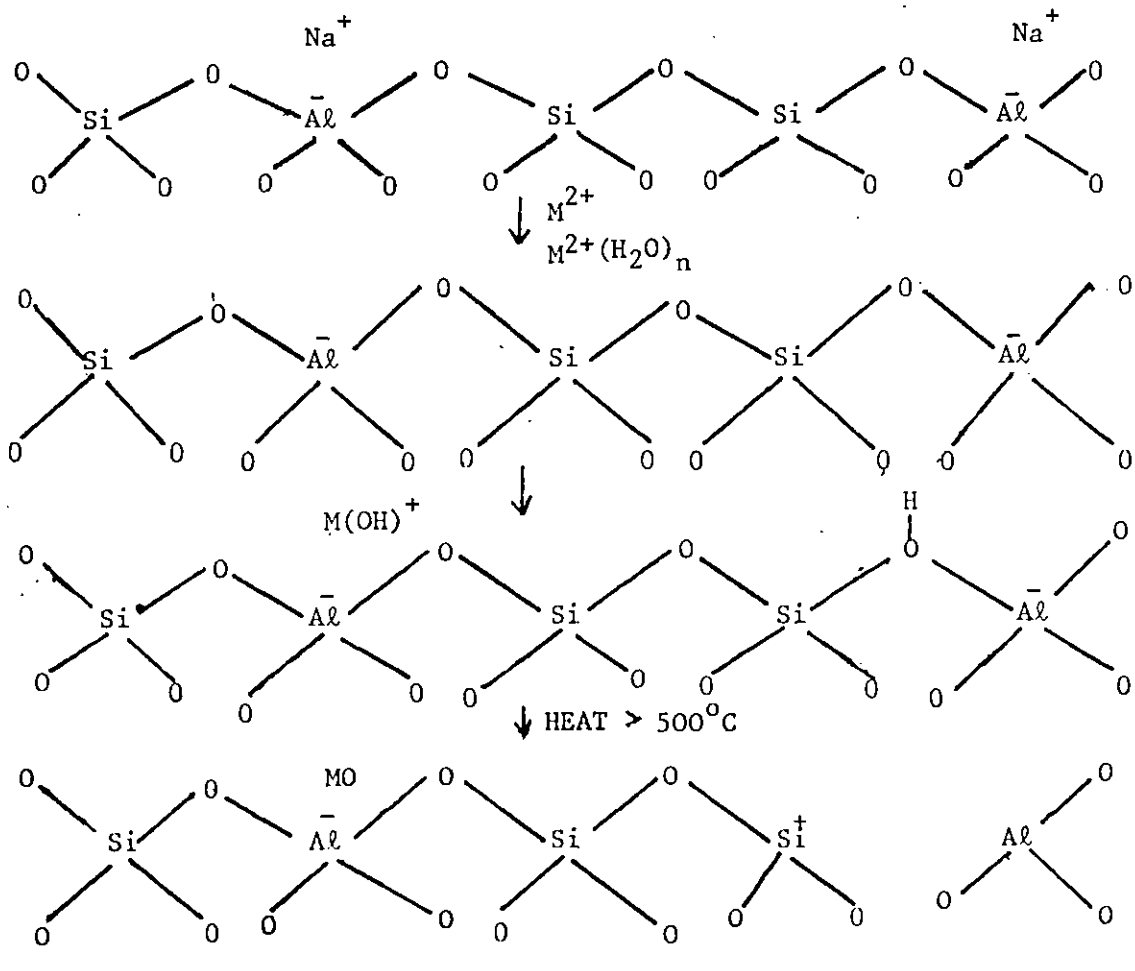

A similar hydrolytic scheme has been proposed for trivalent ions by Venuto et al (71) and Rabo (72). Hall (73) has also proposed a hydrolytic scheme for magnesium. Thus one structural hydroxyl group is formed for every two exchanged sites. These hydroxyl groups would be similar to those presented in hydrogen Y zeolite and the cation form would, therefore dehydroxylate at high calcination temperatures accompanied by the conversion of the Brönsted acidity to Lewis acidity. In the absence of much water, the cation cannot satisfy the charge distribution requirements of the zeolite lattice. The localized cation then induces dissociation of the coordinated water molecules to produce MOH^+ and H^+ species. The variation of the hydroxyl content and Brönsted acidity of the various alkaline earth forms may mean that an equilibrium exists:

$$M^{2+}(H_2O)_n \rightleftarrows MOH^+ + H^+$$

The small cations with their associated high electrostatic field and polarizing power would result in the equilibrium moving to the right while the larger cation would be expected to produce less dissociation. Thus, the polarizing power of alkaline earth cations has been found to be inversely related to their cationic radii (70) $Mg^{2+} > Ca^{2+} > Sr^{2+} > Ba^{2+}$. With the exception of Ba^{2+}, alkaline earth cations in zeolite X behave differently from the univalent cation and exhibit a strong band at 3650 cm^{-1} in the i.r. spectra.

The Brönsted acid sites may be preserved if a bridged cation species is formed, e.g.,

$$M(OH)^+ + M^{2+} \rightarrow \overset{+}{M} - O - \overset{+}{M} + H^+$$

and for trivalent cations:

$$M(H_2O)_n^{3+} \rightarrow M^{2+}(OH) + H^+$$

$$M(OH)^{2+} + M^{3+} \rightarrow M^{2+} - O - M^{2+} + H^+$$

Thermal decomposition of ammonium exchanged zeolites, such as zeolite Y, may be represented by the following scheme:

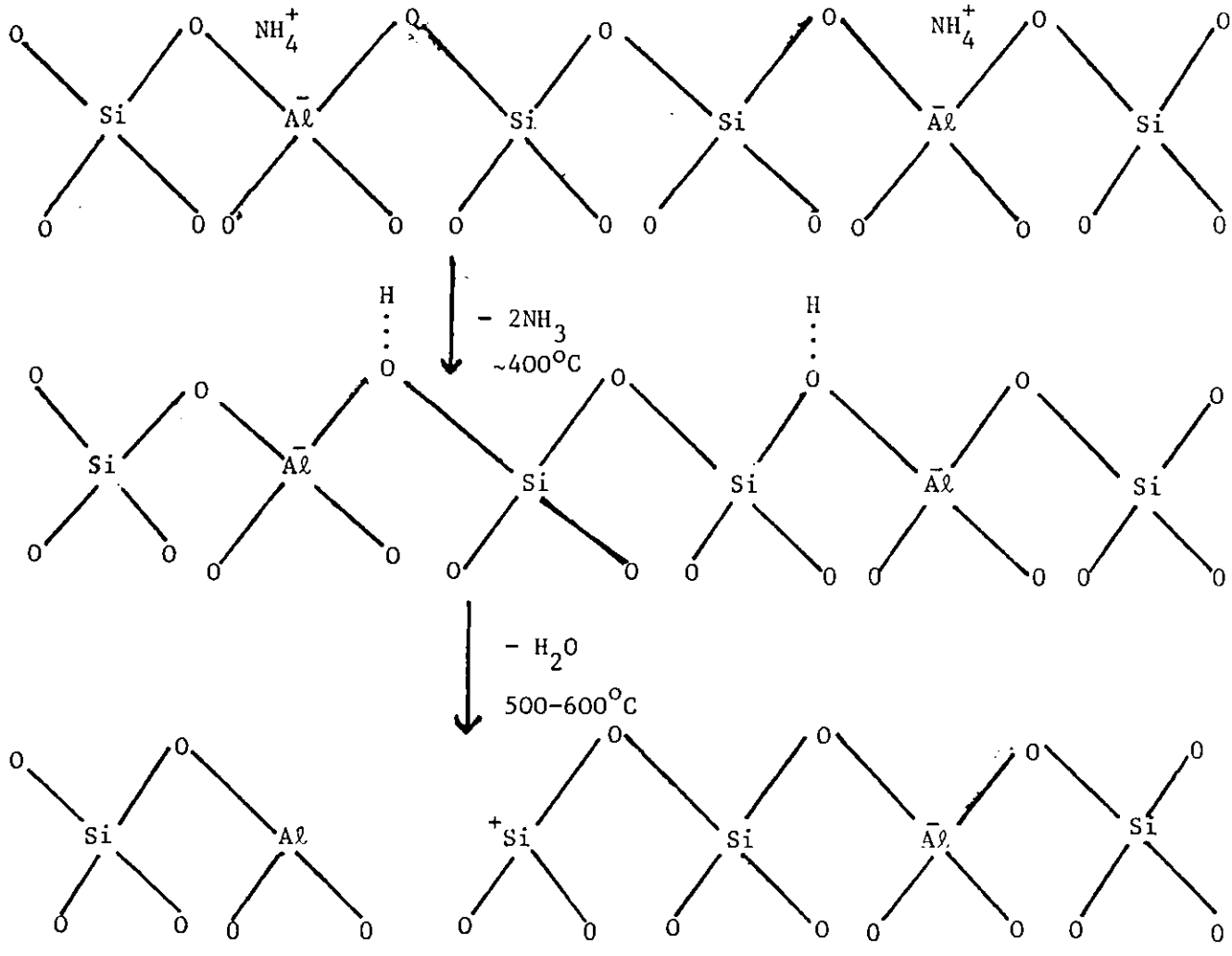

By controlling the degree of ammonium exchange the concentration of structural hydroxyl groups in the "hydrogen" zeolite can be controlled. It has been suggested that protons are initially formed but rearrange to form hydroxyl groups.

The zeolite can contain a maximum of one ammonium ion for each aluminium atom. The electrostatic charge remains neutral and the proton of the hydroxyl group acts as the charge balancing species. Deammoniation occurs at about 400°C. The protons are thought to be located on the bridging oxygen atoms O1 and O3 (74). Further heat treatment at 500-600°C results in the loss of one H_2O molecule from two nearby OH groups or one H_2O for each two tetrahedral aluminium atoms. This causes the loss of oxygens, thus producing a lattice vacancy, and the adjacent Aℓ and Si atoms will tend to assume a planar type sp^2 configuration with the remaining three oxygen atoms.

The intensity of the ir bands of the two types of hydroxyl groups vary with the calcination temperature after deammoniation of the zeolite. Increasing temperature causes the intensity to increase and remain constant up to 500°C, while above 500°C the intensities rapidly decrease for the HF and LF bands. It is found that the initial stage of dehydroxylation overlaps with the final stage of deammoniation in zeolite X, whereas these two processes are distinct in zeolite Y. Ward (70) ascertained that the frequencies of the absorption bands of the hydroxyl groups on divalent cation forms were similar to those of the hydrogen form. Their intensity is considerably less, which indicated a lower hydroxyl group concentration.

2.6 Dehydration and Thermal Stability of Zeolites X and Y

Differential Thermal Analysis (DTA) and Thermogravimetric Analysis (TGA) have shown that physically adsorbed water can be removed by heating at 250-300°C; without major alteration to the crystal structure. The zeolites can be subsequently rehydrated, i.e. adsorb water from the vapour or liquid phase. In zeolites that undergo dehydration reversibly and continuously, there is no substantial change in the topology of the framework structure. In zeolite X which has several cation sites, the effect of dehydration or partial dehydration may be pronounced. Crystallographic dimensions change with dehydration, which can be due to framework distortion or to relocation of cations. It must be stressed that all molecular sieve separations are judged by an "effective pore size" which will be larger than the measured crystallographic dimensions (for dehydrated zeolites).

Based on dehydration behaviour, zeolites may be classified as (a) those which upon dehydration do not show major structural changes, and which exhibit continuous dehydration curves as a function of temperature, and (b) those zeolites which undergo structural change with dehydration and which show steps or other discontinuities in the dehydration curves. The factors affecting the nature of the DTA curves include particle size, heating rate and the atmosphere surrounding the specimen.

The DTA curve for zeolite X indicates a continuous loss of water over a broad range commencing from slightly above room temperature to about 350°C with a maximum at about 250°C. Exothermic peaks at 772°C and 933°C indicate decomposition followed by recrystallization of the zeolite. Zeolite Y shows a broad endothermic peak with a maximum at 208°C and an exothermic peak at 790°C. After prolonged heating in air at 760°C no structural change occurs; at 800°C, the structure collapses to an amorphous residue.

$$\text{Zeolite X} \xrightarrow{1000^{0}\text{C}} \text{Carnegeite}$$

$$\text{Zeolite Y} \xrightarrow{1000^{0}\text{C}} \text{Glass}$$

The thermal stability of zeolites can be increased by cation exchange, e.g. Na^{+} by Ce^{3+}. Zeolites with high SiO_2/Al_2O_3 ratios are known to be more stable than their low ratio counterparts (76). Bremer et al (77) distinguished three groups of cation exchange in Y type zeolites to increase thermal stabilities; they are (1) Mg^{2+}, Ca^{2+}, Co^{2+}, Ni^{2+} or Zn^{2+}; (2) Ce^{3+}, H^{+}; (3) Cu^{2+}. With the first group, minimal stability was exhibited at 20-40% level of exchange. At low loadings the framework distortion is significant when the cations enter the hexagonal prism. At higher level of exchange the lattice distortion is partly compensated. The second group exhibits increasing stability with the degree of exchange; the continuous rise in thermal stability of Ce^{3+} - exchanged zeolite has been attributed to the existence of a sodalite unit complex proposed by Olson et al (78). This complex reduced the polarizing power of Ce^{3+} ions and hence the lattice distortion. The third group exhibits continuous decreasing stability with increasing level

of exchange. E.S.R. studies have shown that when the degree of exchange is $\geq$ 19%, the Cu^{2+} ions can be located in sites I, I', II and large cages. With increasing level of exchange, the concentration of Cu^{2+} ions in I' and II' increases and this has been attributed to cause a distortion in the hexagonal prism and resulting in a decrease in thermal stability.

CHAPTER III

CHROMATOGRAPHY

Historically, the word chromatography was used by Tswett in 1903 to describe the separation of plant pigments by percolating a petroleum-ether extract through a glass column packed with powdered calcium carbonate. Coloured zones were produced by the various pigments migrating through the column at different rates, the components being isolated by extrusion and sectioning of the calcium carbonate packing. Modern chromatographic techniques are more complex and are used for a wide variety of separations frequently involving colourless substances, but the original term is retained.

All the techniques depend upon the same basic principle, i.e. variation in the rate at which different components of a mixture migrate through a stationary phase under the influence of a mobile phase. Rates of migration vary because of differences in distribution ratios. A stationary phase (porous medium) can either be a solid (e.g. Alumina, charcoal, silica, Molecular sieves, etc..) or a liquid which is coated onto an inert, granular or powdered solid support which is either packed into a column or spread on a supporting sheet in the form of a thin layer. The solid stationary phases used in some chromatographic techniques have no need of a support if packed into a column but still require a supporting sheet for thin-layer operation. A mobile phase can either be liquid or gas.

The process whereby a solute is transferred from a mobile to a stationary phase is called sorption. Chromatographic processes are based on two different sorption mechanisms, namely surface adsorption and partition. The original method employed by Tswett involved surface adsorption where the relative polarities of solute and solid stationary phase determines the rate of movement of that solute through a column or across a surface. If a liquid is coated onto the surface of an inert solid support, the sorption process is one of partition, and movement of the solute is determined solely by its relative solubility in the two phases or by its

volatility if the mobile phase is a gas. This process was introduced in 1941 by Martin and Synge. Both adsorption and partition may occur simultaneously, and the contribution of each is determined by the system parameters, i.e. the nature of the mobile and stationary phases, solid support and solute. For example, a stationary phase of aluminium oxide is highly polar and normally exhibits strong adsorptive properties. However, these may be modified by the presence of adsorbed water which introduces a degree of partition into the overall sorption processes by acting as a liquid stationary phase.

Stationary Phase	Mobile Phase	Process
Liquid	Liquid	Partition
Liquid	Gas	Partition
Solid	Liquid	Adsorption
Solid	Gas	Adsorption

Table 3.1 Showing the types of processes that can be achieved in Chromatography.

3.1 Gas-chromatography - Apparatus and Instrumentation

The technique is beyond doubt the most extensively employed for analytical purposes of all the instrumental separation methods, and so merits detailed consideration. It provides a quick and easy way of determining the number of components in a mixture, the presence of impurities in a substance and, in many instances, prima facie evidence of the identity of a compound. The only requirement is some degree of stability at the temperature necessary to maintain the substance in the gas state.

A schematic diagram of a gas chromatograph is shown below and details of the components are discussed.

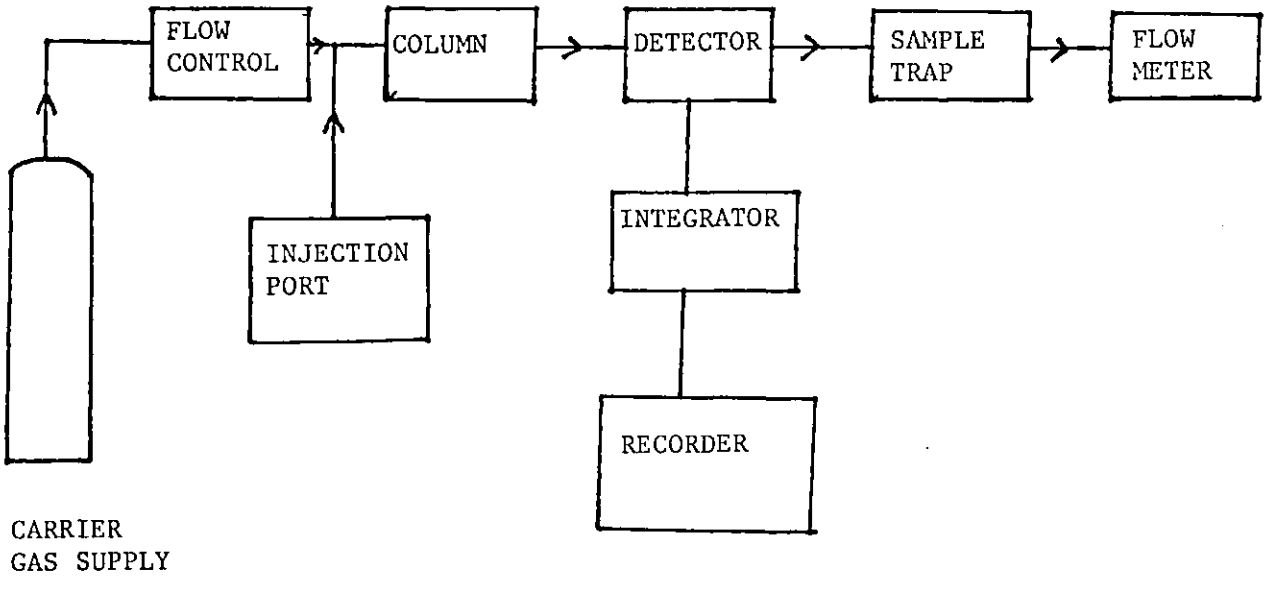

3.1.1 Mobile Phase and Flow Control

The mobile phase or carrier-gas is supplied from a cylinder via a pressure reducing head at a pressure of 40 psi giving a flow-rate of 10 to 100 ml/min. Fine control of carrier-gas pressure is achieved either by a needle-valve or by a mass flow controller. The latter enables a constant flow rate to be maintained when the temperature is increased during a separation. Water vapour, hydrocarbons, and other impurities in the gas affect column performance and detector response, but they can be removed by passing it through a trap containing a molecular sieve. The most common carrier gas is helium, inspite of its cost. There are two principal reasons for this choice. One of the most useful detectors depends on the thermal conductivity of the gas, a property that is much greater for hydrogen and helium than for any other gases. The other advantage of helium, also shared by hydrogen, is that because of its low density greater flow rates can be employed, thus reducing the time required for a separation. Hydrogen has two drawbacks, its fire and expolsion hazard and, more fundamentally, its reactivity toward reducible or unsaturated sample components. Other gases, such as argon or nitrogen, are required by certain detectors.

3.1.2 Sample Injection System

For liquid samples, they are simply introduced into the carrier-gas stream by injecting a small quantity (0.2 to 5 µl) through a self sealing silicone rubber septum using an hyperdermic syringe.

For gaseous samples either gas tight syringes may be used (sample size 0.5 to 5 ml) or a gas sampling valve incorporated in the system where usually a calibrated gas loop may be filled with sample and then flushed onto the column by altering the direction of the carrier gas flow.

Solid samples can be introduced as a solution or in a sealed glass ampoule which is crushed in the gas stream by means of a gas-tight plunger. Only solids which have appreciable vapour-pressures at the operating temperature of the column can be successfully chromatographed.

3.1.3 The Column

The column is the heart of the gas chromatograph in which the separation process occurs, therefore the choice of column packing material is of upmost importance. It consists of a coil of tubing, usually stainless steel, glass or copper, with an o.d. of $\frac{1}{16}$" to $\frac{1}{4}$" and anything from a few metres to several hundred metres long.

For Gas Liquid Chromatography, the stationary phase is either coated on to a granular solid support which is packed uniformly into the column - packed column - or coated on to the walls tearing an unrestricted narrow path through the centre of the column - open tubular or capillary column. Capillary columns may be prepared by coating the stationary phase directly on to the walls, WCOT (wall coated open tubular) or coating with a porous solid support, SCOT (support coated open tubular). The advantages of the latter type columns are an increased sample capacity compared to capillary columns due to a higher loading of stationary phase, and increased efficiency arising from the thinner coating. The sample capacity of ordinary capillary columns is much lower than that of a packed column necessitating the use of a stream splitter to avoid overloading. This device, located between the injection port and the top of the column, diverts the bulk of the sample to waste allowing only a very small fraction to pass down the column.

To ensure operation under reproducible conditions, the column is enclosed in a thermostatically controlled oven whose temperature can be held constant to within 0.5 K. Operating temperatures range from ambient to over 400°C and may remain constant during a separation - isothermal operation - or automatically increased at a predetermined rate to speed the elution process - temperature programmed. Rapid temperature equilibration and changes in operating temperature are

achieved by circulating the oven air with a fan.

3.1.4 Solid Support

The function of a solid support is to hold the liquid phase used for glc immobile during the separation process. It should be inert, easily packed and have a large surface area. The solid support ideally should have no effect on the chromatographic process, but only to serve as a mechanical matrix for the liquid phase. Calcined diatomaceous earth and firebrick, both mainly silica, are commonly used, being marketed under various trade names such as Celite, Chromosorb and Stermachol. The materials must be rendered chemically inert before coating with the stationary phase because trace metal impurities and surface silanol (Si-OH) groups produce surface sites which promote undesirable adsorption effects. Adsorption causes tailing and may result in catalysed decomposition or rearrangements of the solutes passing through the column. Pretreatment consists of acid - or alkali - washing to remove the trace metals, and silanizing to convert the Si-OH groups to the innocuous silyl ethers, e.g. $Si-O-Si(CH_3)_3$. Dimethyl dichlorosilane or hexamethyl disilazane are frequently used for this purpose. If highly polar compounds are to be separated, silanized glass beads or granular PTFE are supports less likely to cause tailing. Because they are non-porous, they can support a maximum of only about 3% of stationary phase, and the size of the sample that can be chromatographed is smaller than with the silaceous solid supports.

The particle size of a solid support is critical in striking a compromise between column efficiency and speed of separation. Typical

diameter ranges are 60 to 80 mesh (about 0.25 to 0.18 mm), 80 to 100 mesh (0.18 to 0.15 mm) and 100 to 120 mesh (0.15 to 0.13 mm). The smaller the grains, the more pressure is required to force gas through the columns.

3.1.5 Stationary Phase

The number of stationary phases suitable for gas chromatography is quite extensive, and choice is dictated largely by the nature of the sample. A liquid stationary phase should be non-volatile and thermally stable at the operating temperature of the column, otherwise it will 'bleed' during operation and cause a drifting baseline on the recorder. In addition, it should be chemically stable and inert towards samples to ensure reliable results. Stationary phases are described as non-polar or polar according to their structure and separating abilities. Non-polar types include hydrocarbon and silicone oils and greases. Polar types cover a wide range of polarity and include high molecular weight polyesters, ethers, carbowaxes, amines, etc.

In general, the most suitable stationary phase for a given sample is that which is chemically similar to it. Thus, non-polar solutes, such as saturated hydrocarbons can be resolved easily on a non-polar liquid such as squalane, Apiezon-L grease or silicone oil DC 200, whereas their peaks fall much closer together on a column of similar dimensions but containing a polar liquid such as one of the succinates. The converse applies to the separation of polar solutes such as alcohols. Where a sample contains unknowns or compounds of varying polarity, a compromise stationary phase must be chosen, usually by trial and error. The order of elution can be altered by changing the liquid phase. For example, on a non-polar paraffin-type column, t-butyl alcohol (b.p. 82.6°C) will elute before cyclohexane (b.p. 80.8°C). If a more polar liquid phase containing hydroxyl groups is

used, the cyclohexane elutes first because of hydrogen - bonding between the alcohol and the stationary phase.

Stationary phases can be made highly selective by adding compounds to them which have affinities for certain chemical species. For example, silver nitrate, incorporated into a polar liquid preferentially retards the elution of olefins by formation of weak π - complexes. The amount of stationary phase or 'loading' carried by a solid support affects the efficiency of the column and the size of the sample to be injected. Loadings of 1 to 10% are to be preferred, although at the lower end of this range the sample size may have to be restricted to prevent overloading the column. In general lower loadings allow the use of a lower operating temperature which is an important factor when handling thermally sensitive compounds.

A selection of stationary phases with their maximum operating temperatures is given in Table 3.2.

Table 3.2 Some stationary-phase liquids, in order of increasing polarity.

Stationary Phase	Max. TEMP (°C)
Squalane ($C_{30}H_{62}$)	150
Apiezon-L grease	250-300
Didecyl phthalate	165-170
Di-(2-ethyl hexyl) sebacate	150
Methyl silicone oil DC-200	200
Phenyl silicone oil DC-550	180-220
Methyl silicone gum SE30	300-350
Polyethylene glycol (Carbowax 1540)	150
Polyalkylene glycol (Ucon Oil-LB-550-X)	180-200
Polyalkylene glycol (Ucon Oil-HB-2000)	180-200
Polyphenyl ether (OS-138)	200-225
Butane diol succinate polyester "BDS"	200-225
Diethylene glycol succinate polyester "DEGS"	205-210

3.1.6 Detectors

Detectors are devices used to sense and measure, the small amounts of components present in the carrier gas stream, leaving the chromatographic column. Ideally, a detector should have the following characteristics: rapid response to the presence of a solute, a wide range of linear response, high sensitivity,stability of operation.

The detectors normally used in GC are of a differential nature, i.e. their response is proportional to the concentration or mass flow rate of the eluted component. They depend on changes in some physical property of the gas stream, e.g., thermal conductivity, density, flame ionization, β-ray ionization, in the presence of a sample component. The signal from the detector is fed to a chart recorder and an integrator via suitable electronic amplifying circuitry where the data are presented in the form of an elution profile and area units respectively. Detectors most widely used in industry are those based on thermal conductivity, flame ionization, electron capture and perhaps gas density.

Detector	Minimum Detectable Quantity/gs^{-1}	Linear Range	Temp Limit/°C	Remarks
Thermal Conductivity	10^{-9}	10^{4}	450	non-destructive, temperature and flow sensitive.
Flame ionization (F.I.D.)	10^{-11}	10^{7}	400	destructive, excellent stability.
Electron Capture	10^{-13}	10^{2}	350	non-destructive, easily contaminated, temperature sensitive.
Gas density	10^{-8}	10^{4}	150	non-destructive, requires no calibration

Table 3.3. Shows Detector Characteristics

3.1.6a Thermal Conductivity Detector (TC) or Katharometer

This detector was introduced by Ray (79) and is based on the principle that a hot body loses heat at a rate which depends on the thermal conductivity and therefore the composition of the surrounding gas. It consists of two heated filaments of a metal which has a high coefficient of resistance, e.g. platinum, and so requires a high degree of temperature and gas flow control. The matched filaments form part of a Wheatstone Bridge arrangement, which gives a signal when resistances are not balanced. This imbalance is due to the filaments being at different temperatures. Pure carrier gas flows through one channel and the effluent from the column through the other. The rate of heat loss from each filament determines its temperature and therefore its resistance. A change in thermal conductivity of the gas flowing through the sample channel arising from elution of a sample component alters the temperature and hence the resistance of the filament in that channel and this produces an out-of-balance signal in the bridge circuit. Sensitivity, which is determined by the difference in thermal conductivity between the reference and sample streams, is highest when hydrogen or helium is used as the carrier-gas. The thermal conductivity detector is robust and reliable but has only moderate overall sensitivity which varies widely from compound to compound. Response is non-linear and sensitive to changes in temperature and flow-rate so that it is not particularly suitable for quantitative work.

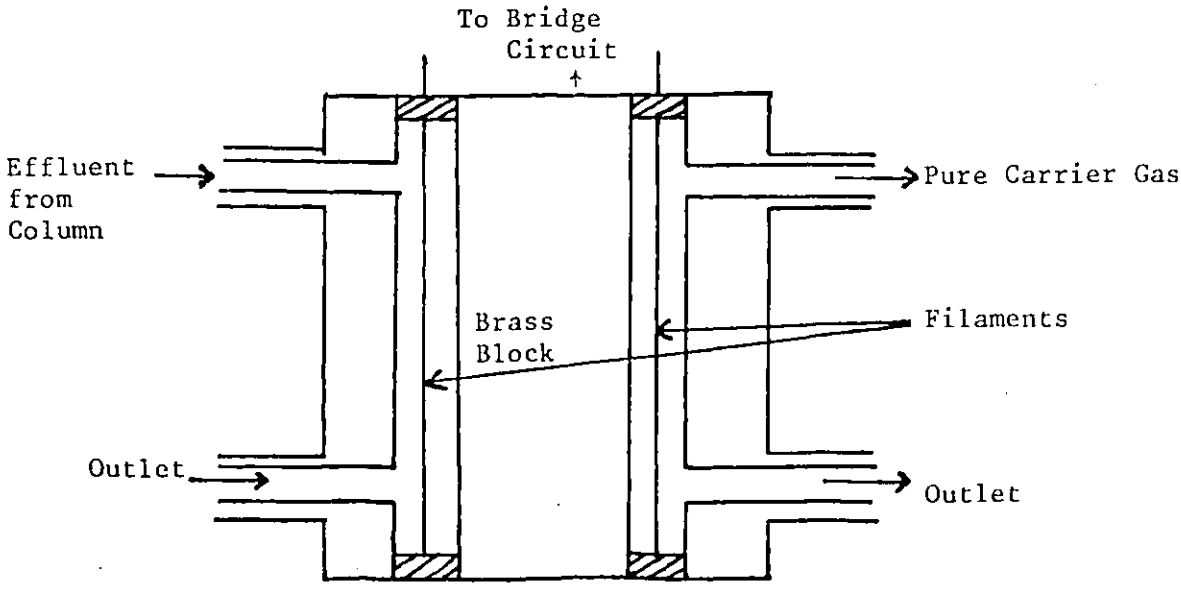

FIG. 3.1 Thermal Conductivity Detector

3.1.6b Flame Ionization Detector (FID)

This type of detector measures the variation of the ionisation current of an air-hydrogen flame or an oxygen-hydrogen flame into which the gases leaving the column are sent. Many organic compounds are readily pyrolyzed in this flame to produce ions. The carrier gas (usually He or N_2) emerging from the column is mixed with about an equal amount of hydrogen and burned at a metal jet in an atmosphere of air. The jet (or a surrounding ring) is made the negative electrode, and a loop or cylinder of inert metal surrounding the flame is made positive. The sensitivity to organic solutes varies roughly in proportion to the number of carbon atoms; it is perhaps a thousandfold more sensitive than the Thermal Conductivity detector. The FID has become one of the most popular detectors, superior for quantitative analysis, since there is no flow dependence. It is also insensitive to water, and therefore can analyse aqueous solutions directly.

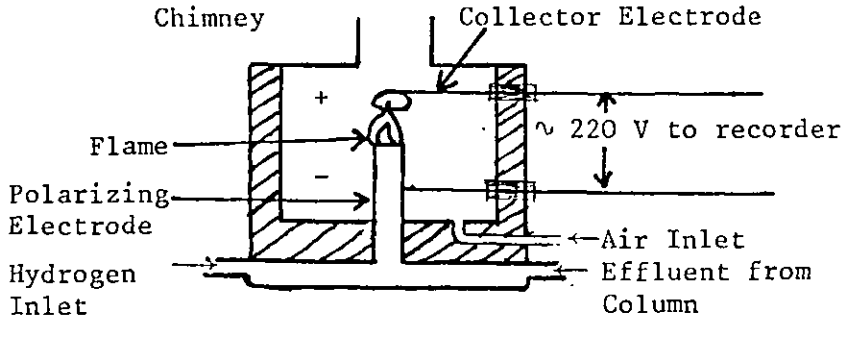

FIG. 3.2 Flame Ionization Detector

3.1.6c Electron Capture Detector

This is the most widely used of several detectors which employ a β-ray ionizing source. It exploits recombination effects for the detection of compounds having an affinity for free electrons, and therefore measures a reduction in signal. The principle of detection depends on the fact, that the rate of combination between positive and negative ions, is 10^5-10^8 times greater than that of recombination between free electrons and positive ions. As the nitrogen carrier-gas flows through the detector a tritium or ^{63}Ni source ionizes the gas forming 'slow' electrons which migrate towards the wire anode under an applied potential difference of 20 to 50 V. The drift of 'slow' electrons constitutes a steady current while only carrier-gas is present. If a solute with a high electron affinity is eluted from the column, some of the electrons are 'captured' thereby reducing the current in proportion to its concentration. The detector is very sensitive to halogenated compounds and insensitive to hydrocarbons, therefore can determine former in vast excess of latter. Additional selectivity can be obtained by increasing the applied potential when the response of weakly electron-capturing compounds is eliminated. It is particularly useful in the analysis of halogen - containing pesticides which can be detected in the sub-picogram range. Although the electron capture detector is the most sensitive available, its linear range is restricted to only 10^2 and it is sensitive to temperature changes.

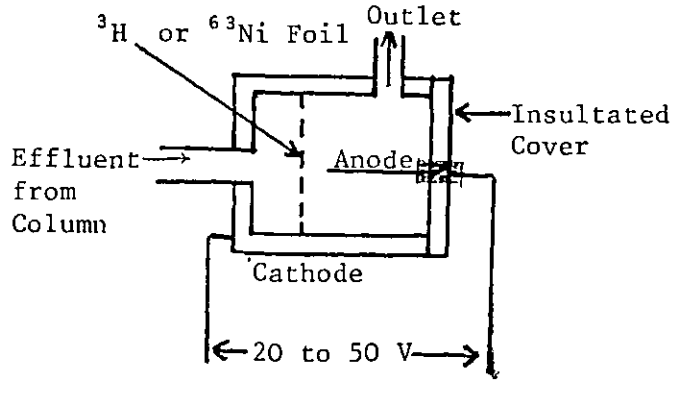

FIG. 3.2 Electron Capture Detector

3.2 G.C. Retention Data and Systems

Retention data is the means of identifying components in a sample mixture, and is obtained from the chromatogram itself.

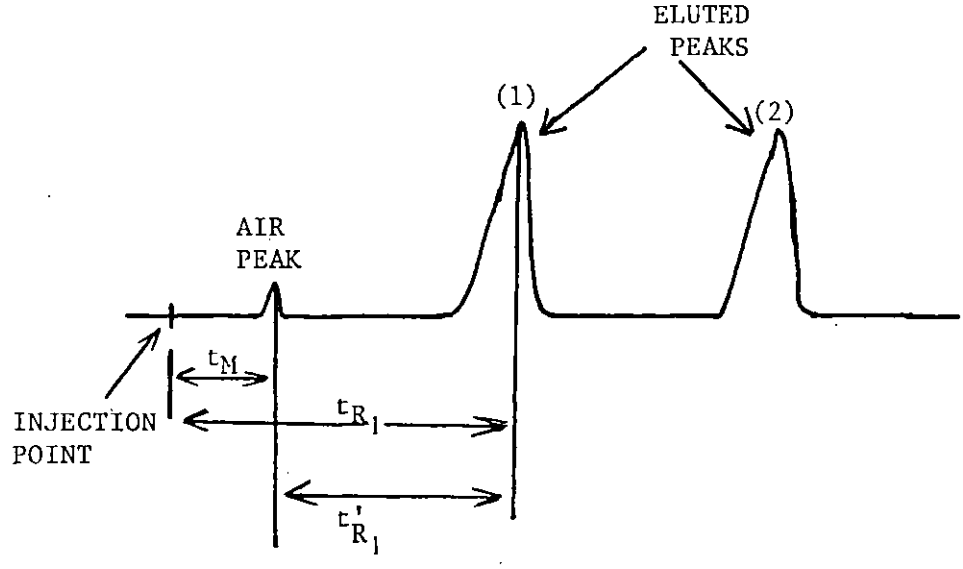

Retention time t_R = time taken from injection point for peak maximum to appear.

Holdup time t_M = time taken from injection point for air peak to appear.

Retention volume $V_R = t_R \times f_c$ (f_c = flow rate).

Adjusted Retention Volume $V'_R = V_R - V_M$ (V_M = holdup volume = $t_M \times f_c$).

However, for many analytical purposes a more useful and convenient parameter is Relative Retention γ,

where $$\gamma_{1:2} = \frac{V'_{R_1}}{V'_{R_2}} \quad \ldots \quad (3.1)$$

Ideally one would wish to refer all samples to the same standard, however, due to the wide range of volatilities encountered in gas chromatography this is clearly impracticable.

The most widely used method of calculating and expressing retention data is that due to Kovats (80) Retention Index (I) System. The basic idea of this system of peak identification is that the retention of a component is expressed relative to a series of closely related standard compounds (n-paraffins).

The Retention Index for unknown (I_x) is given by:

$$I_x = 100\,N + 100\,n\left[\frac{\log V'_{R_X} - \log V'_{R_N}}{\log V'_{R_{(N+n)}} - \log V'_{R_N}}\right] \qquad \ldots \quad (3.2)$$

where V'_{R_X} = Adjusted retention volume sample x.

V'_{R_N} = " " " n-paraffin C_N.

$V'_{R_{(N+n)}}$ = " " " " $C_{(N+n)}$

where $V'_{R_N} < V'_{R_X} < V'_{R_{(N+n)}}$

Also by definition I for n-paraffins = 100 N e.g. 400, 500 for n-butane, n-pentane, for all columns and all temperatures. In the determination of I a logarithmic scale is used, because log V'_R is linear to chain length and hence retention index. Retention indices can assist in determining a tentative structure for a compound, by using an additive technique for the ΔI's of the effective zones (functional groups etc.) of the compound.

e.g.

Ethyl chloride	I	=	671	∴	ΔICℓ	= 471
n-Propyl chloride	I	=	772	∴	ΔICℓ	= 472
n-Butyl chloride	I	=	870	∴	ΔICℓ	= 470

Further observations on the applications of the Retention Index concept where:-

1) Kovats (80).

"If the difference in boiling points of two isomers is ΔT, then the difference in their retention indices ΔI on a "non-polar" stationary phase is given by:

$$\Delta I \times 5\Delta T$$

2) Smith and Evans (81)

The authors put forward the observation that, "If the retention indices of two symmetrically substituted substances are $I_{(RxR)}$ and $I_{(R'xR')}$ respectively, then the retention index of the unsymmetrically substituted compound RxR' is given by:

$$I_{(RxR')} = \frac{1}{2}(I_{(RxR)} + I_{(R'xR')})$$

The retention index has now been widely adopted to systematise the compilation of retention data, and has also made it possible for the classification of stationary phases to be put on a more quantitative basis in the Rohrschneider system which uses ΔI values. (See section 3.4.3).

In gas chromatography, correction must be made for the difference in pressure at the inlet (P_i) and outlet (P_o) of the column. (This correction is not necessary if the mobile phase is a liquid, since liquids are not compressible). A temperature correction is also needed. These factors can be combined to give:

$$V_g = V_R' \, j \, \frac{273}{T_c} \, \frac{1}{W_s} \qquad \ldots \quad (3.3)$$

$$\text{where } j = \text{pressure correction} = \frac{3\{(P_i/P_o)^2 - 1\}}{2\{(P_i/P_o)^3 - 1\}} \quad \ldots \quad (3.4)$$

T_c is the temperature of the column (in K), and W_s is the weight of stationary phase in the column. V_g represents the volume of carrier fluid required to move one-half of the solute through a hypothetical column containing 1.00 g of stationary liquid, operating at 0^oC, and causing no pressure drop. One can show that

$$V_g = \frac{273\ K}{T_c \rho_s} \quad \ldots \quad (3.5)$$

where ρ_s is the density of the stationary phase. V_g, the specific retention volume, provides a convenient way in which to report retention data.

3.3 Column Performance

Two contributing factors are responsible for the performance of column in carrying out a particular separation. They are column efficiency and solvent efficiency.

The column efficiency, is rather a mechanical concept which is a function of column packing and expressed in terms of a theoretical plate number n where n may be calculated from the chromatogram.

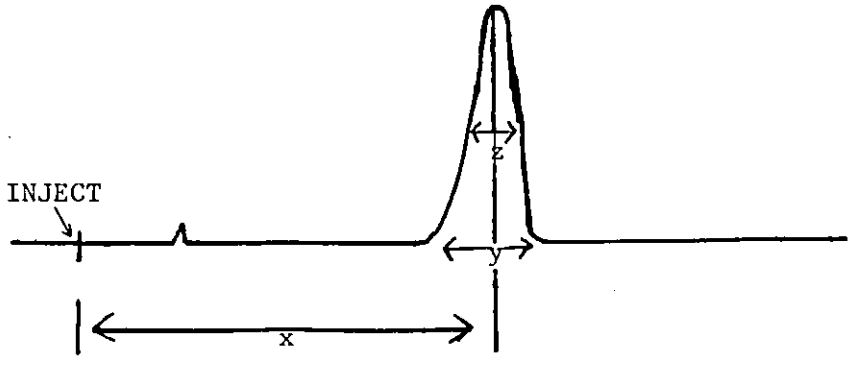

$$n = 16 \frac{x^2}{y^2} \quad \text{or} \quad n = 5.54 \frac{x^2}{z^2} \quad \ldots \quad (3.6)$$

Also expressed as Height Equivalent of a Theoretical Plate (HETP). It is defined as that length of column which will yield an effluent in equilibrium with the mean concentration over that length in the stationary phase. For high efficiency, a large number n of theoretical plates is desirable and, to avoid very long columns, the HETP must be as short as possible. Thus the lower the HETP, the more efficient the column. The efficiency can be expressed as:

$$H = HETP = \frac{\text{Length of column}}{\text{Number of plates}}$$

H is not the same for all solutes, and varies with linear flow rate as per Van Deemter equation, of the form:

$$H = A + \frac{B}{u} + Cu \qquad \ldots \quad (3.7)$$

where A, B and C are constants for a given system, and u is the velocity of the carrier gas in cm/s. The A term arises from the fact that not all solute molecules in the mobile phase travel exactly the same distance in passing through the column; this effect is enhanced by non-uniformity of particle size. A is given by the relation:

$$A = 2\lambda d_p \qquad \ldots \quad (3.8)$$

where d_p is the average diameter of the solid particles, and λ expresses the irregularity of packing. The B term, which becomes less important as the velocity u increases, has to do with the longitudinal diffusion of the solute within the mobile phase. If the diffusion coefficient is designated by Dg, then:

$$B = 2YD_g \qquad \ldots \quad (3.9)$$

where γ is the ratio of the actual velocity of solute molecules down the column to the velocity of the carrier gas u. The B/u term can be lowered by decreasing the temperature or increasing the flow rate. The last term, Cu, which predominates at higher flow rates, is contributed by transverse diffusion in the mobile phase, as from one channel to another, and by the kinetic lag in attaining equlibrium between phases. The pertinent relation is:

$$C = \frac{8}{\pi^2} \frac{K}{(1 + K)^2} \frac{d_f^2}{D_s} \quad \ldots \quad (3.10)$$

where K is the partition coefficient, and d_f is the average thickness of the film of stationary liquid phase.

A fourth term must be added if more precision is required; this involves second-order interactions between the previously mentioned factors.

The Van Deemter equation is plotted below, to show the qualitative relations between the three terms. There is an optimum flow velocity u_{opt} for the system at which H will be a minimum. In practice this is usually determined by trial and error. The optimum velocity will not be the same for different substances in a mixture, and should be selected for the component most difficult to separate.

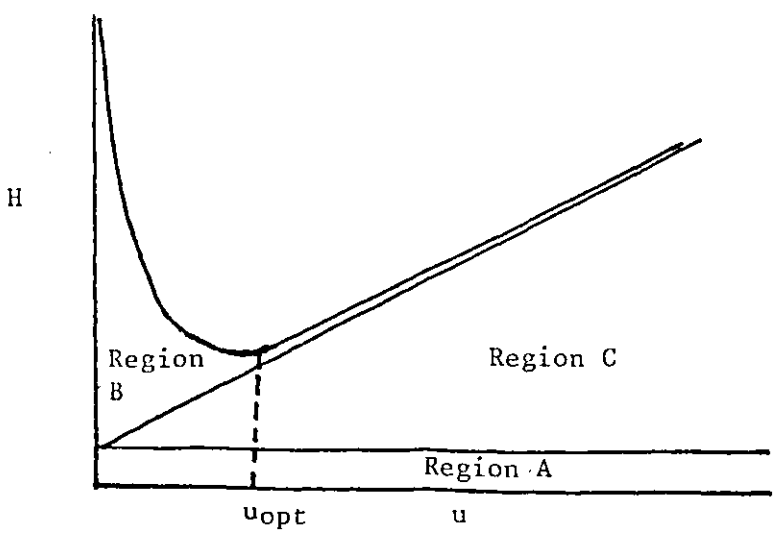

FIG. 3.4 Plot of Van Deemter Equation

The solvent efficiency (or resolution) is a function of the chosen solvent and the column temperature. The numerical value of resolution R, may be determined from the chromatogram.

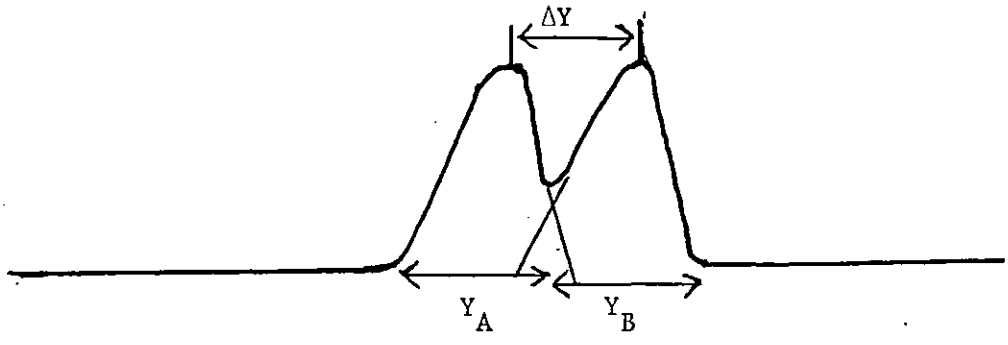

$$R = \frac{\text{separation of peak maxima}}{\text{average peak width}} = \frac{2\,\Delta Y}{Y_A + Y_B} \qquad \ldots \quad (3.11)$$

Purnell has shown that R = 1.5 is required for just complete resolution.

3.4 Choice in Stationary Phase in Gas Chromatography

It is important to remember that any separation is achieved by the solutes spending differing amounts of time dissolved in the liquid solvent phase, all components spend the same time in the gas phase. The time spent in the solvent is characteristic of the solvent/solute interactions.

The above indicates the importance of the correct choice of the partitioning solvent (stationary phase). An equilibrium is attained between the molecules of the solute in the liquid phase and the gas phase:

i.e. Partition coefficient $K = \frac{\text{g. per ml in stationary phase}}{\text{g. per ml in gas stationary phase}}$

3.4.1 Solute-Solvent Interactions

The solute molecules spend most of their time in the column in the liquid phase, constantly vapourising and dissolving. In order to escape (vapourise) from the liquid, molecules must overcome the attractive forces of surrounding molecules of solvent. If the attractive forces were the same for all substances then the order of elution would always be in order of boiling point, but ideal solutions are not formed, therefore we must apply Henry's Law, not Raoult's Law i.e. $p = \gamma x p^{o}$ where γ depends on attractive forces. As $V_R \propto p$, it also therefore depends on the attractive forces involved. There are four types of forces of interaction.

3.4.1a Dispersion (London Forces)

These arise from variations in the instantaneous (transient) dipoles of the interacting species; these are due to looseness of the electron cloud relative to the positive nucleus, these forces are always present between solute and solvent, and are the only attraction between the two non-polar substances.

3.4.1b Induction (Debye Forces)

These are the result of an interaction between a permanent dipole in one molecule (either solute or solvent) and an induced dipole in the other molecule.

3.4.1c Orientation (Keesom Forces)

These result from the interaction between two permanent dipoles; they are temperature dependent and the most important orientation force in gas liquid chromatography is hydrogen bonding.

3.4.1d Specific Interactions

These are infact chemical bonds and include loose adducts and other reversible complex formations e.g. Olefin's with $AgNO_3$ - ethylene glycol.

3.4.2 Classification Methods

Correct choice of stationary phase is fundamental, but not always easy due to lack of quantitative treatment. Basic "law of similarity" of polarity, i.e. like dissolves like applies. Keulemanns extended this qualitative approach and introduced five classes in order of decreasing cohesive forces.

1. Molecules capable of forming three dimensional networks of multiple hydrogen bonds, e.g. water, polyalcohols, hydroxy acids and dicarboxyllic acids.

2. Molecules possessing active hydrogen atoms as well as an electronegative atom with a donor pair of electrons (O, F, N) e.g. alcohols, oximes, phenols, primary amines.

3. Molecules possessing electronegative atoms but no active H e.g. ethers, ketones, aldehydes and esters.

4. Molecules possessing active H but no donor atom (weak dipole) e.g. 1) compounds with two or three halogen atoms on the same C atom as a H; ($CHCl_3$, CH_2Cl_2, CH_3CHCl_2). 2) Aromatic and Olefinic hydrocarbons.

5. Molecules possessing no functional groups, no dipoles. e.g. saturated hydrocarbons, CS_2, CCl_4, sulphides.

N.B. Both solute and solvent are classified by this method, and a solute is most strongly retained by a solvent of the same class.

3.4.3 Selection of Stationary Phases

Systematic approach - use of "Rohrschneider constants"

It must be borne in mind, selection if haphazard is wasteful. Earlier ideas developed on polarity of stationary phase (with respect to retarding aromatics); this was not sufficient as it was solute dependent.

The Rohrschneider system is based on "polarity" being dependent on solvent and the solute to be analysed, and is dependent on the use of Kovats Retention Indices recognising additivity of ΔI's consisting of two parts:

(1) Solute specific a, b, c, d, e. (2) Phase specific x, y, z, u, s.

Determine

Benzene RI on 20% Squalane = I_{Sq}

Benzene RI on 20% D.E.G.s = I_{DEGS}

(under constant conditions).

Difference is a measure of the polarity of D.E.G.S

$\Delta I = I_{polar} - I_{non\text{-}polar} = ax$ (x is column polarity).

i.e. one should be able to characterise a column by reference to a compound chromatographed on the column and on a non-polar standard column.

Rohrschneider then suggested "polarity" of column depends on solute being analysed, therefore determine ΔI with several different types of compounds. e.g. with EtOH, $\Delta I = I_{polar} - I_{non\text{-}polar} = by$

CH_3COEt $\Delta I =$ " " $= cz$

CH_3NO_2 $\Delta I =$ " " $= du$

pyridine $\Delta I =$ " " $= es$

then he defined $\Delta I = ax + by + cz + du + es$ where x is polarity when benzene is analysed = $I/_{100}$ for benzene, and where y, z, u, and s is polarity when EtOH, CH_3COEt, CH_3NO_2, pyridine is analysed = $I/_{100}$ for the respective compound. Therefore to characterise a group of stationary phases, determine I for the above five compounds on a squalane column and stationary phase under investigation under identical conditions i.e. % stationary phase and temperature. Numerical values obtained are very valuable in column selection for a particular separation. Note that the variations in values of x, y, z, u & s for column, often indicate selectivity available and the structural electronic reason for this.

Silicone QF_1 (containing tri fluoro propyl groups - electron attracting) is selective for ketones which are electron donors, compared with alcohols which are electron acceptors also. Other constants a, b, c, d and e refer to compounds being chromatographed and are equal to 100 for

C_6H_6, EtOH, CH_3COEt, CH_3NO_2 and pyridine respectively. Therefore, to determine a, b, c, d & e for other compounds X:

1. Chromatograph X on at least five columns of known x, y, z, u & s values.
2. Determine I(X) on each column.
3. Calculate $\Delta I(X) = I_{(St.phase)} - I_{(squalane)}$ gives experimental ΔI for each column.
4. Now calculate a, b, c, d & e by fitting the data to Rohrschneider equations (82) for method.

N.B. a, b, c, d & e constants for compounds regardless of column x, y, z, u & s characterise columns.

When all data is available in handbook, the prediction of separation should be possible.

McReynolds - proposed (1) for practical reasons for three of five test substances use higher homologues and (2) use ten test substances to fully characterise stationary phase.

Proposal (1) is accepted and proposal (2) is rarely used.

i.e. test substances used by McReynolds were: x (benzene), y (butanol-1), z (methyl n-propyl ketone), u (nitropropane), s (pyridine).

3.5 Quantitative Analysis

Gas chromatography has become one of the most useful separation techniques because quantitative information can so readily be obtained from it. Standardization of operating conditions is of prime importance and detector response factors must be known for each compound to be determined. The integrated area of a peak is directly proportional to the amount of solute eluted. Measurement of area is accomplished by one of the following methods, which vary considerably in precision.

Method of Measurement	Relative Precision %
Electronic Integrator	0.4
Ball and Disc Integrator	1.3
Cutting out and Weighing Peaks	1.7
Geometric Methods	3-4
Planimetry	4.0

Table 3.4 Precision of methods of peak area measurement

Electronic integrators have a digital output derived by feeding the detector signal into a voltage-to-frequency converter which produces a pulse-rate proportional to the input signal. The total number of pulses is a measure of the peak area and this can be printed out directly or stored until required. Electronic integrators have a wide linear range, a high count-rate and automatic correction for baseline drift. In addition, the more expensive versions will print retention data along side peak areas. Automatic integration methods are the most precise available.

There are three methods of calculation of quantitative results, and are discussed.

Internal Normalisation

If the components of a mixture are similar in chemical composition and if all are detected, the percentage weight of each is given by:

$$\text{Percentage X} = \frac{\text{Area for component X}}{\text{Total area for all components}} \times 100 \quad \ldots \quad (3.12)$$

The formula assumes that the detector sensitivity is the same for each component. If this is not the case, the response of each must first be determined using a set of standards. Areas are then multiplied by correction factors obtained by setting the response of one component equal to unity.

Internal Standardization

An accurately known amount of a standard is added to the sample before it is chromatographed. The ratio of peak area of standard to that of the component of the sample to be determined is calculated and converted to weight of component using a previously prepared calibration curve. The internal standard should have a retention volume close to those of the components being determined but well resolved from them. Preferably it should be present at a similar concentration level.

Standard Addition

If a pure sample of the component to be determined is available, the sample can be chromatographed before and after the addition of an accurately known amount of the pure component. Its weight in the sample is then derived from the ratio of its peak areas in the two chromatograms.

The advantages of internal standardization are that the quantities of sample injected need not be measured accurately and the detector response need not be known, as neither affect the area ratios. Standard addition is particularly useful in the analysis of complex mixtures where it may be difficult to find a suitable internal standard which can be adequately resolved from the sample components.

3.6 GC as a Member of a Team

GC can play a valuable role in combination with any other instrumental technique that can accept gaseous or volatile liquid samples and that is compatible in speed. Another difficulty is in the analysis of very complex mixtures by gas chromatography, in resolving and identifying all the components. To overcome this problem, gc can be coupled directly to either mass spectrometer or infra red spectrometer.

Coupling gc to any other instrument or another separation process (e.g. thin layer) to improve resolution is often the solution to complex problems.

3.7 Applications of GC

GC has become one of the most widespread techniques for use in industrial research. It is particularly suited to the rapid analysis of volatile mixtures containing dozens or even hundreds of components and as a result is much used by the food and petroleum industries. Only lack of volatility or thermal stability are likely to preclude its use in the solving of a particular problem. In some instances, volatile derivatives can be prepared with the necessary properties, e.g. the silyl ether derivatives of sugars or the methyl esters of fatty acids. The pyrolysis of polymeric materials leads to the production of degradation products that can be characterised by gc and much use is made of this technique in the plastics, paint and rubber industries.

CHAPTER IV

SORPTION FROM LIQUID PHASE

As has already been discussed, the nature, degree and size of cation, type of zeolite ($\frac{SiO_2}{Al_2O_3}$ ratio), and calcination temperature (H_2O content) affect the molecular sieving properties of zeolites. In this chapter, I would like to discuss the factors which contribute to the selectivity of molecules, and in particular to the separation of isomeric molecules. The number of oxygen atoms forming a zeolite aperture is an obvious indication of the molecular size capable of entering the internal structure. Selectivity can also be altered by the introduction of a larger cation to partially block windows or a more subtle effect relying on a cation resiting to restrict bulk access to part of the zeolite channels. The "effective pore size" determines all molecular sieve separations in dehydrated zeolites.

The separation of normal paraffins from isoparaffins is today a large-scale use for molecular sieves involving adsorption of components present as major stream constitutents. Molecular sieve type 5A is employed and the process is in the C_4- C_9 range to produce a normal paraffin for chemical and solvent uses plus a high octane gasoline blending stock, and with kerosene feed streams in the C_{10} - C_{18} range for high purity n-paraffins used in the manufacture of biodegradable detergents. However, due to volatilities and size of isomeric hydrocarbons being very similar, separation with molecular sieves has received a lot of attention over the last decade. For an adsorbent to be selective in a separation process, it must possess the following characteristics: adsorptive capacity for some volume of desired hydrocarbons per volume of adsorbent, reduced or no catalytic activity for undesired side reactions such as polymerization and isomerization, and selectivity of adsorption both for hydrocarbons and for the desired carbon number range of hydrocarbons.

The pore sizes of the Type 4A, 5A, 10X, 13X, and Y zeolites fall in the range of the molecular diameters of many organic compounds. This leads

directly to the use of molecular sieves to separate certain of these compounds using the molecular sieve principle. For those components of a mixture which cannot be separated by molecular size many can still be effectively separated by using a molecular sieve with pores large enough to adsorb all of these components. In this latter case; the strong selectivity of the molecular sieve for the more polar and unsaturated materials makes possible the purification of many organic materials as well as the separation of the components of many organic mixtures. The sorbed molecules can be envisaged as jumping rapidly from site to site in the cages with an occasional escape through a window into the next cage. The greater the chemical attraction between a molecule and the cations or framework species, the greater will be the residence time. The more asymmetric a molecule, the lower will be frequency of rotation. The larger a cage, the greater will be the delocalization of the molecules.

4.1 Factors Influencing Competitive Adsorption of Isomers at the Solid-Liquid Interface

In adsorption from binary mixtures preferential or "selective" adsorption occurs, but to emphasize that both components are absorbed, it is preferable to refer to competitive adsorption. There are several factors which influence the nature of this competitive adsorption. Clearly the different interaction energies between different isomer configurations and the zeolite surface are important. These are dependent upon: cation-sorbate, lattice-sorbate, steric hindrance and differences in polarizability, field-dipole and field-quadrupole interactions. It seems likely that quite small differences in adsorptive forces may be responsible for preferential adsorption which can readily be detected experimentally.

The chemical nature of the zeolite surface is of profound importance. Its force field (e.g. in Y, ion exchange of Ca^{2+} or K^{+}; the electrostatic field can be increased or decreased) is such that preferential adsorption is appreciably greater than that which occurs

at other interfaces, but the extent, and even the sign, of selectivity varies considerably. This is most clearly evident when adsorption takes place with polar or polarizable molecules. The very strong adsorptive forces due primarily to localized positive charge of the cations, electrostatically attract the negative end of polar molecules. The more polar the molecule, i.e. the greater the dipole moment, the more strongly will it be attracted by the cationic charge and the more strongly it will be adsorbed. Polar molecules are generally those which contain O, N, S or Cℓ atoms and/ or are asymmetrical. Some examples are listed below:

	μ (Debyes)
CH_3OH	1.7
C_2H_5OH	1.69
$CH_2C\ell_2$	1.60
$(CH_3)_2CO$	2.88
CH_3CN	3.92

(The dipole moments are quoted as in the gas phase)

In addition to polar molecules, polarizable molecules are strongly adsorbed. Under the influence of the localized, strong positive charge of the cations molecules have dipoles induced in them. This polarized molecule is then adsorbed strongly due to the electrostatic attraction of the cation. The more unsaturated the molecule, the more polarizable it is, and the more strongly it is adsorbed in the molecular sieve adsorbent.

In adsorption by zeolites from liquid solutions an important role is played (apart from solution concentration and temperature) by the geometrical and chemical structure of porous crystals (the presence or absence of the molecular-sieve effect with respect to solution components, the chemical composition of its skeleton, the type of exchange cation) as well as the molecular field of free solution. Even when it is impossible for the solvent to penetrate into zeolite cavities because of the molecular-sieve effect, molecules of one and the same solvent

are distributed differently between zeolite cavities and free solution, with different solvents due to the difference in the molecular field of this solution. In the absence of the molecular-sieve effect, competition of the molecules of the two components in the adsorbent field is added. With respect to molecules having links with electron density concentrated on the periphery, the cationised surface of zeolite is more specific than hydroxylated surface of silica gel.

In the Russian literature (84), molecules which have common functional or structural features leading to a specific type of adsorption behaviour in zeolites are classified into groups. Their so called "B-group molecules" include compounds having π-electron bonding structures, such as alkenes, aromatics, and naphthalenes. Molecules possessing permanent dipole groups, e.g. alcohols and amines are classified as D group. Considerable experimental evidence from infrared and electron-spin resonance studies shows that these two groups are capable of interacting specifically with zeolites. Molecules in their A group include the permanent gases and the alkanes. These latter substances do not interact with zeolites any more strongly than with other sorbents, such as activated carbon and silica gel (84). According to this classification (84), the authors found that the heats of adsorption for B-group molecules on NaX are about 8.4 to 12.6 KJ/g-mol higher, and for D-group molecules about 42 KJ/g-mol higher than for the corresponding A-group molecules of similar size and structure. In the absence of specific polar groups, the π-electrons of aromatic systems ensure that aromatic compounds are absorbed preferentially to corresponding aliphatic compounds by the zeolites. An example is benzene and cyclohexane, because the two molecules are similar in shape and size. Specific interaction with the heteropolar nature of the zeolite and the π-electrons of the benzene ring enables separation to be achieved.

An interesting comparison of "chemical" with "geometrical" or "steric" effects is shown in sorption from mixtures of benzene and n-hexane by molecular sieves. The openings of the Linde molecular sieve 5Å are

too small to admit molecules of benzene, but molecules of n-hexane are admitted; n-hexane is therefore preferentially sorbed at all concentrations. The sieves 10X and 13X, however, have wider openings which admit both molecules. Sorption is thus competitive on a normal basis. The interaction between the π-electron system of the benzene and the ionic lattice of the zeolite is so strong that the n-hexane is completely excluded over virtually the whole range of concentration (85).

Adsorption of alkanes and alkenes on cation exchanged forms of zeolites X and Y, affords an opportunity to study the σ and π-bond interactions on the zeolite surface. Interaction with the π-bond in various positions, as in isomers makes the study even further interesting when faced with a separation problem. The various interactions that have been mentioned are related to $\Delta\bar{H}_1$, the heat of adsorption, i.e., at 0K

$$\Delta H_1 = \phi_D + \phi_R + \phi_P + \phi_{F-Q}$$

The dispersion (D) and repulsion (R) energy terms are given by:

$$\phi_D = -\frac{A}{r^6}$$

$$\phi_R = \frac{B}{r^{12}}$$

where A and B are constants and r is the separation distance. But the electrostatic terms polarizability (P) and field quadrupole(F - Q) depend on the characteristics of the adsorbate and adsorbent.

Adsorption is always exothermic. This can be explained on the basis of well-known thermodynamic expression: $\Delta G = \Delta H - T\Delta S$. Since the adsorption process involves the loss of certain degrees of freedom of the adsorbed molecules as well as a decrease in entropy in going from a less to a more ordered configuration, both ΔG and ΔS are negative. It follows

then that ΔH must also be negative; and that consequently, heat is given up. Ordinarily, the heat of adsorption is greatest for the first amounts of adsorbate taken up by the surface becoming smaller as less active parts of the surface are occupied. Because of the strong surface forces characteristic of zeolites, heats of adsorption are generally higher than with other adsorbents.

4.2 Theoretical Background of Liquid Phase Adsorption

The experimental measurement in adsorption from liquid solutions is the change in concentration of the solution which results from adsorption. The fact that a change in concentration is measured emphasizes that there are at least two components in the solution. Adsorption of a single gas by a solid represents directly the quantity (weight, or volume under standard conditions) of the gas adsorbed by unit weight of the solid. Equilibrium data from gas phase is normally plotted: as isotherms(variable amount sorbed and pressure at constant temperature), as isosteres (variable pressure and temperature at constant amount sorbed), and as isobars (variable amount sorbed and temperature at constant pressure). Since the principle of sorption data from the two phases (gas and liquid) is different, the nature of the adsorption isotherm from liquid phase will be dealt with in this section. Equations relating adsorption of gases on solids by many workers (86-89) will not be discussed here.

4.2.1 The Surface Excess (n_1^e)

The surface excess is the measure of adsorption from solution. It is obtained by measurements of the isothermal change in the composition of the bulk liquid when the solid adsorbent is immersed into the liquid mixture. The significance of the adsorption isotherm is shown by deriving an equation to relate the preferential adsorption from a two-component mixture to the actual adsorption of each component. This derivation is not based on any supposed mechanism of adsorption except that each component of the liquid mixture may be adsorbed at the interface.

When a weight m of solid is brought into contact with n^o moles of liquid, the mole fraction of the liquid decreases by ΔX with respect to component 1. This change in concentration is brought about by the transfer of n_1^s moles of component 1 and n_2^s moles of component 2, onto the surface of unit weight of solid. At equilibrium, there remains in the liquid phase n_1^ℓ and n_2^ℓ moles, respectively, of the two components, giving a mole fraction, x, with respect to component 1, the initial mole fraction having been x_1^o.

Then

$$n^o = n_1^\ell + n_2^\ell + n_1^s\, m + n_2^s\, m \qquad \ldots \quad (4.1)$$

and $$X_1^o = \frac{n_1^\ell + n_1^s\, m}{n^o}, \quad x_1^\ell = \frac{n_1^\ell}{n_1^\ell + n_2^\ell} \quad \text{and } 1 - x_1^\ell = \frac{n_2^\ell}{n_1^\ell + n_2^\ell}$$

$$\therefore \quad \Delta X = (x_1^o - x_1^\ell) \qquad \ldots \quad (4.2)$$

$$\Delta X = \frac{n_2^\ell n_1^s m - n_1^\ell n_2^s m}{(n_1^\ell + n_2^\ell) n^o} \qquad \ldots \quad (4.3)$$

$$n_1^e = \frac{n^o \Delta X}{m} = n_1^s\,(1 - x_1^\ell) - n_2^s\, x_1^\ell \qquad \ldots \quad (4.4)$$

If molecular sieving action takes place (sorption of one component to the complete exclusion of another or others), then $n_2^s = 0$ and equation (4.4) reduces to:

$$n_1^e = \frac{n^o \Delta X}{m} = n_1^s\,(1 - x_1^\ell) \qquad \ldots \quad (4.5)$$

In the absence of molecular sieving action, equation (4.4) becomes:

$$n_1^e = \frac{n^o \Delta X}{m} = n_1^s - x_1^\ell (n_1^s + n_2^s) \quad \ldots \quad (4.6)$$

now $n^s = n_1^s + n_2^s$

and $n_1^s = x_1^s n^s$ ... (4.7)

where X_1^s = mole fraction of component 1 in the adsorbed layer

$$\therefore \quad n_1^e = \frac{n^o \Delta X}{m} = n^s x_1^s - x_1^\ell n^s \quad \ldots \quad (4.8)$$

$$= n^s (x_1^s - x_1^\ell) \quad \ldots \quad (4.9)$$

$$\frac{n_1^s}{n_{m1}^s} + \frac{n_2^s}{n_{m2}^s} = 1 \quad \ldots \quad (4.10)$$

where n_{m1}^s and n_{m2}^s are the numbers of moles of the individual components, respectively, required to cover the surface of unit weight of solid completely. These values can be obtained by applying the Langmuir or B.E.T. equation to the isotherms for adsorption of the individual vapours by the solid, if (a further assumption) the orientations of the molecules are the same whether adsorbed from the vapour phase or from a liquid mixture.

From equations (4.4) and (4.10) we get

$$n_1^s = \frac{x_1^\ell + \frac{n_1^e}{n_{m2}^s}}{\left(\frac{1}{n_{m1}^s} - \frac{1}{n_{m2}^s}\right) x_1^\ell + \frac{1}{n_{m2}^s}} \quad \ldots \quad (4.11)$$

now $$\beta = \frac{n_{m2}^s}{n_{m1}^s} \quad \ldots \quad (4.12)$$

This ratio in the case of zeolites (2) is the ratio of mole volumes of the solution components.

$$\text{So } n_1^s = \frac{n_{m1}^s \beta x_1^\ell + n_1^e}{1 + (\beta - 1) x_1^\ell} \quad \ldots \quad (4.13)$$

The equilibrium constant (or separation factor) relating to the adsorption of binary mixtures can be given for an ideal behaviour in both the liquid phase and the adsorbed layer by the following expression:

$$K = \frac{x_1^s x_2^\ell}{x_1^\ell x_2^s} \quad \ldots \quad (4.14)$$

where x_1^s represent the mole fraction in the adsorbed phase, component 1 refers to the preferentially adsorbed compound.

The mole fraction of a component in the adsorbed solution is given by:

$$x_1^s = \frac{K x_1^\ell}{1 + (K - 1) X_1^\ell} \quad \ldots \quad (4.15)$$

From the definitions of x_1^s, n_1^s and K it follows that:

$$n_1^e = \frac{n_{m1}^s \beta (K - 1)(1 - x_1^\ell) x_1^\ell}{1 + (\beta K - 1) x_1^\ell} \quad \ldots \quad (4.16)$$

Using the linear form of (4.16), n_{m1}^s can be calculated (in the first approximation $\beta \approx 1$ for isomers is assumed). A more detailed discussion to the application of equation (4.16) is given in (91, 92, 93).

If the mixtures are ideal solutions

$$K = \exp\left[\left(\frac{u_1^o - u_{a,1}^o}{RT}\right) - \left(\frac{u_2^o - u_{a,2}^o}{RT}\right)\right] \quad \ldots \quad (4.17)$$

where u_1^o and $u_{a,1}^o$ are the Gibb's free energy per mole of pure component 1 in the liquid and zeolite-adsorbed phases, respectively, at the temperature and pressure under consideration.

Equation (4.17) indicates that the separation factor for a given adsorbent (zeolite) and a binary system is a function of temperature and pressure only if the assumption of ideal solution in both phases is valid. The extent to which the separation factor varies with temperature can be readily obtained in terms of the heat of adsorption.

At constant pressure, differentiating equation (4.17) with respect to T gives:

$$\frac{\partial \ell n\, K}{\partial T} = \frac{1}{RT^2}\left[(H_{a,1} - H_1) - (H_{a,2} - H_2)\right] \quad \ldots \quad (4.18)$$

noting that

$$\left[\frac{\partial \left(u_{i/T}^o\right)}{\partial T}\right]_P = -\frac{H_i}{T^2} \quad \ldots \quad (4.19)$$

where H_i is the enthalpy per mole of pure i at the temperature T. The term $(H_{a,i} - H_i)$ is the change in enthalpy $\Delta H_{i,ads}$ of the pure component i from its liquid state to its zeolite - adsorbed state. It is the negative of the heat evolved when one mole of pure compound i is adsorbed by a zeolite at constant temperature and pressure.

Over small ranges it may be assumed that $\Delta H_{1,ads}$ and $\Delta H_{2,ads}$ are independent of temperature. Upon integration of equation (4.18) the

following relationship is obtained:

$$K = K_o \exp\left[- \frac{\Delta H_{1,ads} - \Delta H_{2,ads}}{RT} \right] \quad \ldots \quad (4.20)$$

This equation indicates that the separation factor K and its variation with temperature depend on the relative magnitudes of the heats of adsorption of the two compounds.

The Gibbs equation, quoted only for dilute solutions can be represented by:

$$- d\gamma = \sum_i n_i^\sigma \, du_i^\ell = RT \sum_i n_i^\sigma \, d\ell n \, a_i \quad \ldots \quad (4.21)$$

where γ is the surface tension of a solution in which the chemical potential and activity of component i are u_i and a_i respectively, and n_i^σ is the Gibb's surface adsorption. Thus for a two-component mixture:

$$- d\gamma = n_1^\sigma \, du_1^\ell + n_2^\sigma \, du_2^\ell \quad \ldots \quad (4.22)$$

whence, from the Gibbs-Duhem equation ($x_1^\ell du_1^\ell + x_2^\ell du_2^\ell = 0$),

$$n_1^e \equiv - \frac{x_2^\ell d\gamma}{RTd\ell n \, a_i} = n_1^\sigma (1 - x_1^\ell) - n_2^\sigma x_1^\ell \quad \ldots \quad (4.23)$$

By comparison with equation (4.4) we find $n_i^\sigma = n_i^s$. Calculation of thermodynamic functions for liquid phase adsorption is based on equation (4.23).

4.2.2 Thermodynamics of Adsorption from Liquid Phase Solutions

The thermodynamic treatment of adsorption from solution involves a satisfactory treatment of the solution itself as well as that of the interfacial phenomena. For adsorption from solution, this is essentially a heat transfer of one component from the bulk phase to the interface. It thus depends on the initial environment of the component being considered. For dilute solutions, this can be considered to be approximately constant for all surface coverages. When the complete concentration range for binary liquid mixtures is considered, however, the initial environment varies very considerably. Some care is therefore desirable in defining the precise significance of such terms in relation to adsorption from solution.

By reference to section (4.2.1) we can say; that in the adsorbed phase:

$$N^s = N_1^s + N_2^s \qquad \ldots \quad (4.24)$$

and in the liquid phase

$$N^\ell = N_1^\ell + N_2^\ell \qquad \ldots \quad (4.25)$$

these represent the total number of lattice points in each phase. The model is based on the assumption that the adsorbed phase be termed as a perfect adsorbed monolayer, and has been used by many workers (94-97) to calculate the surface tensions of solutions.

The total number of arrangements Ω of the system is:

$$\Omega = \Omega^s \Omega^\ell = \frac{N^s!}{N_1^s!\ N_2^s!} \quad \frac{N^\ell!}{N_1^\ell!\ N_2^\ell!} \qquad \ldots \quad (4.26)$$

where Ω^s and Ω^ℓ are the number of ways of arranging the molecules in the surface and in solution respectively.

Using Stirling's theorem, which is:

$$N! = N(N-1)(N-2)\ldots(2)(1) \qquad \ldots (4.27)$$

$$\ell n\, N! = \sum_{m=1}^{N} \ell n\, m \qquad \ldots (4.28)$$

as m becomes large, this sum can be approximated even more closely by an integral, so that:

$$\ell n\, N! \approx \int_1^N \ell n\, m\, dm = \left| m\, \ell n\, m - m \right|_1^N \qquad \ldots (4.29)$$

Since when $N \gg 1$, the lower limit is negligible,

$$\ell n\, N! \approx N\, \ell n\, N - N \qquad \ldots (4.30)$$

the configurational entropy of the system, $K\, \ell n\, \Omega$ is therefore:

$$S^{config} = R\left[n^s \ell n\, n^s - n_1^s \ell n\, n_1^s - n_2^s \ell n\, n_2^s + n^\ell \ell n\, n^\ell - n_1^\ell \ell n\, n_1^\ell - n_2^\ell \ell n\, n_2^\ell \right] \qquad \ldots (4.31)$$

where n denotes the numbers of moles. To this must be added the internal vibrational and rotational entropy (thermal entropy) of the molecules. The molar thermal entropies are denoted by $S_1^{o,s}$, $S_2^{o,s}$, $S_1^{o,\ell}$ and $S_2^{o,\ell}$ and are assumed to be independent of the composition of both surface and solution.

The thermal entropy of the system is thus:

$$S^{thermal} = n_1^s s_1^{o,s} + n_2^s s_2^{o,s} + n_1^\ell s_1^{o,\ell} + n_2^\ell s_2^{o,\ell} \quad \ldots \quad (4.32)$$

Furthermore, since the model has been assumed to be perfect and all adsorption sites to have identical properties, the energy of the system:

$$U = n_1^s u_1^s + n_2^s u_2^s + n_1^\ell u_1^\ell + n_2^\ell u_2^\ell \quad \ldots \quad (4.33)$$

where u_1^s, u_2^s and u_1^ℓ, u_2^ℓ are the molar energies of molecules of the two kinds in the adsorbed and liquid phases respectively: these again are independent of composition.

The free energy F of the whole system is

$$F = U - T\,(S^{config} + S^{thermal}) \quad \ldots \quad (4.34)$$

The equilibrium state is that for which dF/dn is zero for a process in which at constant T and V, dn moles of component 1 are transferred from the surface to the solution and are replaced by the same number of moles of component 2 transferred from the solution, i.e., the number of surface molecules (and hence the area of contact between solution and solid) remains constant. In effect, an equilibrium constant of the phase-exchange reaction is required:

$$(1)^s + (2)^\ell \rightleftarrows (1)^\ell + (2)^s \quad \ldots \quad (4.35)$$

This leads to the condition:

$$\ell n \frac{n_2^\ell}{n_1^\ell} - \ell n \frac{n_2^s}{n_1^s} = \frac{\Delta_a U_2 - \Delta_a U_1}{RT} - \frac{\Delta_a S_2^o - \Delta_a S_1^o}{R} \quad \ldots \quad (4.36)$$

(cf equation $K = \frac{kT}{h}\, e^{-\frac{1}{R}\left(\frac{\Delta H}{T} - \Delta S\right)}$).

where $\Delta_a U_i$ and $\Delta_a S_i^o$ are the changes of energy and of the thermal part of the entropy on adsorption:

$$\Delta_a U_i = U_i^s - U_i^\ell ; \quad \Delta_a S_i^o = S_i^{o,s} - S_i^{o,\ell}; \quad i = 1,2 \qquad \ldots \quad (4.37)$$

in terms of mole fractions x_1^s ($= n^s_{1/n^s}$) and x_1^ℓ ($= n^\ell_{1/n^\ell}$) ,

we have:

$$\ell n \frac{x_1^s \, x_2^\ell}{x_1^\ell \, x_2^s} = - \left[\frac{\Delta_a U_1 - \Delta_a U_2}{RT} - \frac{\Delta_a S_1^o - \Delta_a S_2^o}{R} \right] \qquad \ldots \quad (4.38)$$

K has already been defined in equation (4.14) and equation (4.38) can be written as:

$$K = \exp - \left[\frac{\Delta_a U_1 - \Delta_a U_2}{RT} - \frac{\Delta_a S_1^o - \Delta_a S_2^o}{R} \right] \qquad \ldots \quad (4.39)$$

Equation (4.14) can be regarded as the "Langmuir equation" for adsorption from solution, and its close analogy with the Langmuir adsorption isotherm for a gas/solid interface is seen by writing (4.14) as:

$$K \frac{x_1^\ell}{x_2^\ell} = \frac{x_1^s}{1-x_1^s} \qquad \ldots \quad (4.40)$$

and comparing with the Langmuir isotherm written in the form (86):

$$K_1 P = \frac{\theta}{1-\theta} \qquad \ldots \quad (4.41)$$

θ is the fraction of the surface sites occupied and

$$K_1 = \exp -\left[\frac{\Delta_a h}{RT} - \frac{\Delta_a S^o}{R}\right] \quad \ldots \quad (4.42)$$

where $\Delta_a h$ is the differential heat of adsorption and $\Delta_a S^o$ the standard differential entropy of adsorption. It is therefore possible to derive heats and entropies of adsorption from the temperature coefficient of adsorption from solution. For perfect systems, it follows clearly from equation (4.39) that the quantities:

$$\Delta_a U_1 - \Delta_a U_2$$

and $$\Delta_a S_1^o - \Delta_a S_2^o \quad \ldots \quad (4.43)$$

can be calculated from the temperature dependence of K.

The heat of immersion of the solid in the solution, for perfect systems can also be readily derived.

In the initial state, when there are n^o moles of solution, and n^a moles of solid separate from it

$$H^i = n_1^o h_1^\ell + n_2^o h_2^\ell + n^a h^a$$

$$= n^o (x_1^o h_1^\ell + x_2^o h_2^\ell) + n^a h^a \quad \ldots \quad (4.44)$$

After immersion and the attainment of adsorption equilibrium (assuming that the adsorption process does not affect the enthalpy of the solid)

$$H^f = n_1^\ell h_1^\ell + n_2^\ell h_2^\ell + n_1^s h_1^s + n_2^s h_2^s + n^a h^a$$

$$= n^\ell (x_1^\ell h_1^\ell + x_2^\ell h_2^\ell) + n^s (x_1^s h_1^s + x_2^s h_2^s) + n^a h^a \quad \ldots \quad (4.45)$$

where h^s and h^ℓ are the molar enthalpies of solid and liquid phases.

The enthalpy change is therefore:

$$\Delta H = n^o \left[(x_1^\ell - x_1^o)h_1^\ell + (x_2^\ell - x_2^o)h_2^\ell\right] + n^s \left[x_1^s h_1^s - x_1^\ell h_1^\ell + x_2^s h_2^s - x_2^\ell h_2^\ell\right] \quad \ldots (4.46)$$

which simplifies to:

$$\Delta H = x_1^s \Delta H_1^o + x_2^s \Delta H_2^o \quad \ldots (4.47)$$

where $\Delta H_1^o = n^s \Delta_a h_1$ and $\Delta H_2^o = n^s \Delta_a h_2$ are the heats of immersion of the solid in the two pure liquids. Since x_1^s and x_2^s can be calculated from equilibrium data the correctness of this general equation can then be tested by immersing the solid in solutions of varying composition, and combining the calorimetric data with the equilibrium data.

Equation (4.16) can also be written as:

$$\frac{X_1^\ell X_2^\ell}{n_1^e} = \frac{1}{n^s}\left(x_1^\ell + \frac{1}{K-1}\right) \quad \ldots (4.48)$$

rearranging and combining with equation (4.46) gives:

$$\Delta H - (x_1^\ell \Delta H_1^o + x_2^\ell \Delta H_2^o) = \frac{x_1^\ell x_2^\ell}{\left(x_1^\ell + \frac{1}{K-1}\right)}(\Delta H_1^o - \Delta H_2^o) \quad \ldots (4.49)$$

The use of this equation can be made, if K is known from equlibrium experiments, and the calorimetric measurements are made with a large excess of liquid so that $x_1^\ell \approx x_1^o$

CHAPTER V

EXPERIMENTAL

5.1 Materials

The synthetic zeolites used in this work were NaX and NaY; supplied by Laporte Industries Limited, England, with $\frac{SiO_2}{Al_2O_3}$ of 2.45 and 4.97 respectively. Their unit cell composition'swere:

NaX

$$Na_{86}\left[(AlO_2)_{86}(SiO_2)_{106}\right] \cdot xH_2O$$

NaY

$$Na_{55}\left[(AlO_2)_{55}(SiO_2)_{137}\right] \cdot yH_2O$$

1-hexene, trans-2-hexene and trans-3-hexene were obtained from Aldrich Chemical Company. Cis-2-hexene was obtained from Fluorochem Limited. Some secondary and tertiary isomers of hexene were also obtained from Aldrich Chemical Company. Heptane was obtained from B.D.H. Chemicals. The purity of these liquids was checked by gas chromatography and was > 99%. They were further dried over molecular sieve type 4A before use in adsorption experiments.

The zeolites as supplied were conditioned in 1M NaCl solution for about two days at ambient temperature, to ensure complete conversion to the Na^+ form and to remove any traces of acidity present.

Ion-exchange with Li^+, K^+, Cs^+, NH_4^+, Ca^{2+}, Ba^{2+} was performed by contacting the original zeolite with a chloride salt of the ingoing cation (Analar grade). The exchange was repeated several times with a fresh solution to achieve complete replacement. Lithium, Potassium and Caesium ion-exchanges was carried out at ambient temperature using 1M solutions. Ammonium exchange was carried out at 50-60°C using 6M NH_4Cl. Calcium and Barium exchanges were carried out at 80°C using 1M solutions.

The samples prepared were contaminated with chloride ions, which were removed by washing the zeolite with copious amounts of hot distilled

water, on a Buchner funnel until the filtrate showed no positive pH test with $AgNO_3$ solution. The samples were left to dry for about 4 hr, then transferred to an evaporating dish and allowed to dry at 120°C overnight. They were then left over saturated ammonium chloride solution for ~ 2 weeks to obtain constant moisture content. T.G.A. was used to determine the water contents in each sample. The degree of ion-exchange was determined by analysis for sodium and the ingoing cation by flame photometry and atomic absorption spectrometry. The unit cell formula weight of zeolites X and Y is given by:

$$M_W = \frac{\text{Formula weight of } Si_p\ Al_q\ O_r}{(1 - \Sigma\ \%)}$$

where $p + q = 192$, $r = 384$. Σ % is the sum of the percentages by weight of the chemical constitutents A, B, ... and H_2O.

The zeolites prepared and used for adsorption experiments had the following unit cell compositions:

NaX $\quad Na_{86}\left[(AlO_2)_{86}(SiO_2)_{106}\right] \cdot 263\ H_2O$

KX $\quad Na_{1.2}\ K_{84.8}\left[(AlO_2)_{86}(SiO_2)_{106}\right] \cdot 240\ H_2O$

CsX(49) $\quad Na_{44}Cs_{42}\left[(AlO_2)_{86}(SiO_2)_{106}\right] \cdot 212\ H_2O$

NaY $\quad Na_{55}\left[(AlO_2)_{55}(SiO_2)_{137}\right] \cdot 253\ H_2O$

KY $\quad NaK_{54}\left[(AlO_2)_{55}(SiO_2)_{137}\right] \cdot 206\ H_2O$

CsY(61) $\quad Na_{21}Cs_{34}\left[(AlO_2)_{55}(SiO_2)_{137}\right] \cdot 200\ H_2O$

It is obvious from the above compositions that the number of water molecules per unit cell decreases with increasing cation size.

5.2 Experimental Conditions of Adsorption Experiments

The ion exchanged zeolites as described in previous section were used as adsorbents. They were weighed into screw cap scintillation vials (5.5 cm x 2.5 cm) and activated in air at two calcination temperatures (T_c), (~ 1.0 g for T_c 120°C and ~ 1.1 g for T_c 350°C) for 24 hr. They were then removed from the oven(s), stoppered immediately and allowed to cool in a glove box, which had been evacuated, and filled with dry air. The vials were then reweighed to ascertain the amount of water in the zeolite; and transferred back to the glove box.

An equimolar mixture of two hexene isomers in n-heptane as solvent was prepared and added to the cooled zeolites. In all adsorption experiments, 200 mg /5 ml of solution was added; i.e. 100mg of each isomer. The capped glass vials were further sealed with teflon tape and allowed to shake in a constant temperature water bath at 25-26°C. Sorption was generally rapid and complete within a few hours. Establishment of equilibrium was assumed when no significant changes were observed after 24 hr. Microlitre size samples of the liquid phase were analysed by gas chromatography and compared with the original solution analysed in an identical manner. The separation factor or selectivity observed is defined as:

$$K_{A/B} = \frac{\text{A adsorbed on zeolite}}{\text{B adsorbed on zeolite}} \times \frac{\text{B in solution}}{\text{A in solution}}$$

If $K_{A/B}$ is > 1, then component A is selectivity adsorbed over component B. If $K_{A/B}$ is ~ 1.0, there is no preferential adsorption of one component by the adsorbent.

Complete recovery of the adsorbed isomers was obtained by washing the zeolite bed with methanol.

5.3 G.C. Model

The gas chromatograph used a 204 series manufactured by Pye Unicam. Limited, Cambridge, England. The unit was coupled with an S8 autojector, DP88 computing integrator and PM8110 mini recorder. The detector used was anF.I.D.

Samples for analysis were introduced into special g.c. vials and placed on a turntable for automatic injection. The chromatograph was usually left to run overnight by programming the integrator to activate the autojector. The action of the autojector was controlled by a computerised programme tape.

To check the linear response of the F.I.D., the original solution was diluted to various concentrations and injected into the chromatograph before, during and after analysis. This calibration was carried out for all analysis to ensure that the area under the peak was proportional to the concentration of the solute. The integrator printed out both retention time and peak area for each component.

GLC conditions used for analysis:

Stationary phase:	Squalane
Detector:	F.I.D.
Column temperature:	$50^{o}C$
Injector temperature:	$80^{o}C$
Detector temperature:	$130^{o}C$
Carrier gas:	N_2
Flow rate:	30 ml/min

5.4 Adsorption of 1-hexene: trans-2-hexene in Heptane on Partially Exchanged Na^+ by K^+ in Zeolite Y

Adsorption of the above isomeric mixture was investigated on partially ion-exchanged Na^+ by K^+ forms of zeolite Y. The conditions of the experiment and the analysis by glc were identical to that described before.

This experiment was performed to ascertain the level of exchange at which the selectivity change occurs.

5.5 Effect of Change in Solvent on Selectivity

Adsorption of 1-hexene: trans-2-hexene in methylcyclohexane as solvent was investigated on NaX, KX, NaY and KY to observe the effect of solvent on selectivity. Experimental details and analysis were identical to that described before.

5.6 Adsorption Studies on Vacuum Calcined Zeolites

This study was carried out to ascertain any differences in adsorption or selectivity as a function of the method of calcination.

The zeolite was weighed as before in scintillation vials and transferred into a long glass tube which was then connected to the standard vacuum gas line. High vacuum (~ 10^{-6} torr) was obtained by backing the rotary oil pump with a mercury diffusion pump. Water in the zeolite was pumped out under vacuum with the aid of a liquid nitrogen trap. The sample was heated from ambient temperature to 350°C at a controlled rate, and left at this temperature for ~ 24 hr.

After the calcination period, the zeolite was allowed to cool to room temperature on the gasline. The tap was closed, and the long tube disconnected and transferred to the dry glove box. The glass vial was removed, stoppered immediately and weighed. Addition of sorbates and further conditions of experiment were identical to that described before.

5.7 Adsorption of Hexene Isomers as a Function of Calcination Temperature

The two methods of calcination have shown variation in selectivity. It is important to make an attempt to describe the distribution of water molecules in sodalite and supercages as a function of calcination temperature, and to show if these analyses reflect on the values of the separation factor so obtained.

Hydrated samples of zeolites NaX and NaY (~ 1.1 g) were calcined to various temperatures at a pressure of 10^{-6} torr for ~ 24 hr. The experimental details as described in sec 5.6 were employed. 1-hexene: trans-2-hexene in heptane as solvent was used as the adsorption mixture.

5.8 Sorption Isotherms of 1-hexene, cis-2-hexene, trans-2-hexene, trans-3-hexene in Heptane on Zeolites NaX, NaY and KY

Sorption isotherms of individual isomers in heptane in the zeolites NaX, NaY and KY were investigated at 24-26°C. This information was extremely important to explain the competition, interaction and the relative extent of adsorption of each isomer with the zeolite type and the cation contained.

To about 0.8 g of activated zeolite (24 hr at ~ 400°C at a pressure of 10^{-6} torr) was added five millilitres of a binary liquid solution of known composition, and allowed to reach equilibrium overnight at 25-26°C. The composition of the bulk phase was analysed by means of g.c. as before.

5.9 Adsorption of cis-2-hexene: trans-2-hexene and cis-2-hexene: trans-3-hexene in Heptane as Solvent on Zeolites NaX, KX, NaY and KY

Adsorption of the above isomeric mixtures were investigated on vacuum calcined zeolites (~ 24 hr at 350°C, 10^{-6} torr). Experimental conditions and analysis were identical to that described before.

This study was useful to show if the type and size of cation substituted in zeolites with different $\frac{SiO_2}{Al_2O_3}$ ratio affect selectivity, in the case of more closely related isomers.

5.10 Variation of Separation Factor as a Function of Concentration of Hexene Isomers in Heptane on Zeolite NaX

This study was carried to ascertain the concentration dependence of hexene isomers on separation factor, taking zeolite NaX for example.

The zeolite was heated at 350°C at a pressure of 10^{-6} torr for ~ 24 hr 1-hexene: trans-2-hexene in heptane was used as stock solution. Concentrations starting from 0.15 to 1 ml of each isomer diluted to 5 ml with heptane were used. Experimental conditions and analysis of the bulk phase were identical to that described before.

Also investigated was the variation of separation factor as a function of various ratios of 1-hexene: trans-2-hexene in heptane as solvent.

5.11 Effect of Adsorption and Isomerization of Hexenes on Lithium Exchanged X and Y Zeolites

NaLiX (56%) and NaLiY (57%) were activated in air at ~ 350°C for 24 hr and used for adsorption or isomerization experiments, conditions being the same as before.

Firstly, experiments with 1-hexene in heptane were carried out on these zeolites, and these were compared with NaX and NaY zeolites. On

the same zeolites was added 2-methyl-1-pentene in heptane.

This study allowed to ascertain if the formation of new sites of the type:

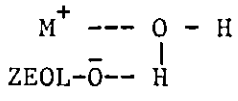

are formed. This mechanism results in the formation of a new but very weak hydroxyl group, the strength of which depends directly on the electrostatic potential of the alkali metal cation, as shown:

M^+	Ionic radius (nm)	Electrostatic potential, $e/_r$ (nm^{-1})
Li	0.06	16.7
Na	0.095	10.5
K	0.133	7.5
Rb	0.148	6.7
Cs	0.169	5.9

5.12 Experiments of Hexene Isomers on Divalent and Hydrogen Forms of X and Y Zeolites

The formation of active hydroxyl groups on these zeolites has already been discussed (Chapter II). It was essential to ascertain what kind of reactions take place on these active sites, when hexene isomers were added.

The zeolites were calcined in air at ~ 350°C for 24 hr and used as catalysts. The reaction was monitored by GC/MS.

Isomerization kinetics were carried out on HY zeolite at three temperatures (4, 15 and 32°C) to find the respective activation energies. A secondary carbonium-ion mechanism was suggested after obtaining evidence from isomerization studies of 3,3, dimethyl-1-butene.

CHAPTER VI

RESULTS AND DISCUSSION

6.1 Air Calcined Zeolites

Experimental results are tabulated for three different isomeric mixtures of hexenes adsorbed on Na, K, and Cs forms of X and Y zeolites, calcined in air at two temperatures.

The number in brackets in some zeolite sample denotes percentage degree of ion-exchange.

6.1.1 Stock Solution: 1-hexene: trans-2-hexene

Table 6.1.1 A

Zeolite	Hydrated weight (g)	Dehydrated weight (g)	Number of H_2O mols/Unit cell	$K_{\frac{1\text{-hexene}}{\text{trans-2-hexene}}}$
T_c=120±1°C				
NaX	0.9998	0.8259	91	1.4(4)
KX	1.0025	0.8718	111	1.0
CsX(49)	1.007	0.8902	78	0.4(5)
T_c=350±5°C				
NaX	1.1002	0.8173	5	2.0(2)
KX	1.0967	0.8512	4	1.6(2)
CsX(49)	1.1013	0.8932	-	1.0(9)

Table 6.1.1 B

Zeolite	Hydrated weight (g)	Dehydrated weight (g)	Number of H_2O mols/Unit cell	$K_{\frac{1\text{-hexene}}{\text{trans-2-hexene}}}$
T_c=120±1°C				
NaY	1.0031	0.8139	74	~ 1.0
KY	1.0029	0.8575	85	0.6
CsY(61)	1.0053	0.8726	64	0.3(2)
T_c=350±5°C				
NaY	1.1004	0.8214	1	0.9
KY	1.1016	0.8607	3	0.3(2)
CsY(61)	1.1050	0.9012	-	0.4(9)

6.1.2 Stock Solution: 1-hexene: cis-2-hexene

Table 6.1.2 A

Zeolite	Hydrated weight (g)	Dehydrated weight (g)	Number of H_2O mols/Unit cell	$K_{\frac{1\text{-hexene}}{\text{cis-2-hexene}}}$
T_c=120±1°C				
NaX	0.9997	0.8042	68	0.7(1)
KX	1.0005	0.8303	71	0.6(9)
CsX(49)	1.0042	0.8917	83	0.3(5)
T_c=350±5°C				
NaX	1.102	0.8237	11	1.1(1)
KX	1.0936	0.8507	6	1.6(9)
CsX(49)	1.1006	0.8935	-	1.6(1)

Table 6.1.2 B

Zeolite	Hydrated weight (g)	Dehydrated weight	Number of H_2O mols/Unit cell	$K_{\frac{1\text{-hexene}}{\text{cis-2-hexene}}}$
T_c=120±1°C				
NaY	1.0087	0.8296	87	0.7(1)
KY	1.007	0.8669	90	0.5(8)
CsY(61)	1.0007	0.8706	66	0.3(4)
T_c=350±5°C				
NaY	1.1015	0.7935	-	0.6(8)
KY	1.10	0.8591	-	0.4(8)
CsY(61)	1.1047	0.9013	-	0.5(6)

6.1.3 Stock Solution: 1-hexene: trans-3-hexene

Table 6.1.3 A

Zeolite	Hydrated weight (g)	Dehydrated weight (g)	Number of H_2O mols /Unit cell	$K_{\frac{1\text{-hexene}}{\text{trans-3-hexene}}}$
T_c=120±1°C				
NaX	0.9968	0.8534	138	0.8(6)
KX	0.9921	0.8726	128	2.0(7)
CsX(49)	1.0011	0.8967	96	0.7(1)
T_c=350±5°C				
NaX	1.1005	0.8135	-	3.3(5)
KX	1.1062	0.8535	-	1.3(2)
CsX(49)	1.101	0.8998	-	1.7

Table 6.1.3 B

Zeolite	Hydrated weight	Dehydrated weight	Number of H_2O mols/Unit cell	$K_{\frac{1\text{-hexene}}{\text{trans-3-hexene}}}$
T_c=120±1°C				
NaY	1.0045	0.8308	105	1.2(1)
KY	1.0	0.8658	89	0.4(7)
CsY(61)	0.9993	0.8976	100	0.3(5)
T_c=350±5°C				
NaY	1.1052	0.812	-	1.2(4)
KY	1.10	0.8624	-	0.1(5)
CsY(61)	1.0965	0.8863	-	0.5(1)

The results show that by increasing the size of the cation in zeolites X and Y, and treating them under the conditions mentioned, selectivity for each isomer can be effected. The factors responsible for selectivity have been mentioned (Chapter IV) and will be discussed later. The variation in selectivity suggests that there is competition of the respective isomers for the sorption sites, and the isomer that interacts more strongly with the zeolite lattice is adsorbed to a greater extent. This variation is particularly noticeable in the case of zeolite Y, i.e. with increasing cation size, selectivity for the more symmetrical isomer was indicated. With zeolite X, increasing cation size, and partial dehydration show interesting features compared to complete dehydration. The presence of water in zeolite does reveal interesting features.

A useful experiment from these results is to observe the decrease in separation factor of 1-hexene: trans-2-hexene on partially exchanged Na^+ by K^+ in zeolite Y.

6.1.4 Adsorption of 1-hexene: trans-2-hexene on partially exchanged Na^+ by K^+ in Zeolite Y.

Table 6.1.4

Zeolite	Hydrated weight (g)	Dehydrated weight (g)	Number of H_2O mols./Unit cell	$\frac{K_{1\text{-hexene}}}{\text{trans-2-hexene}}$
T_c=120±1°C				
KY(11)	1.0022	0.8117	75	0.8(3)
KY(42)	1.0146	0.8615	109	0.6(8)
KY(54)	1.0012	0.8548	109	0.5(8)
KY(88)	1.0022	0.8692	97	0.5(6)
T_c=350±5°				
KY(11)	1.10	0.8208	-	0.6(6)
KY(42)	1.1014	0.8335	7	0.3(7)
KY(54)	1.1087	0.8495	10	0.2(7)
KY(88)	1.0969	0.8730	20	0.2(6)

A plot of separation factor against degree of ion exchange (Fig. 6.1) indicates preference for trans-2-hexene as the K^+ ion exchanges with Na^+ in site II.

FIG. 6.1 Variation of separation factor against degree of ion-exchange

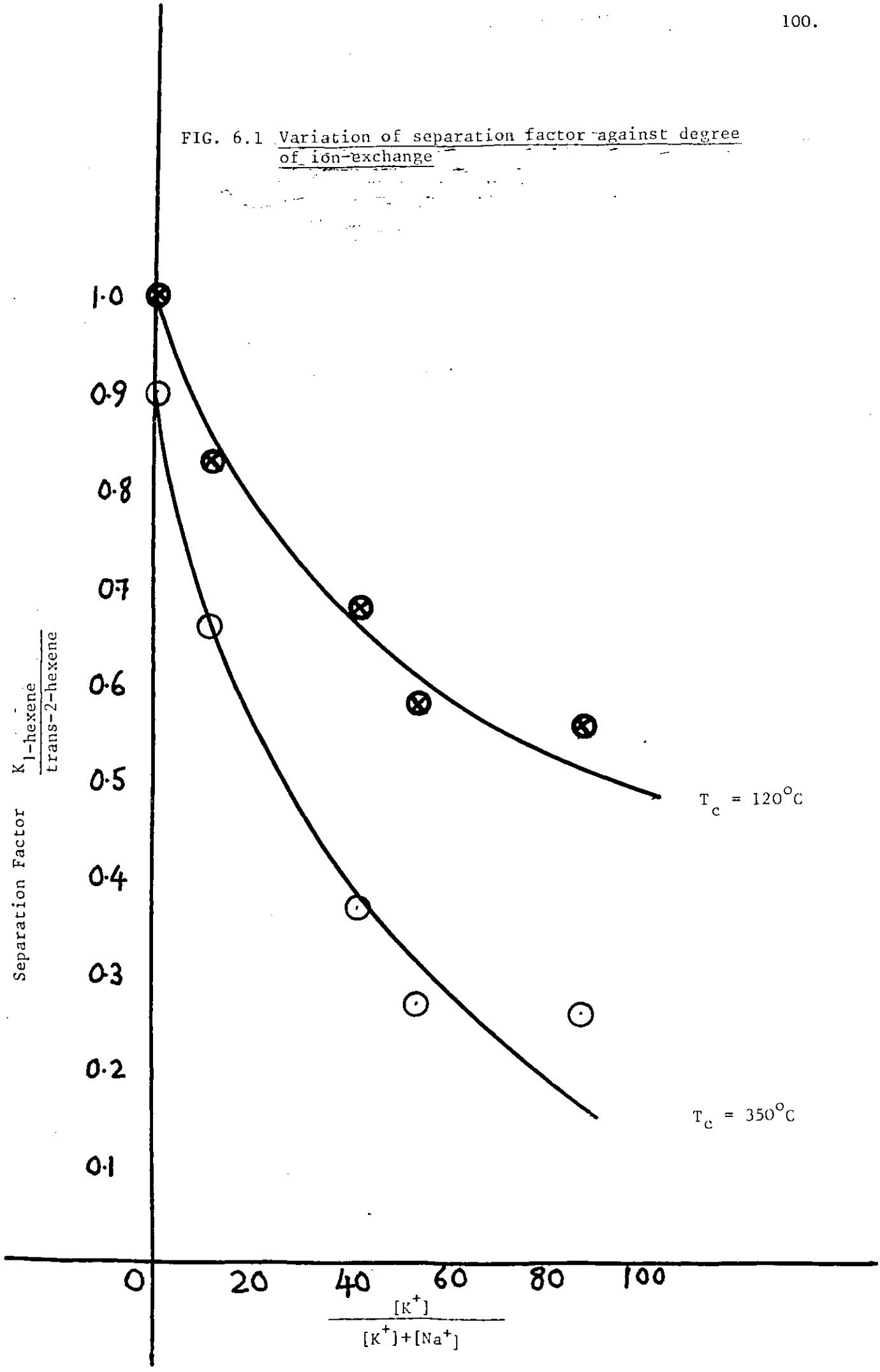

6.1.5 Effect of Change in Solvent on Selectivity

Table 6.1.5 A solvent-methylcyclohexane

Zeolite	Hydrated weight (g)	Dehydrated weight (g)	Number of H_2O mols/Unit cell	$\frac{K_{1\text{-hexene}}}{K_{\text{trans-2-hexene}}}$
$T_c = 120 \pm 1^{\circ}C$				
NaX	1.009	0.8626	128	~ 1.0
KX	1.0078	0.8854	124	~ 1.0
$T_c = 350^{\circ} \pm 5^{\circ}C$				
NaX	1.0975	0.826	3	0.9(1)
KX	1.0992	0.8432	-	0.4(4)

Table 6.1.5 B

Zeolite	Hydrated weight (g)	Dehydrated weight (g)	Number of H_2O mols/Unit cell	$K_{\frac{1\text{-hexene}}{\text{trans-2-hexene}}}$
T_c=120±1°C				
NaY	1.0046	0.8361	97	1.5(9)
KY	1.007	0.8672	95	0.9(4)
T_c=350±5°C				
NaY	1.0953	0.806	-	2.5(6)
KY	1.0959	0.8439	-	1.3(8)

This experiment has shown that a change in shape of solvent compared to n-heptane, both of which should be able to penetrate into the supercages alters selectivity in each case. By comparison to tables 6.1.1 A and 6.1.1 B the following can be deduced:

1) KX showed selectivity for trans-2-hexene at high T_c.

and 2) K^+ in zeolite Y showed a drop in separation factor but selectivity for trans-2-hexene was better when heptane was used as solvent.

This tends to suggest that the solvents compete for the sorption sites, which in turn influences the interaction between the adsorbates and the adsorbent. Steric considerations and physicochemical interactions may be important factors, e.g. the cyclic molecule (methylcyclohexane) interacts with the zeolite much more strongly than the linear molecule (heptane).

6.2 Vacuum Calcined Zeolites

Adsorption of same isomeric mixtures in heptane as solvent was carried out.

In all experiments, final $T_c = 350 \pm 5^{\circ}C$.

6.2.1 Stock solution: 1-hexene: trans-2-hexene

Table 6.2.1

Zeolite	Hydrated weight (g)	Dehydrated weight (g)	Number of H_2O mols/Unit cell	$K_{\frac{1\text{-hexene}}{\text{trans-2-hexene}}}$
NaX	1.0983	0.8173	7	2.4(3)
KX	1.1066	0.861	6	2.1(9)
CsX(49)	1.0987	0.9122	7	1.1(1)
NaY	1.1008	0.815	5	0.9(1)
KY	1.1046	0.8688	1	0.3(7)
CsY(61)	1.1048	0.9128	11	0.6(3)

6.2.2 Stock solution: 1-hexene: cis-2-hexene

Table 6.2.2

Zeolite	Hydrated weight (g)	Dehydrated weight (g)	Number of H_2O mols/Unit cell	$K_{\frac{1\text{-hexene}}{\text{cis-2-hexene}}}$
NaX	1.1044	0.8274	14	1.10
KX	1.0977	0.8551	-	2.0(6)
CsX(49)	1.0956	0.9038	-	1.4(3)
NaY	1.0968	0.8149	9	0.7(9)
KY	1.103	0.8681	2	0.7
CsY(61)	1.102	0.9108	12	0.5(7)

6.2.3 Stock solution: 1-hexene: trans-3-hexene

Table 6.2.3

Zeolite	Hydrated weight (g)	Dehydrated weight (g)	Number of H_2O mols/Unit cell	$\frac{K_{1\text{-hexene}}}{\text{trans-3-hexene}}$
NaX	1.104	0.8192	4	3.5(3)
KX	1.1022	0.8547	3	1.7(2)
CsX(49)	1.102	0.9061	-	1.3(2)
NaY	1.1027	0.8193	8	1.5
KY	1.1022	0.8683	3	0.1(8)
CsY(61)	1.1028	0.9106	10	0.5(9)

Results from these experiments indicate considerable differences in separation factors compared to those obtained from air calcined zeolites. Although the values for K are not identical, preference for each isomer is same from the two methods of calcination. This suggests that the random distribution of water molecules in sodalite and supercages during the calcination period is different for each type of zeolite and these analyses in turn reflect on the values of K obtained from the two methods of calcination.

A further experiment was carried out to ascertain the effect of partial dehydration on adsorption of hexene isomers.

6.3 Adsorption of hexene isomers as a function of calcination temperature

Results for NaX, which contained 263 H_2O molecules per unit cell at saturation.

Table 6.3.1

Hydrated weight of NaX (g)	Dehydrated weight of NaX (g)	T_c ±5(°C)	Number of H_2O mols/Unit cell (N_w)	mg of sorbates adsorbed/g of dehydrated NaX	$\frac{K_{1\text{-hexene}}}{K_{\text{trans-2-hexene}}}$
1.0983	0.8173	350	7	112.2(8)	2.4(3)
1.1004	0.8199	260	8	106.9	2.4(9)
1.0948	0.8228	145	17	101.4	2.3(7)
1.101	0.8316	110	22	92.3	2.3(1)
1.1068	0.8492	100	37	66.0	2.2(3)
1.0978	0.8549	80	51	53.7(4)	2.0(7)
1.1019	0.9011	25	97	38.5(7)	1.7

Results for NaY, which contained 253 H_2O molecules per unit cell at saturation.

Table 6.3.2

Hydrated weight of NaY (g)	Dehydrated weight of NaY (g)	T_c ±5(°C)	Number of H_2O moles/Unit cell (N_w)	mg of sorbates adsorbed/g of dehydrated NaY	$\frac{K_{1\text{-hexene}}}{K_{\text{trans-2-hexene}}}$
1.1008	0.815	350	5	94.1(7)	0.9(1)
1.0981	0.822	300	16	90.5(7)	0.9(8)
1.0969	0.8333	190	29	86	0.9(5)
1.1031	0.8438	130	36	79.2(3)	0.9(4)
1.1007	0.8535	100	48	66.7(9)	0.9(3)
1.1064	0.8638	70	55	65.9(1)	0.9(1)
1.1014	0.8746	25	70	48.7(7)	1.0(4)

From these two sets of experimental data, the following graphs were plotted for each zeolite:

Figs 6.2 and 6.3, showing the variation of adsorption of hexene isomers, and separation factor verses the number of water molecules per unit cell (N_w) on NaX and Figs 6.4 and 6.5 showing the same on NaY.

The graphs indicate different behaviour of adsorption of hexene isomers, i.e., exponential in the case of zeolite NaX, and linear in the case of zeolite NaY, as a function of number of water molecules per unit cell left. They also indicate decrease in separation factor as the number of water molecules per unit cell left increases.

There are three or possibly four types of water molecules present in zeolites X and Y. They are (1) loose water, (2) water in supercages and sodalite cages, (3) water associated with the cations and (4) dehydroxylation. Each of these types of water is removed as a function of T_c.

The results suggest that during the calcination period, continuous redistribution and removal of water molecules from supercages and sodalite cages of these isomorphic X and Y zeolites affect the uptake of hexene isomers with different relationships, but the separation factor linearly.

For zeolite NaX, the uptake of sorbates (mg/g of dehydrated zeolite) can be estimated, when the zeolite is totally dehydrated (i.e. $N_w = 0$) using the kinetic relationship below:

As adsorption (A) is dependent on N_w then:

$$-\frac{dA}{dN_w} = K A \qquad \ldots \quad (6.1)$$

where K is a constant. On integration of equation (6.1) we get:

$$\ell n\ A = -K N_w + C \qquad \ldots \quad (6.2)$$

where C is the integration constant.

When $N_w = 0$, then:

$$\ell n\ A_o = C \qquad \ldots \quad (6.3)$$

FIG 6.2 – Graph showing variation of adsorption of hexene isomers verses number of H_2O molecules per unit cell left on NaX.

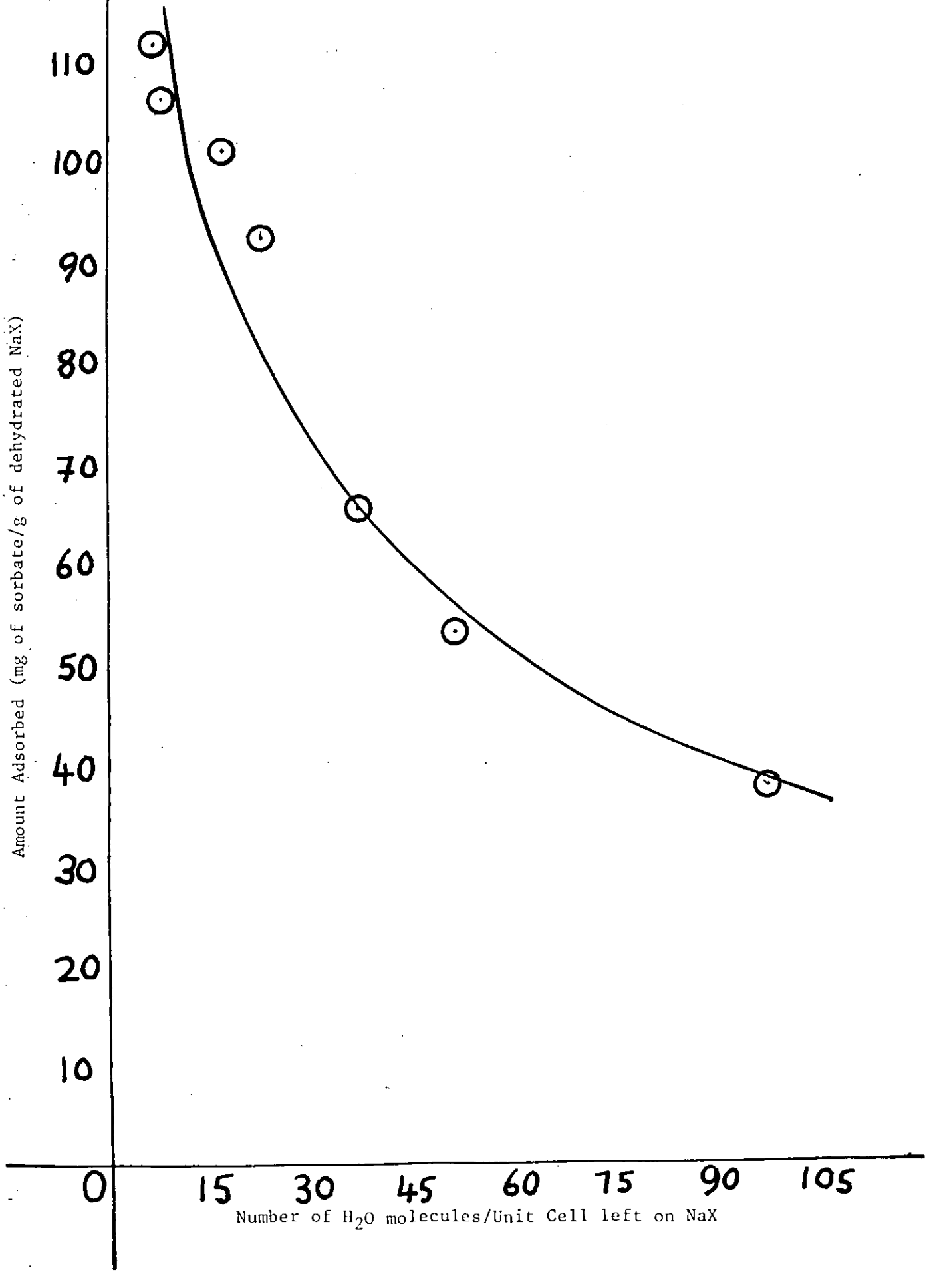

FIG 6.3 - Graph showing variation of separation factor verses number of H_2O molecules per unit cell left on NaX.

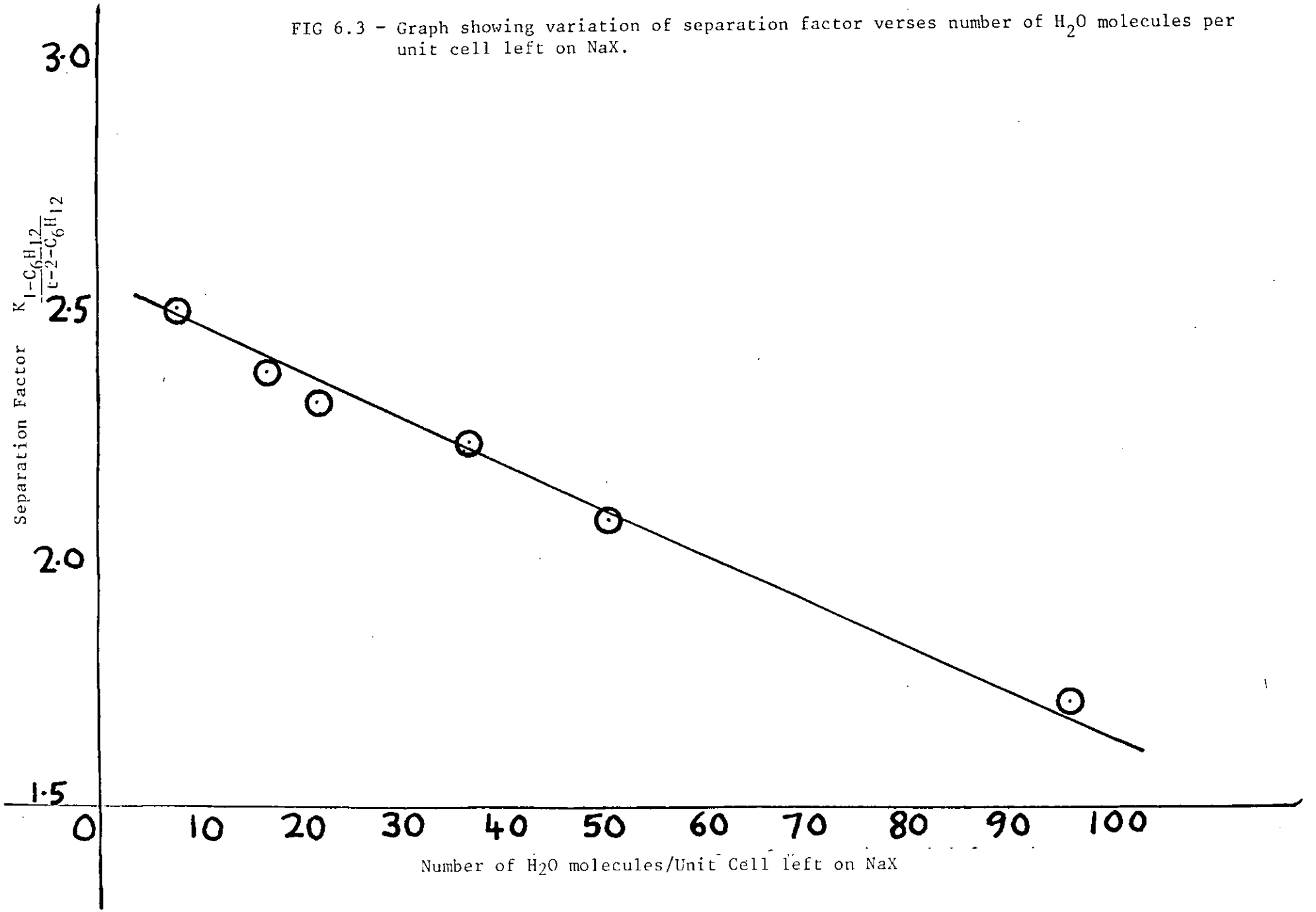

FIG 6.4 - Graph showing variation of adsorption of hexene isomers verses number of H_2O molecules per unit cell left on NaY.

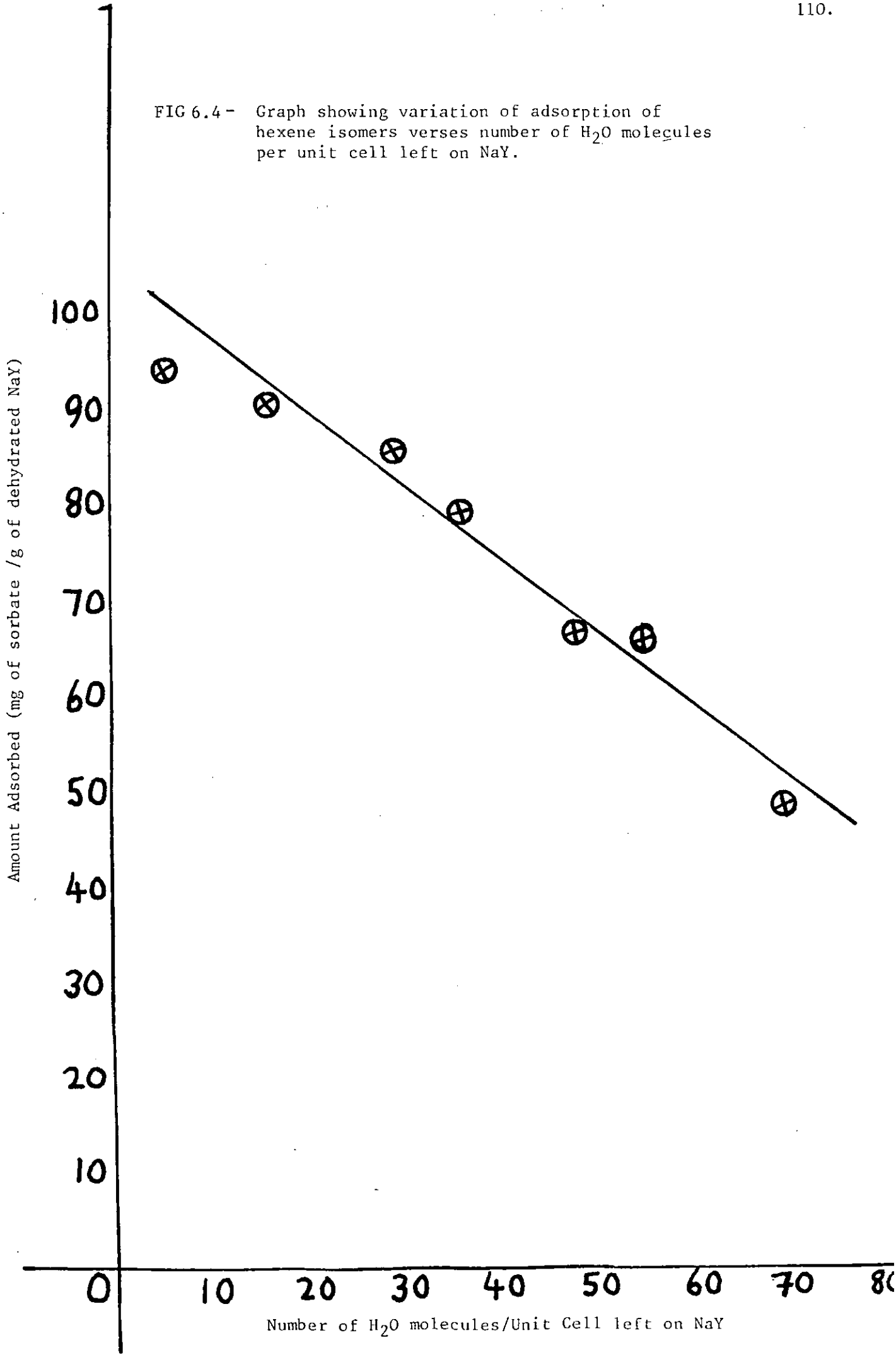

FIG 6.5 - Graph showing variation of separation factor verses number of H_2O molecules per unit cell left on NaY.

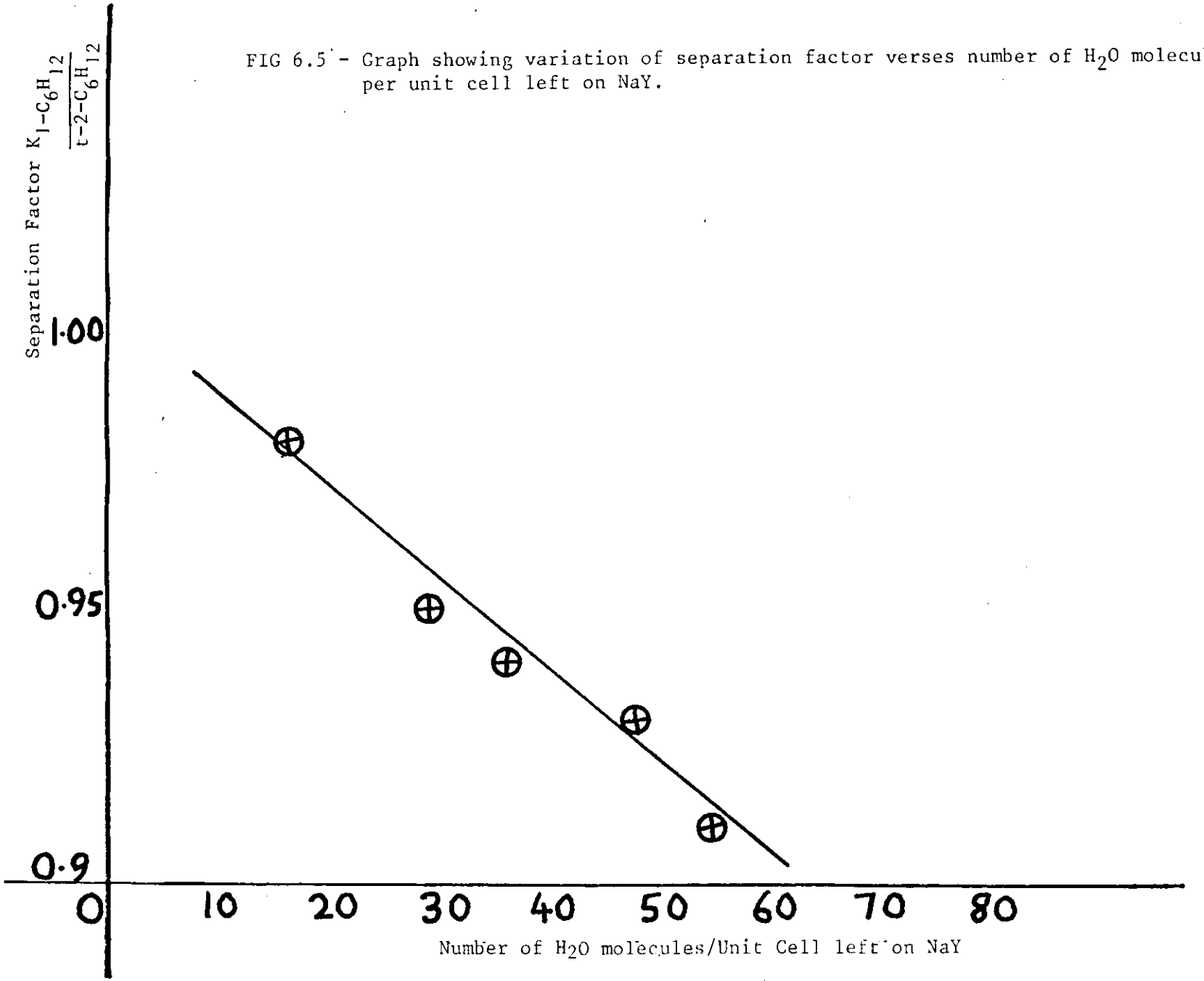

where A_o represents the uptake when the zeolite is fully dehydrated

$$\therefore \quad \ln A = - K N_w + \ln A_o \qquad \ldots \quad (6.4)$$

$$\text{or} \qquad A = A_o e^{- K N_w} \qquad \ldots \quad (6.5)$$

So a graph of ln A verses N_w should result in a straight line with slope - K, and intercept ln A_o, and hence A_o can be deduced. From Fig. 6.6, it was found that A_o for zeolite X was 134.3 mg/g, indicating that there is competitive adsorption between the two isomers for adsorption sites. From Fig. 6.4, by extrapolation (when $N_w = 0$), the value of uptake of isomers on zeolite Y was 105 mg/g. However, quantitative adsorption for each isomer needs to be established.

FIG 6.6 - Graph of ln A verses number of H_2O molecules per unit cell left on NaX.

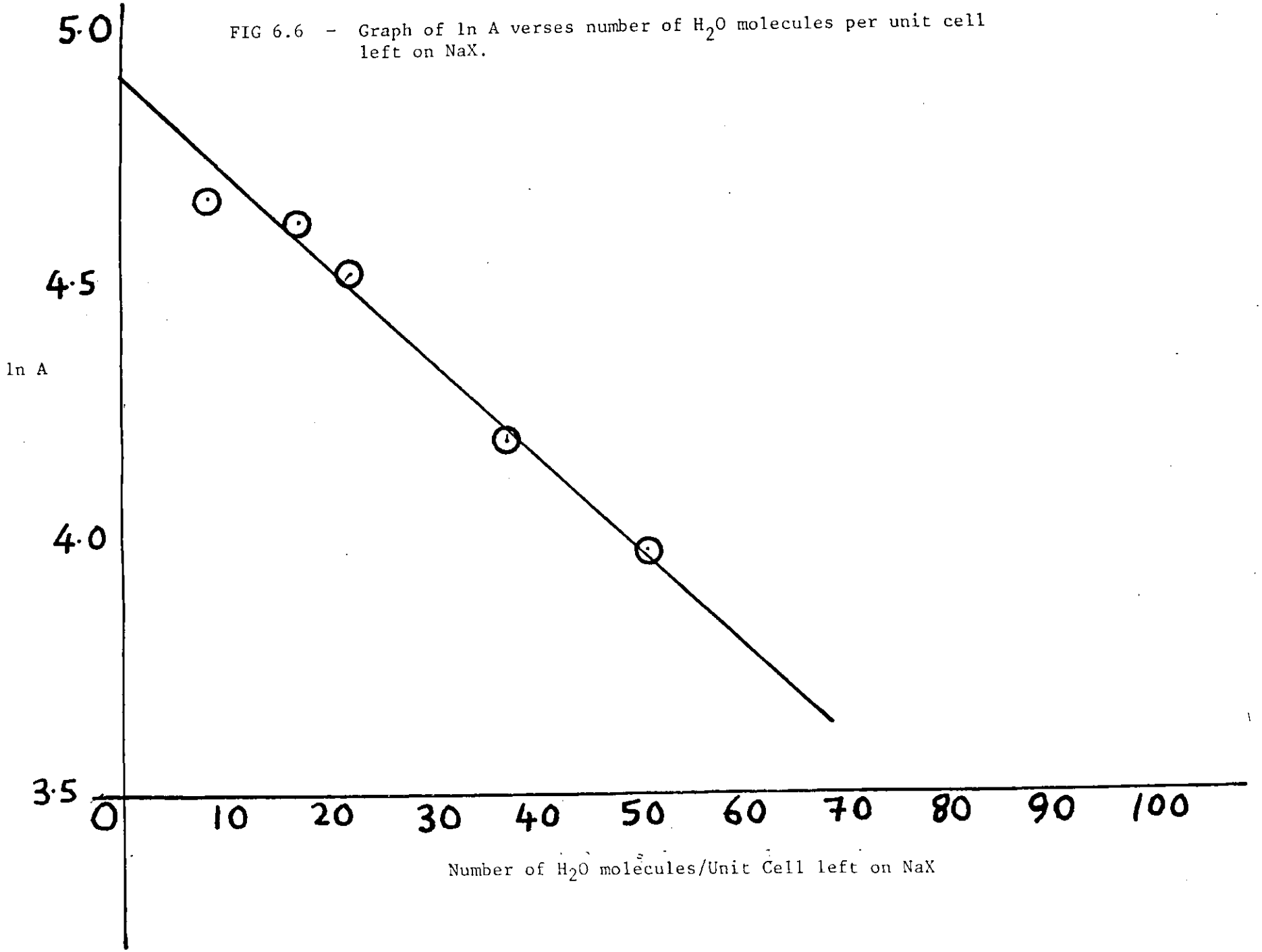

6.4 Sorption Isotherms

The densities of the hexene isomers that were used were as follows:

Isomer	Density (g/ml)
1-Hexene	0.673
cis-2-Hexene	0.687
trans-2-Hexene	0.669
trans-3-Hexene	0.677

density of n-heptane = 0.683 g/ml

The binary mixtures that were prepared and added to each of the zeolites under investigation had the following compositions:

A) 1-Hexene/Heptane

Total number of moles of mixture added $n^o \times 10^{-3}$	Mole fraction of 1-hexene added X_o
34.442	0.058
34.735	0.115
35.027	0.1713
35.32	0.2265
36.49	0.4384
37.66	0.6372
38.83	0.8241

B) cis-2-Hexene/Heptane

Total number of moles of mixture added $n^o \times 10^{-3}$	Mole fraction of cis-2-hexene added X_o
34.4871	0.059
34.824	0.117
35.1614	0.174
35.4985	0.23
36.8471	0.444
38.1957	0.642
39.5442	0.8272

C) trans-2-Hexene/Heptane

Total number of moles of mixture added $n^o \times 10^{-3}$	Mole fraction of trans-2-hexene added X_o
34.4335	0.0578
34.7171	0.1147
35.0	0.17
35.2842	0.2257
36.4185	0.4373
37.5528	0.636
38.6871	0.8234

D) trans-3-Hexene/Heptane

Total number of moles of mixture added $n^o \times 10^{-3}$	Mole fraction of trans-3-hexene added X_o
34.4573	0.0584
34.7647	0.1159
35.0721	0.1723
35.3795	0.2278
36.609	0.44
37.8385	0.639
39.068	0.825

6.4.1) Zeolite NaX

Table 6.4.1 A 1-hexene/heptane system

Hydrated weight of NaX (g)	Dehydrated weight of NaX (g)	Number of H_2O mols/Unit Cell	Mole fraction of 1-hexene after eqm. x_1	n_1^e (mmol/g)
1.1047	0.8186	3	0.026	1.38
1.1023	0.8206	8	0.083	1.47
1.1033	0.8183	4	0.14	1.59
1.104	0.8265	13	0.20	1.41
1.105	0.8219	6	0.4226	1.21
1.1013	0.8268	16	0.631	0.765
1.0993	0.820	9	0.8226	0.396

Table 6.4.1 B cis-2-hexene/heptane system

Hydrated weight of NaX (g)	Dehydrated weight of NaX (g)	Number of H_2O mols/Unit Cell	Mole fraction of cis-2-hexene after eqm. x_1	n_1^e (mmol/g)
1.1048	0.8258	12	0.0266	1.39
1.0951	0.8177	10	0.071	2.108
1.1051	0.8263	12	0.131	2.105
1.1014	0.8243	13	0.191	2.07
1.1085	0.8286	11	0.424	1.54
1.10	0.8234	13	0.635	0.89
1.0994	0.8245	15	0.825	0.388

Table 6.4.1 C trans-2-hexene/heptane system

Hydrated weight of NaX (g)	Dehydrated weight of NaX (g)	Number of H_2O mols/Unit Cell	Mole fraction of trans-2-hexene after eqm. x_1	n_1^e (mmol/g)
1.0969	0.817	8	0.035	1.0
1.1034	0.8275	15	0.078	1.67
1.1012	0.8231	11	0.134	1.77
1.1063	0.8314	17	0.1978	1.47
1.0988	0.8183	8	0.421	1.25
1.1046	0.8244	10	0.629	0.86
1.1049	0.8283	14	0.822	0.367

Table 6.4.1 D trans-3-hexene/heptane system

Hydrated weight of NaX (g)	Dehydrated weight of NaX (g)	Number of H_2O mols/Unit Cell	Mole fraction of trans-3-hexene after eqm. x_1	n_1^e (mmol/g)
1.097	0.8215	13	0.038	0.89
1.0961	0.8147	6	0.09	1.21
1.1028	0.8211	7	0.147	1.267
1.098	0.8232	14	0.2	1.49
1.1017	0.822	9	0.425	1.16
1.102	0.8265	15	0.633	0.748
1.1026	0.8261	14	0.8238	0.32

6.4.2) Zeolite NaY

Table 6.4.2 A 1-hexene/heptane system

Hydrated weight of NaY (g)	Dehydrated weight of NaY (g)	Number of H_2O mols/Unit Cell	Mole fraction of 1-hexene after eqm. x_1	n_1^e (mmol/g)
1.1021	0.8196	9	0.0338	1.05
1.0923	0.8098	7	0.083	1.497
1.0945	0.8125	8	0.1373	1.709
1.0993	0.8187	11	0.1924	1.83
1.0994	0.816	8	0.4173	1.65
1.1007	0.8173	8	0.6295	1.0
1.1008	0.8173	8	0.8223	0.54

Table 6.4.2 B cis-2-hexene/heptane system

Hydrated weight of NaY (g)	Dehydrated weight of NaY (g)	Number of H_2O mols/Unit Cell	Mole fraction of cis-2-hexene after eqm. x_1	n_1^e (mmol/g)
1.1048	0.8189	6	0.034	1.09
1.0964	0.8117	5	0.0836	1.56
1.1022	0.8158	5	0.1378	1.80
1.0993	0.814	5	0.19	2.14
1.1072	0.8212	7	0.42	1.84
1.1051	0.8229	11	0.6339	1.01
1.1028	0.818	7	0.8258	0.382

Table 6.4.2 C trans-2-hexene/heptane system

Hydrated weight of NaY (g)	Dehydrated weight of NaY (g)	Number of H_2O mols/Unit Cell	Mole fraction of trans-2-hexene after eqm. x_1	n_1^e(mmol/g)
1.0982	0.8129	5	0.0374	0.897
1.1028	0.8207	10	0.0885	1.216
1.0974	0.8181	12	0.14168	1.44
1.1023	0.8213	11	0.193	1.74
1.104	0.8219	10	0.4192	1.378
1.1055	0.8137	-	0.6288	0.895
1.1008	0.8137	4	0.8222	0.32

Table 6.4.2 D trans-3-hexene/heptane system

Hydrated weight of NaY (g)	Dehydrated weight of NaY (g)	Number of H_2O mols/Unit Cell	Mole fraction of trans-3-hexene after eqm. x_1	n_1^e (mmol/g)
1.0982	0.8215	15	0.0397	0.816
1.0976	0.8183	12	0.09688	0.894
1.103	0.8208	10	0.15	1.12
1.0991	0.8204	13	0.2	1.49
1.108	0.8179	3	0.425	1.167
1.0923	0.8053	1	0.6324	0.84
1.1011	0.8148	5	0.824	0.272

6.4.3 Zeolite KY

Table 6.4.3 A 1-hexene/heptane system

Hydrated weight of KY (g)	Dehydrated weight of KY (g)	Number of H_2O mols/Unit Cell	Mole fraction of 1-hexene after eqm. x_1	n_1^e (mmol/g)
1.0981	0.8677	6	0.0525	0.23
1.103	0.8644	-	0.1055	0.426
1.0933	0.8574	-	0.158	0.655
1.1041	0.8678	1	0.2093	0.896
1.1008	0.8607	-	0.43	0.654
1.0955	0.8611	1	0.634	0.43
1.0988	0.8637	1	0.823	0.33

Table 6.4.3 B cis-2-hexene/heptane system

Hydrated weight of KY (g)	Dehydrated weight of KY (g)	Number of H_2O mols/Unit Cell	Mole fraction of cis-2-hexene after eqm. x_1	n_1^e (mmol/g)
1.0966	0.8597	-	0.054	0.212
1.1001	0.8634	-	0.1017	0.685
1.1036	0.8675	1	0.16	0.673
1.1015	0.8652	-	0.208	1.134
1.1053	0.8698	2	0.43	1.03
1.0925	0.8587	1	0.635	0.84
1.1055	0.8676	-	0.8256	0.40

Table 6.4.3 C trans-2-hexene/heptane system

Hydrated weight of KY (g)	Dehydrated weight of KY (g)	Number of H_2O mols/Unit Cell	Mole fraction of trans-2-hexene after eqm. x_1	n_1^e (mmol/g)
1.1002	0.8653	1	0.0458	0.5
1.1033	0.8626	-	0.0928	0.97
1.0962	0.8604	-	0.15	0.98
1.1056	0.8655	-	0.195	1.55
1.0953	0.8536	-	0.4182	1.4
1.0965	0.8593	-	0.6276	0.98
1.0984	0.8613	-	0.8214	0.5

Table 6.4.3 D trans-3-hexene/heptane system

Hydrated weight of KY (g)	Dehydrated weight of KY (g)	Number of H_2O mols/Unit Cell	Mole fraction of trans-3-hexene after eqm. x_1	n_1^e (mmol/g)
1.0997	0.8621	-	0.0355	0.949
1.0994	0.8635	-	0.08859	1.2
1.1088	0.873	2	0.145	1.28
1.0985	0.8628	-	0.1964	1.6
1.1005	0.8629	-	0.4211	1.385
1.0974	0.8575	-	0.6237	1.02
1.0973	0.8587	-	0.823	0.53

plots of n_1^e versus x_1 for the hexene isomers adsorbed on NaX, NaY and KY are shown in Figs 6.7 to 6.9 respectively.

The sorption isotherms follow type II of the Schay-Nagy isotherm classification (90), and their shape is similar to that of n-octane/1-octene reported by Eltekov and Kiselev (2). The olefins are adsorbed preferentially in the large cavities of zeolites X and Y because of their greater specific interaction energy. From equation (4.16), limiting adsorption values (n_{m1}^s) and maximum of excess isotherms $(X_1)_{max}$ were evaluated and tabulated for each zeolite. The values (V^s) for sorption capacities were calculated with the assumption that the density of the adsorbed phase is the same as that of the liquid bulk-phase olefin. From the density of dehydrated zeolites (i.e. for NaX = 1.43 g/ml, NaY = 1.41 g/ml and KY = 1.51 g/ml) the total void fraction (V_f) in the crystal was calculated.

Table 6.4.4 Data for the olefin/heptane NaX system

Olefin	Limiting adsorption values n_{m1}^s (mmol/g) ± 0.1	Number of molecules of olefin adsorbed/ supercage	Maximum excess isotherms $(X_1)_{max}$	Sorption capacity V^s(ml/g) ± 0.01	Total void fraction V_f(ml/ml) ± 0.01
1-hexene	2.0	3.3	0.15	0.25	0.36
cis-2-hexene	2.45	4.1	0.15	0.30	0.43
trans-2-hexene	1.97	3.3	0.15	0.24	0.34
trans-3-hexene	1.9	3.2	0.18	0.23	0.32

FIG. 6.7 Sorption isotherms of hexenes adsorbed on dehydrated NaX at 26°C.

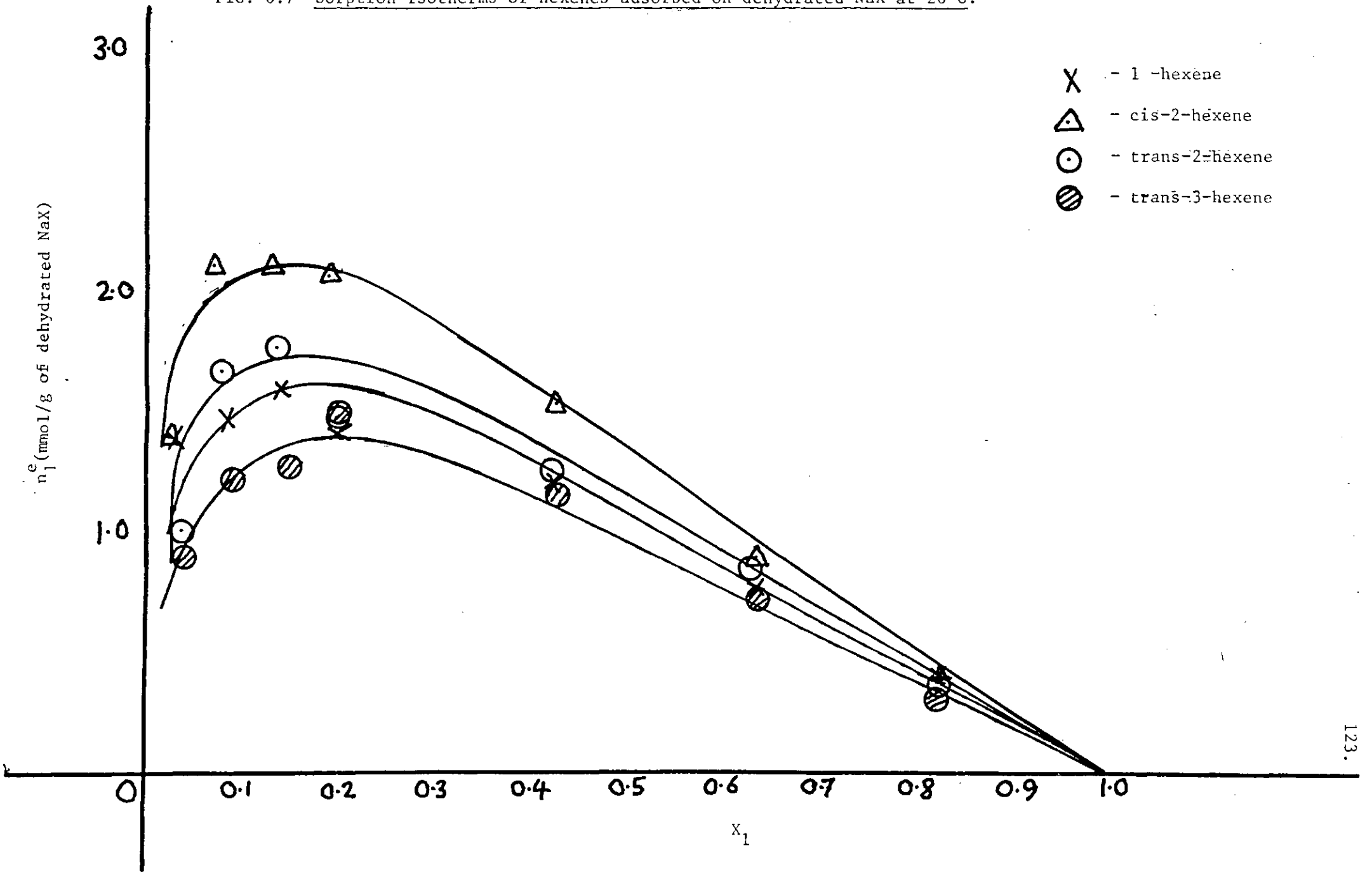

FIG. 6.8 Sorption isotherms of hexenes adsorbed on dehydrated NaY at 26°C.

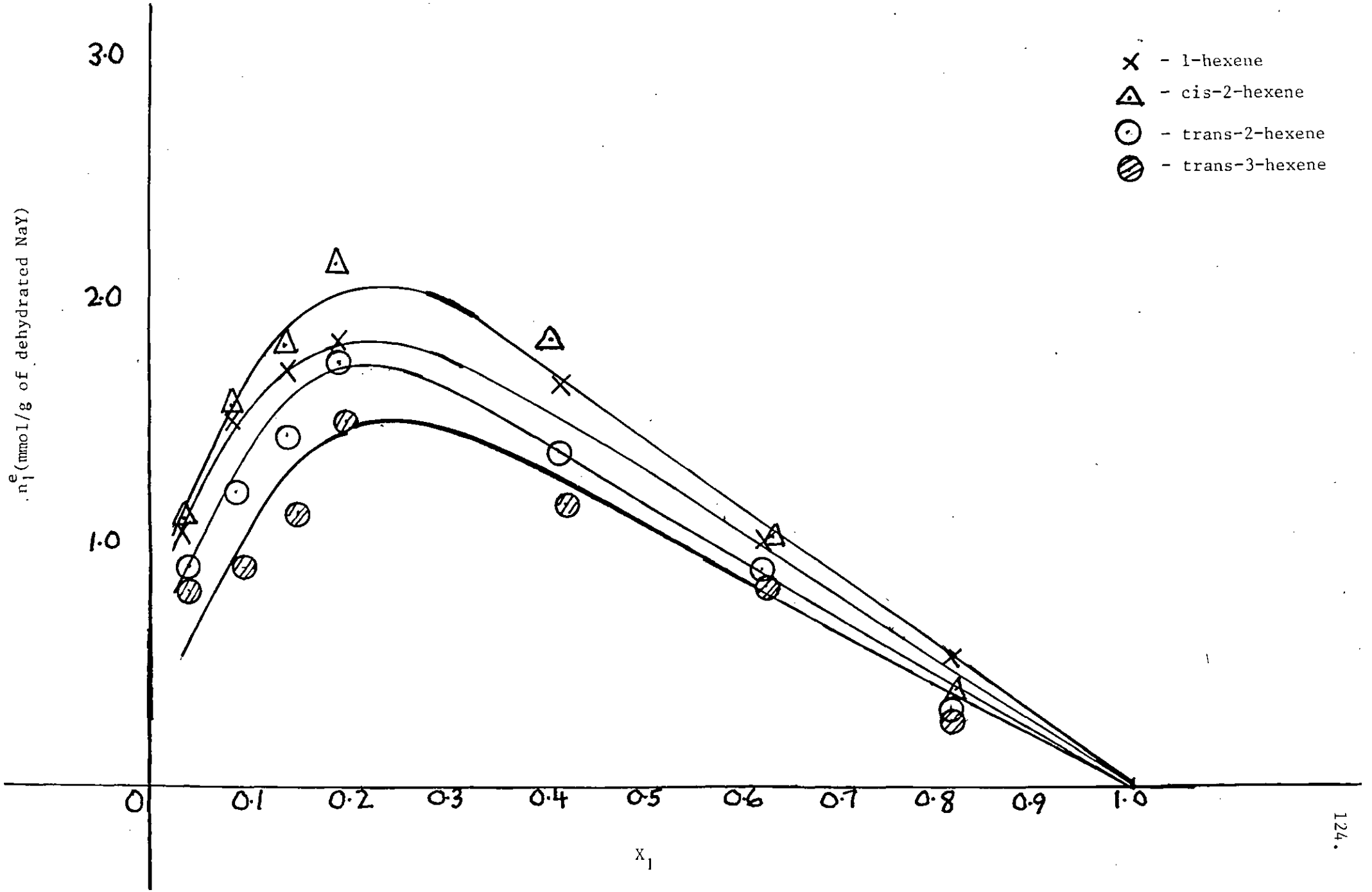

FIG. 6.9 Sorption isotherms of hexenes adsorbed on dehydrated KY at 26°C

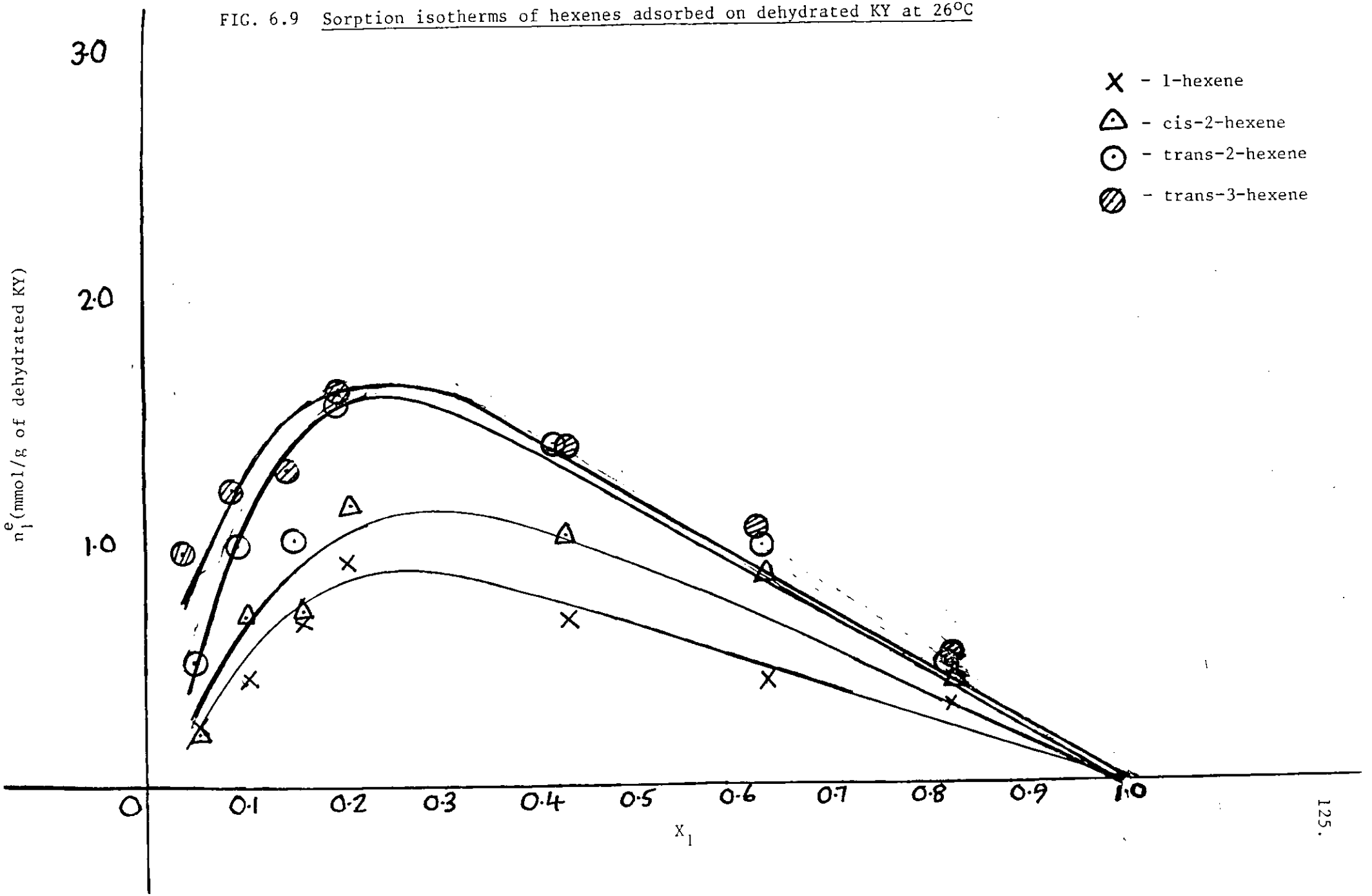

Table 6.4.5 Data for the olefin/heptane NaY system

Olefin	Limiting adsorption values n^s_{ml} (mmol/g) ± 0.1	Number of molecules of olefin adsorbed/ supercage	Maximum of excess isotherms $(X_l)_{max}$	Sorption capacity V^s(ml/g) ± 0.01	Total void fraction V_f(ml/ml) ± 0.01
1-hexene	2.4	3.8	0.21	0.30	0.32
cis-2-hexene	2.5	4.0	0.225	0.31	0.43
trans-2-hexene	2.2	3.5	0.21	0.27	0.38
trans-3-hexene	1.9	3.0	0.23	0.23	0.32

Table 6.4.6 Data for the olefin/heptane KY system

Olefin	Limiting adsorption values n^s_{ml} (mmol/g) ± 0.1	Number of molecules of olefin adsorbed/ supercage	Maximum of excess isotherms $(X_l)_{max}$	Sorption capacity V^s(ml/g) ± 0.01	Total void fraction V_f(ml/ml) ± 0.01
1-hexene	1.07	1.8	0.25	0.13	0.19
cis-2-hexene	1.45	2.4	0.27	0.17	0.25
trans-2-hexene	1.93	3.2	0.25	0.24	0.36
trans-3-hexene	1.90	3.2	0.25	0.23	0.34

The pore volume of zeolite X, as determined from the adsorption of different types of molecules including water, gases and hydrocarbons has been reported by Breck (1). For most molecules, with the possible exception of water, only the large supercages are occupied. The total calculated void volume (V_p) for the large supercages is 0.296 ml/g which is consistent with observed pore volumes as determined from all adsorbates except water and nitrogen (1). The total void fraction (V_f) of supercages in zeolite X covered by molecules of various types has also been reported (1) and found to be about 0.42-0.44 ml/ml. By comparison, it is noticed that heptane is also competing for the adsorption sites, when adsorbed with various hexene isomers. It is also noticed that the molecules of cis-2-hexene pack more efficiently in the large cages of NaX and NaY; whilst trans-2-and trans-3-hexene in KY. So the type and size of the cation has an ultimate effect on the type of isomer preferred; i.e. their orientation and packing efficiency. Results from sorption studies reveal very interesting features which explain the competitive nature of different isomer configurations for the sorption sites.

It is found that the Na^+ form of zeolites X and Y show preference for cis-2-hexene whereas the K^+ form of zeolite Y shows preference for the trans form. For zeolite Y, it may be assumed that contact between cation and adsorbate at site II is approximately the same for Na^+ and K^+ (105). The radius of K^+ being larger than that of Na^+, the electric field is therefore stronger in the vicinity of the Na^+ cation. On the other hand, if K^+ sticks out of plane of window (site II) then electric field gradient is greater than for Na^+ which lies in plane of window. High electric field gradient will interact more strongly with high dipole moment molecules.

By comparing the separation factors obtained in secs 6.1 and 6.2, we find that the values of K dropped in going from NaY to KY significantly when 1-hexene:trans-2-hexene and 1-hexene:trans-3-hexene were compared, but the drop was not so significant with 1-hexene:cis-2-hexene. This drop in K can be explained by considering steric effects. The structure of 1-hexene, cis-2-hexene, trans-2-hexene, and trans-3-hexene can be represented as:

$$CH_2 = CH(CH_2)_3CH_3; \quad CH_3\underset{H}{C} = \underset{H}{C}(CH_2)_2\,CH_3; \quad CH_3\underset{H}{C} = \overset{H}{C}(CH_2)_2CH_3;$$

$$CH_3CH_2\,\underset{H}{C} = \overset{H}{C}\,CH_2CH_3.$$

respectively. The accessibility of the π electrons for interaction with the adsorbed site must therefore increase in the order 1-hexene > cis-2-hexene > trans-2-hexene > trans-3-hexene. The effect of adsorption on the polarization of C-H bonds in the CH_3 group of the adsorbed molecule is also observed in the case of cis-2-hexene, trans-2-hexene and trans-3-hexene. In the case of 1-hexene the effect is weaker owing to the fact that CH_3 group is not adjacent to the C = C double bond.

Selectivity can also be expressed in terms of preferential interaction between species of different acidity-basicity. The acidity of zeolite Y is greater than that of zeolite X, due to lower aluminium content. So by introducing cations of group I in the periodic table in these zeolites, the acidity LiY > NaY > KY > RbY > CsY would be higher compared to the same ions substituted in zeolite X. Olefins act as soft bases, by using the π-electron system and are essentially soft donors. Their ease of reactivity towards acid depends upon the electron availability at the double bond. On this basis, one would expect the basicity of 1-hexene to be less than that of 2- and 3-hexenes, i.e. the methyl groups with their electron repelling property increase the electron density at the double bond in 2- and 3-hexenes. Bearing these interactions in mind, it was found that in going from NaY to KY, selectivity for 2-and 3-hexene was preferred.

However, it is believed in the present study that steric effects and differences in polarizability between hexene isomers as discussed overrule any other contributing factors towards selectivity and that the mechanism of adsorption involves cations of the zeolites as adsorption centres.

Adsorption of more closely related hexene isomers would reveal the effects of the factors mentioned even further.

6.5 Adsorption of more Closely Related Isomers on Zeolites NaX, KX, NaY and KY

Table 6.5 A $T_c = 350 \pm 5^oC$

Stock solution: cis-2-hexene: trans-2-hexene

Zeolite	Hydrated weight (g)	Dehydrated weight (g)	Number of H_2O mols/Unit cell	$K_{\frac{\text{cis-2-hexene}}{\text{trans-2-hexene}}}$
NaX	1.1076	0.8285	12	1.6(2)
KX	1.0993	0.858	10	0.9(4)
NaY	1.0995	0.8196	12	0.9(1)
KY	1.0985	0.8636	1	0.3(8)

Table 6.5 B $T_c = 350 \pm 5^oC$

Stock solution: cis-2-hexene: trans-3-hexene

Zeolite	Hydrated weight (g)	Dehydrated weight (g)	Number of H_2O mols/Unit cell	$K_{\frac{\text{cis-2-hexene}}{\text{trans-3-hexene}}}$
NaX	1.0995	0.8217	11	1.6
KX	1.1038	0.8652	14	0.8(5)
NaY	1.1014	0.8218	13	2.1(9)
KY	1.1003	0.8647	1	0.2(6)

Results show that K^+ substituted in zeolite X shows preference for trans-2-hexene and trans-3-hexene. But the selectivity for these isomers is further enhanced when K^+ is substituted in zeolite Y, indicating once again the importance of the foregoing factors mentioned.

6.6 Variation of K Verses Concentration of Hexene Isomers on Zeolite NaX

The variation of K was studied using the following concentrations of hexene isomers in heptane as solvent.

Firstly in a 1:1 ratio with increasing concentrations of each isomer, per 5 ml of solvent added to the dehydrated NaX.

Experiment Number	ml of each isomer added		mg of each isomer added/5 ml solvent	
	1-hexene	trans-2-hexene	1-hexene	trans-2-hexene
1.	0.15	0.15	100	100
2.	0.25	0.25	168.25	167.25
3.	0.5	0.5	336.5	334.5
4.	0.75	0.75	504.75	501.75
5.	1.0	1.0	673	669

Table 6.6.1 Results from Experiment

Experiment Number	Hydrated weight of NaX	Dehydrated weight of NaX	Number of H_2O mols/Unit cell	$\frac{K_{1\text{-hexene}}}{\text{trans-2-hexene}}$
1.	1.0983	0.8173	7	2.4(3)
2.	1.0971	0.8211	13	2.7(8)
3.	1.1007	0.8215	10	3.3(6)
4.	1.107	0.8278	12	4.5(3)
5.	1.1061	0.8287	14	5.5(8)

A plot of separation factor verses concentration (mg) of each isomer added is shown in Fig. 6.10, and shows a linear dependence of separation factor as a function of concentration added. The significance of this result is that K is proportional to concentration of isomers added.

FIG. 6.10 Variation of separation factor verses concentration of each isomer added on NaX.

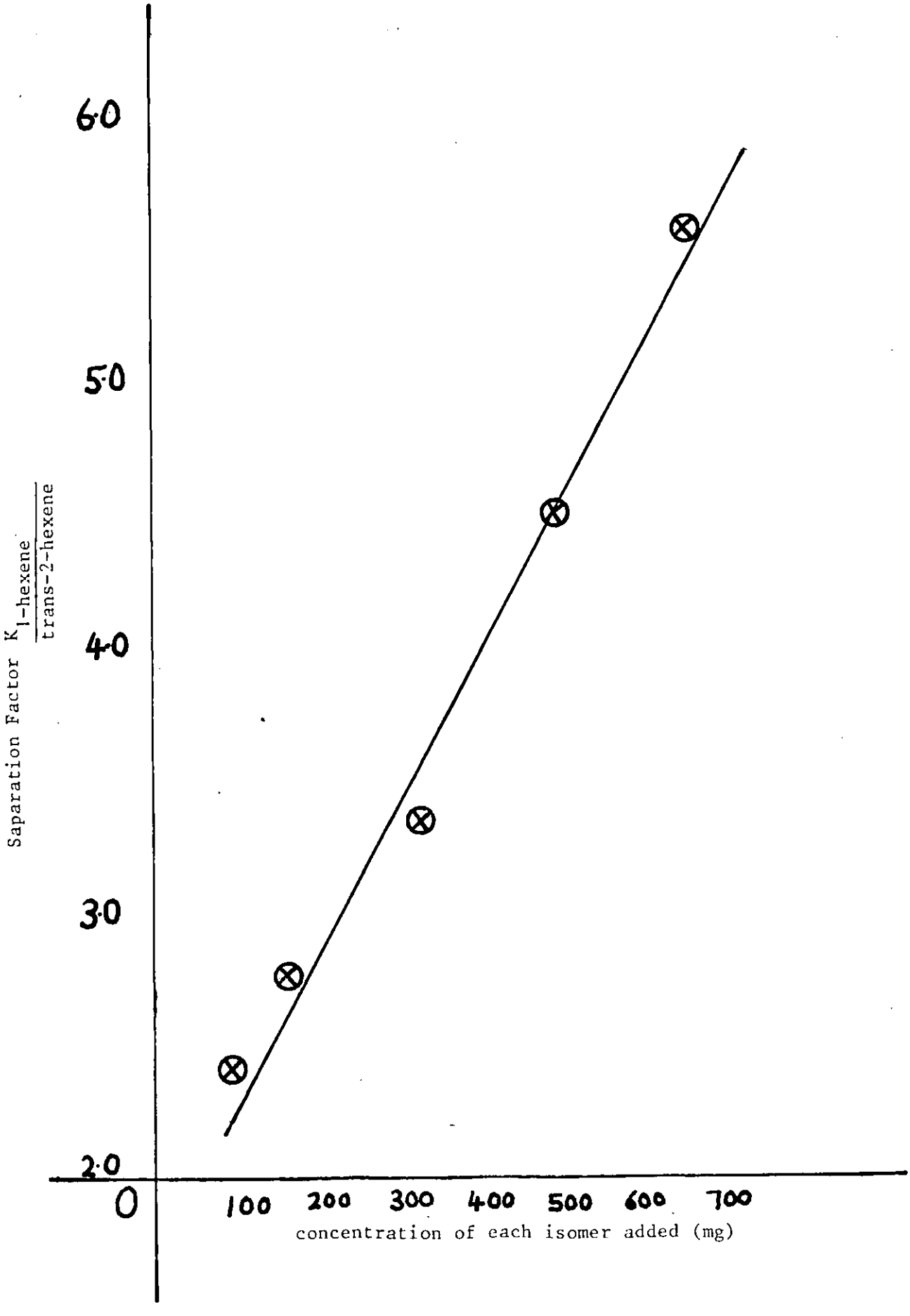

Secondly, loading various ratios of hexene isomers per 5 ml of heptane as solvent.

Table 6.6.2 Results from experiment

Hydrated weight of NaX	Dehydrated weight of NaX	Number of H_2O moles/Unit cell	mg of sorbates added/5 ml heptane		$K_{\frac{1\text{-hexene}}{\text{trans-2-hexene}}}$
			1-hexene	trans-2-hexene	
1.0945	0.8235	18	25	175	3.5(8)
1.1016	0.8254	14	50	150	3.2(1)
1.0983	0.8207	11	75	125	2.7(8)
1.0983	0.8173	7	100	100	2.4(3)
1.1007	0.8264	16	125	75	2.0(7)
1.1034	0.825	12	150	50	1.9(2)
1.097	0.8204	12	175	25	1.6(1)

A plot of separation factor verses concentration of hexene isomers is shown in Fig. 6.11 which indicates a linear drop in separation factor as the concentration of the preferentially adsorbed isomer is increased. This suggests that for efficient separation, a diluted solution of the preferentially adsorbed isomer is recommended.

FIG. 6.11 Varation of separation factor verses concentration of hexene isomers.

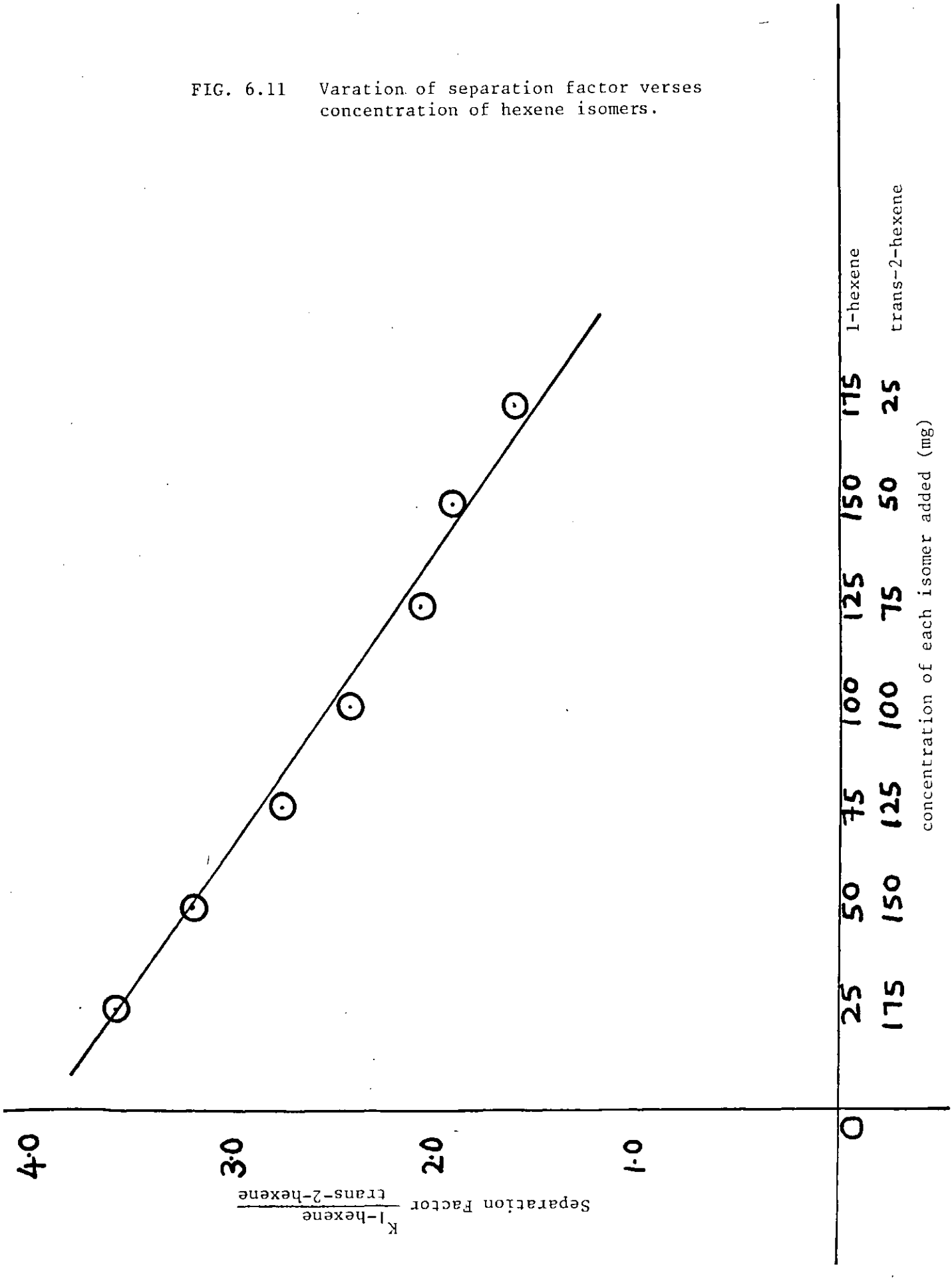

6.7 Li^+ Exchanged X and Y Zeolites

Stock solution: 200 mg 1-hexene/5 ml heptane were added to LiX, NaX, LiY and NaY Zeolites.

NaLiX(56) contained 273 H_2O molecules/Unit cell.
NaLiY(57) contained 272 H_2O molecules/Unit cell.

Table 6.7.1 $T_c = 350 \pm 5^oC$

Zeolite	Hydrated weight (g)	Dehydrated weight (g)	Number of H_2O mols/Unit cell	Isomerization in liquid after contact with Zeolite
LiX(56)	1.1012	0.7998	8	No
NaX	1.0978	0.8238	15	No
LiY(57)	1.0996	0.7928	9	Yes (to trans-2-hexene ~11%)
NaY(57)	1.1002	0.7978	-	No

The results show that isomerization occured on LiY(57), whilst it was practically non-existant on LiX(56), NaX and NaY. This suggests the effect of Li^+ substituted in zeolite Y or the reactivity of the reactant molecule. This was investigated further by loading 2-methyl-1-pentene on these zeolites.

Table 6.7.2 Stock solution: 201.68 mg 2-methyl-1-pentene/5 ml heptane

Zeolite	Hydrated weight (g)	Dehydrated weight (g)	Number of H_2O mols/Unit cell	Isomerization to 2-methyl-2-pentene in the liquid phase after contact with the zeolite
LiX(56)	1.1036	0.7926	-	Yes (~ 56%)
NaX	1.1028	0.8175	3	Yes (~ 3%)
LiY(57)	1.0937	0.7765	-	*
NaY	1.1041	0.8024	-	Yes (~ 57%)

* LiY(57) showed polymerization.
Washings with methanol showed complete recovery.

This experiment does suggest the formation of weak acid sites on zeolites X and Y, and it does reveal the importance of both SiO_{2/Al_2O_3} ratio and the cation size in the zeolite. The effect of methyl group in the two position, enhances reactivity across the double bond, to react with weak acid sites.

So the following two adsorption experiments were conducted, conditions were identical to that described before.

Table 6.7.3 Stock solution: 1-hexene: cis-2-hexene in heptane as solvent.

Zeolite	Hydrated weight (g)	Dehydrated weight (g)	Number of H_2O mols/Unit cell	$K_{\frac{\text{1-hexene}}{\text{cis-2-hexene}}}$
T_c=120±1°C				
LiX(56)	1.0055	0.8475	142	0.4
LiY(57)	0.9997	0.8067	109	0.6(9)
T_c=350±5°C				
LiX(56)	1.1013	0.801	10	1.0(9)

Table 6.7.4 Stock solution: 1-hexene: trans-2-hexene in heptane as solvent.

Zeolite	Hydrated weight (g)	Dehydrated weight (g)	Number of H_2O mols/Unit cell	$K_{\frac{\text{1-hexene}}{\text{trans-2-hexene}}}$
T_c=120±1°C				
LiX(56)	1.0	0.8324	132	0.5(7)
LiY(57)	1.006	0.8069	104	0.8
T_c=350±5°C				
LiX(56)	1.0956	0.7954	8	1.61

These results show preferential adsorption for both cis-and trans-2-hexene by LiX and LiY zeolites when calcined at 120°C. But when LiX was calcined at 350°C preference for 1-hexene was indicated. The effect of different interactions mentioned earlier seem to be reponsible for these differences in selectivity.

6.8 Reaction of 1-hexene on Brönsted Acid Sites

On an essentially hydrogen form of zeolite Y, (ca 1.1 g) which was calcined at 350°C overnight in air, (~ 0.78 g), 1-hexene (10 ml) was added to the cooled zeolite. The contents were agitated in a temperature controlled water bath at 25 to 26°C and samples analysed by GC at various time intervals.

As the reaction proceeded, analysis by GC showed formation of both cis and trans-2-hexene, with the final product being trans-2-hexene, the more thermodynamically favoured form. A sample of the reaction mixture was sent for analysis by GC/MS, which showed a mixture of dimers and trimers (trace) to be formed as well.

The same experiment was carried out with CaX (76%), CaY (59%) and BaY (67%) and similar results were obtained.

Since a mixture of dimers were produced, it was necessary to check if cis or trans-2-hexene were stable to isomerization and/or dimerization. So individual experiments with these isomers were carried out on the hydrogen form of zeolite Y, under identical conditions and the results showed:

$$\text{cis-2-hexene} \xrightarrow{\text{HY}} \text{trans-2-hexene (gradually)}$$

$$\text{trans-2-hexene} \xrightarrow{\text{HY}} \text{trans-2-hexene}$$

samples from both experiments were sent for GC/MS and showed dimerization in both cases (N.B. no trimers were indicated).

These experiments explain the formation of dimers in the major reaction (1-hexene $\longrightarrow$ cis/trans-2-hexene). The fact that these reactions occur on divalent ion-exchanged forms of X and Y zeolites suggest that similar types of hydroxyl groups to those present in HY are involved although the reaction rate is considerably less which indicates a lower hydroxyl group concentration (70).

The reaction follows the scheme below:

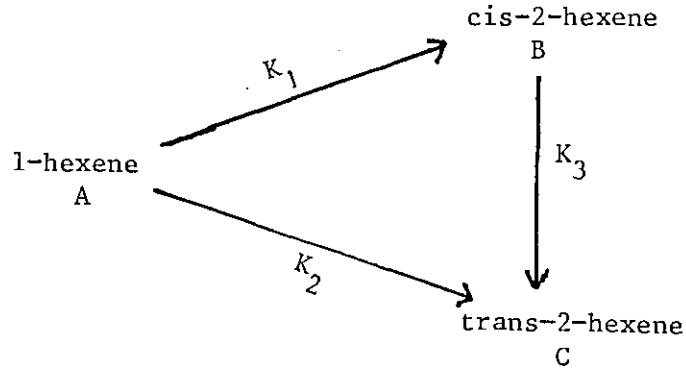

+ (Dimers + Timers)

In constructing the kinetic equations corresponding to the major reaction scheme, the following assumptions were made under the experimental conditions: 1) Although the isomerization is not reversible, first order kinetics was assumed; 2) the active centres are uniform in adsorption and catalytic behaviour.

With these assumptions, the system of differential equations has the form:-

$$\frac{dA}{dt} = -(K_1 + K_2)A$$

$$\frac{dB}{dt} = K_1A - K_3B$$

$$\frac{dC}{dt} = K_2A + K_3B \qquad \ldots \quad (1)$$

$$A + B + C = 1$$

where A, B and C are the mole fractions of the isomers (see above figure for definition of A, B, and C) corresponding to time t; K_1, K_2 and K_3 are the respective rate constants.

The system (1) was solved experimentally using 1-hexene as starting material, the catalyst being HY(~ 1.1g hydrated weight).

To about 0.83 g of HY(T_c = 350°C in air, 24 hr) was added a mixture of 1-hexene in heptane slowly and allowed to shake in a constant temperature water bath. Samples (0.5uℓ) were analysed at time intervals, and kinetic curves were plotted at each reaction temperature.

The reactant was added in a diluted form (336.5 mg of 1-hexene/5 ml heptane) in all experiments, so as to avoid the temperature of the reaction mixture getting too high due to exothermic reaction taking place.

The kinetics of isomerization of 1-hexene at three temperatures are shown in Figs 6.12 to 6.14 and the respective rate constants were evaluated by drawing tangents at suitable points, and solving the simultaneous equations.

Table 6.8.1 shows the values of the calculated isomerization rate constants; the temperature dependence of these rate constants was used to estimate the activation energies (E_a); using the Arrhenius equation:

$$K = Ae^{-E_a/RT}$$

where K = rate constant.
A = pre-exponential factor.
E_a = activation energy.
R = gas constant (8.314 J $mole^{-1}$ K^{-1}).
T = absolute temperature (K).

The Arrhenius equation can be compared to the equation obtained from transition-state theory, i.e.

$$K = \frac{kT}{h} e^{(-\Delta G^{\ddagger}/RT)}$$

where k = Boltzmann constant.
T = Absolute temperature (K).
h = Planck constant.

now $\Delta G^{\ddagger} = \Delta H^{\ddagger} - T\Delta S^{\ddagger}$

where $\Delta G^{\ddagger}$ = free energy of activation.
$\Delta H^{\ddagger}$ = standard enthalpy of activation.
$\Delta S^{\ddagger}$ = standard entropy of activation.

FIG. 6.12 Isomerization of 1-hexene on HY at 4±1°C.

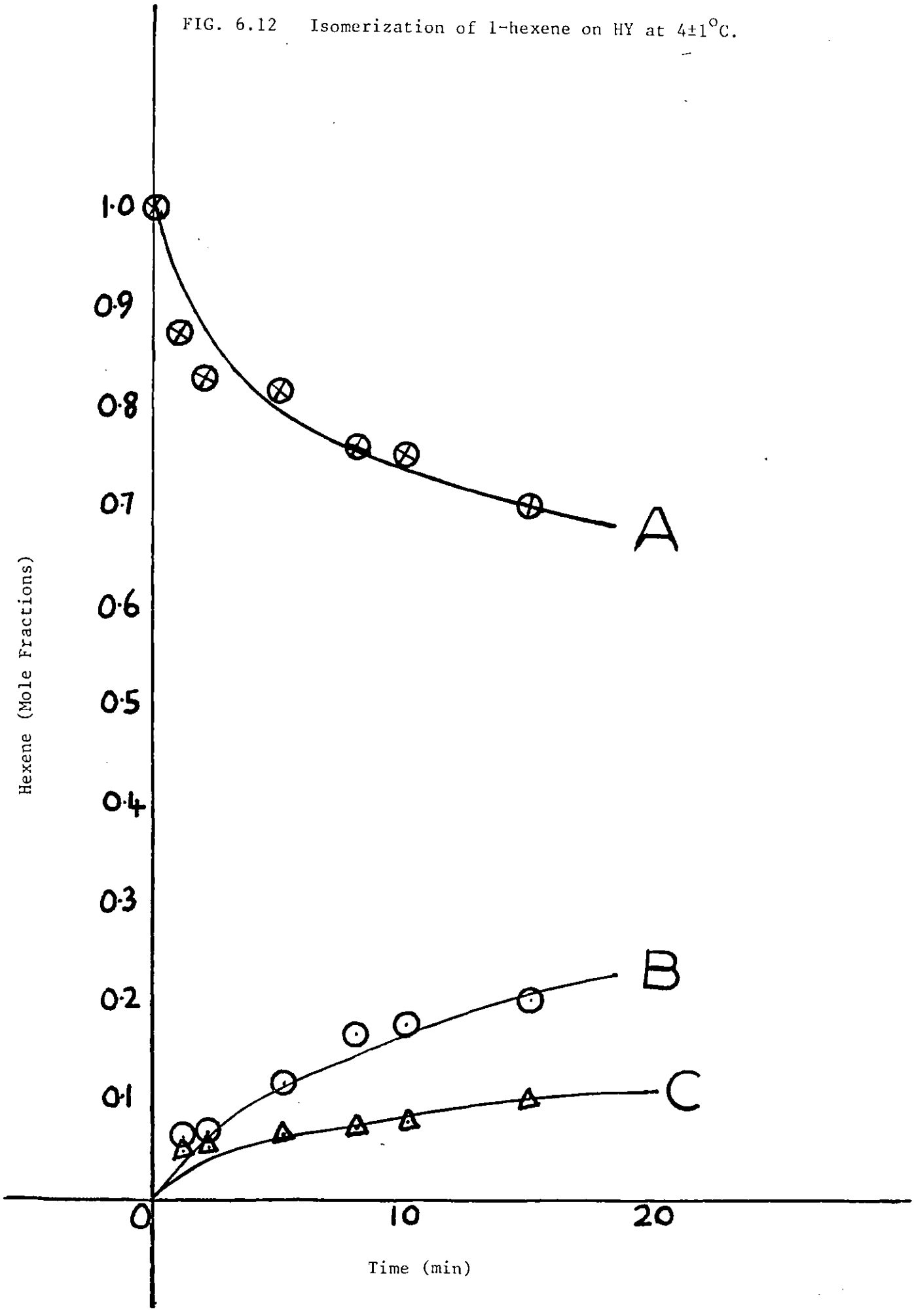

FIG. 6.13 Isomerization of 1-hexene on HY at 15 ± 1°C.

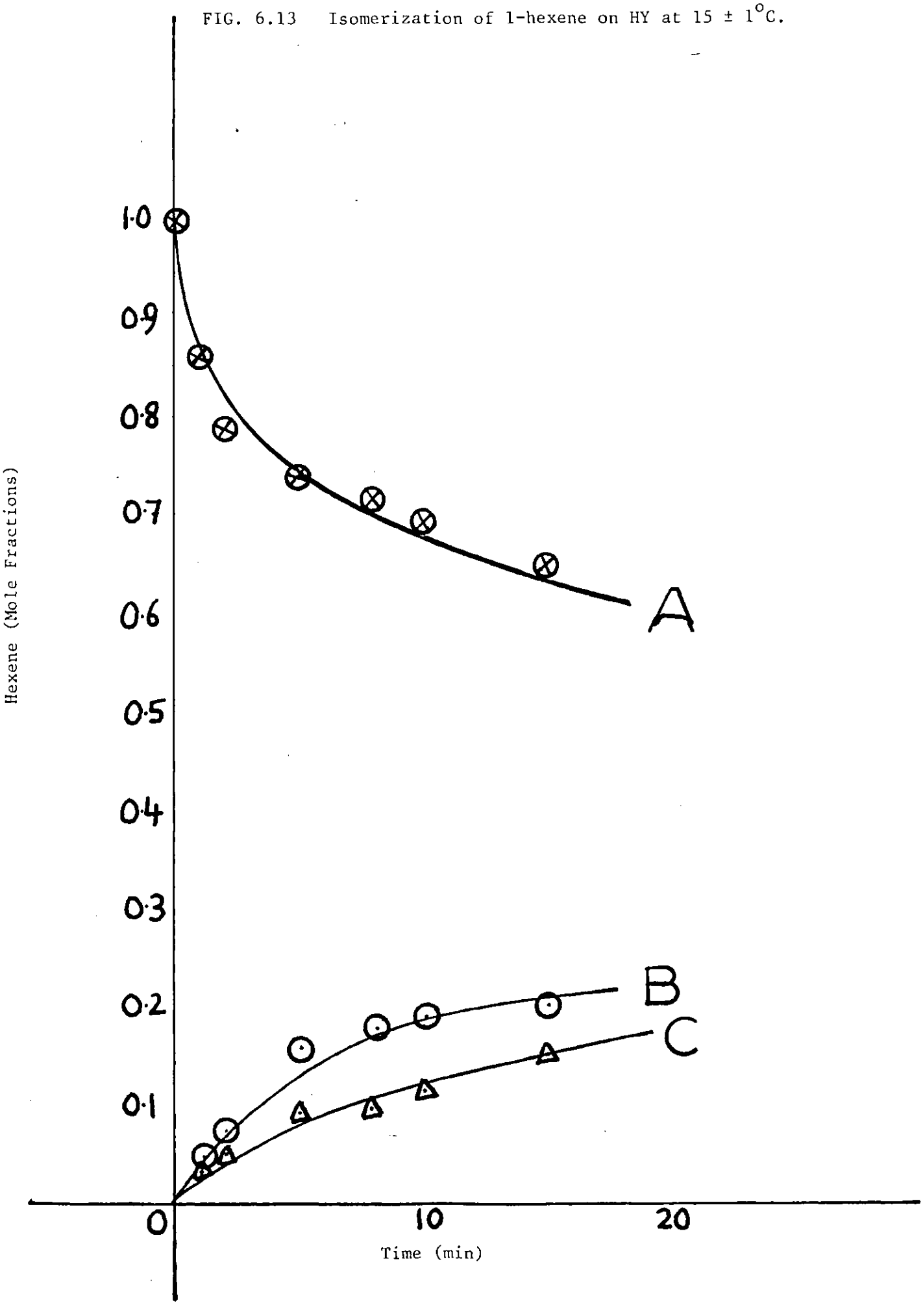

FIG. 6.14 Isomerization of 1-hexene on HY at 32±1°C.

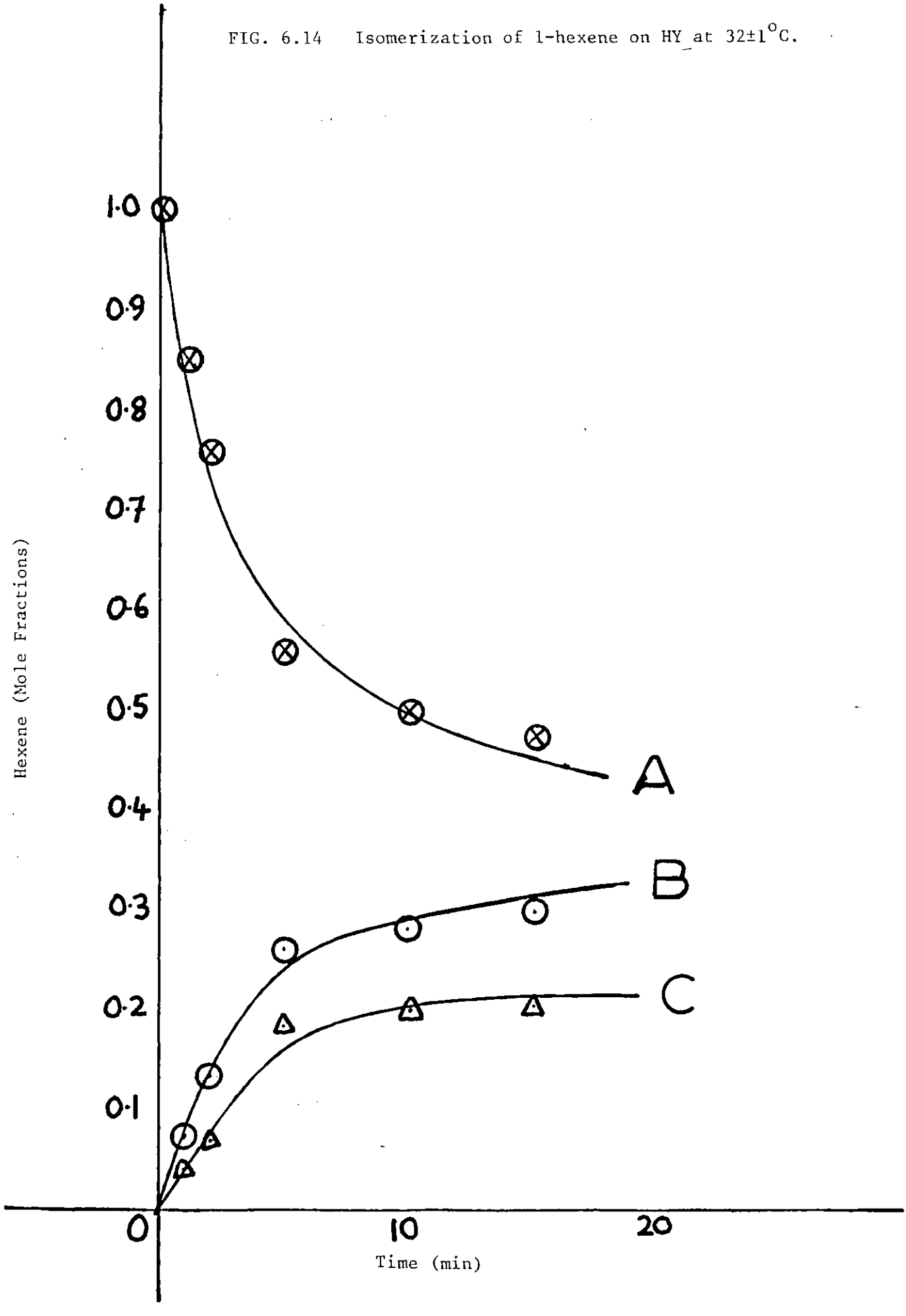

Then:

$$K = \frac{kT}{h} e^{(-\Delta G^{\ddagger}/RT)}$$

$$= \frac{kT}{h} e^{(\Delta S^{\ddagger}/R)} e^{(-\Delta H^{\ddagger}/RT)}$$

so comparing this equation with the Arrhenius equation we see that $-\Delta H^{\ddagger}$ replaces the activation energy E_a and

$$A = \frac{kT}{h} e^{(\Delta S^{\ddagger}/R)}$$

($E_a = -\Delta H^{\ddagger}$ provided there is no further change in the number of molecules in the reaction). So values for $\Delta S^{\ddagger}$ and $\Delta G^{\ddagger}$ at 300 K for each isomerization step was calculated.

Table 6.8.1

Temp(^{o}C) ± 1	Rate constants (x 10^{-4} s^{-1})		
	K_1	K_2	K_3
4	3.12	3.08	1
15	5.1	3.24	2.28
32	10.4	4.09	5.9
E_a(KJ/mole)	32 ± 2	10 ± 2	44 ± 2
At 300 K			
$\Delta S^{\ddagger}$(KJ/mole/K)	- 0.19 ± 0.01	- 0.27 ± 0.01	- 0.16 ± 0.01
$\Delta G^{\ddagger}$(KJ/mole)	91 ± 2	93 ± 2	92 ± 2

From the kinetic data, it can be concluded that the shift of the double bond in 1-hexene is stereoselective. Thus, by comparing the rate constants K_1 and K_2 for the conversion of 1-hexene to cis and trans-2-hexene respectively, it is seen that the cis-2-hexene is formed somewhat more rapidly than the trans-2-hexene, even though the latter is the more thermodynamically stable form. This experimental fact, the high rate of formation of a cis olefin in comparison with the trans isomer, has also been observed in studies of the conversions of n-butenes and n-pentenes (107, 108). The rate constants relative to isomerization of 1-butene to cis-2-butene on silica-alumina at 150°C as reported by Brouwer (108) were:

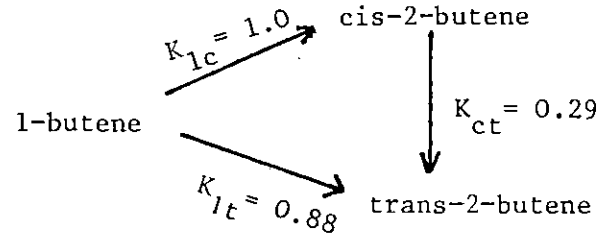

Isomerization of 1-pentene followed the same characteristics as for 1-butene but with slight deviations being inherent in the differences between 1-butene and 1-pentene. Brouwer (108) also reported the isomerization of 1-hexene as well which showed similar patterns as observed with 1-butene and 1-pentene. He found that the steric configuration of the starting material had an influence on the cis/trans ratio of the products and also the shift of the double bond over a greater distance along the carbon chain (1-hexene ⇄ 2-hexenes ⇄ 3-hexenes); particularly 1-hexene ⇄ 3-hexenes was formed by a consecutive reaction mechanism. This scheme was very well supported by recent studies on isomerization kinetics of n-hexenes on NaY zeolite by Sinitsyna et al (154). The isomerization reactions were carried out at three temperatures (210°, 228°and 250°C)respectively; and their relative rate constants corresponding to coversion of 1-hexene to cis and trans-2-hexene were essentially of the same order as for 1-butene conversion. However, conversion of cis-2-hexene to trans-2-hexene proceeded almost $1\frac{1}{2}$ to two times faster compared to conversion of 1-hexene to cis-2-hexene for the above temperature range. Also the activation energy calculated for cis-trans isomerization showed that this process was much strongly favoured compared to double-bond shift, making NaY catalyst more active for the former reaction.

Dimitrov and Leach (107) also studied the isomerization of 1-butene on NaX and CuX zeolites at 305°C for NaX and 105°C for CuX. Their results for the relative rate constants as defined earlier according to the isomerization scheme showed that for the NaX the fastest processes were those in which 1-butene was converted into cis (K_{1c} = 1) and trans (K_{1t} = 0.91) - 2 - butene, whereas the interconversion of the 2-butene stereoisomers were the slowest processes (K_{ct} = 0.1). The NaX catalyst was thus more active for the double-bond shift reaction than for geometrical isomerization.

By comparison, the relative rate constants for the CuX samples revealed some marked differences to those from NaX. With CuX (9.3%) the most important feature was the marked preferential formation of trans-2-butene; but less preference for the double bond shift as NaX (i.e. K_{1c} = 1, K_{1t} = 9.09, K_{ct} = 0.2). The data for CuX (37%) were similar to those for CuX (9.3%) although the preferential formation of trans-2-butene from 1-butene was less marked (K_{1c} = 1, K_{1t} = 1.94, K_{ct} = 0.21).

With catalysts CuX (62%) (K_{1c} = 1, K_{1t} = 0.89, K_{ct} = 0.52) and CuX (68%) (K_{1c} = 1, K_{1t} = 0.79, K_{ct} = 0.37) it was found that cis-2-butene was formed in preference to trans-2-butene, so these samples exhibited a preference for geometrical isomerization rather than double bond shift.

The preferential formation of the thermodynamically less stable cis isomer from 1-butene has been shown by many authors to occur on both basic and acidic catalysts, whereas preferential cis-trans isomerization rather than double bond shift is a feature of acidic catalysts (155). For such catalysts it is generally accepted that the mechanism is ionic, involving a carbanion on basic catalysts and a carbonium ion on acidic catalysts. Catalysts CuX (62%) and CuX (68%) exhibit behaviour characteristic of acidic catalysts and it is concluded that a carbonium ion mechanism was operative.

Paukshtis et al (157) proposed a mechanism of 1-butene isomerization on acidic catalysts to proceed via secondary butyl carbonium-ion. They showed that the formation of the less thermodynamically favoured cis isomer predominates, its content increasing with decreasing strength of the acidic centres (158). This may be explained by the fact that the acid residue on the surface has an influence on the carbonium ion formed by protonation. The positive charge in the carbonium ion is partially delocalized onto adjacent carbon atoms. Interaction of the positive charges on all the carbon atoms with the negative charge of the acid residue results in an orientation of the carbonium-ion such

that the formation of trans-2-butene becomes energetically less favourable. An increase in the strength of the acidic centre, which will weaken the interaction of the acid residue with the carbonium ion, will result in the equally probable formation of both 2-butene isomers.

By comparison, the relative rate constants of isomerization of 1-hexene from gas phase on NaY as reported by Sinitsyna et al (154) and that found in the present work on HY from liquid phase show the following differences:

NaY catalyst:

	K_{1c}	K_{1t}	K_{ct}
At 210°C	1.0	0.81	1.9
At 228°C	1.0	0.8	1.6
At 250°C	1.0	0.85	1.4
E_a(KJ/mole)	30 ± 8	34 ± 8	17 ± 8

HY catalyst:

	K_{1c}	K_{1t}	K_{ct}
At 4 ± 1°C	1.0	0.98	0.32
At 15 ± 1°C	1.0	0.63	0.44
At 32 ± 1°C	1.0	0.4	0.56
E_a(KJ/mole)	32 ± 2	10 ± 2	44 ± 2

i.e. HY catalyst is more active in double bond shift than in cis-trans isomerization; whereas the reverse was found to be true from gas phase on NaY catalyst. So there are differences in relative rates obtained from two phases, indicating that reaction temperature, pore structure of the catalyst, type of cation in the zeolite and the stability of isomer configuration play a significant role in these isomerization processes. The activation energies calculated for the isomeric conversion of 1-hexene on HY from liquid phase suggest that isomerization of 1-hexene to trans-2-hexene is strongly favoured. Since $K_1 > K_2$; the $\Delta G^{\ddagger}$ and $\Delta S^{\ddagger}$ values are in favour of cis-2-hexene. It is noticed

from the values of the relative rate constants that K_{ct} is > K_{lt} at 32°C reaction temperature suggesting that at high reaction temperatures cis-trans isomerization may predominate over double-bound shift. The initial cis:trans-2-hexene ratio was about 1.5:1 at all liquid phase reaction temperatures.

It can be concluded that the hydroxyl groups so formed on dehydration of HY zeolite are responsible for these isomerizations, in particular the O-H group on O_1 of the lattice which extends into the large adsorption cavity is the most active site. The unit cell composition of HY zeolite is $H_{55}[(A\ell O_2)_{55}\ (SiO_2)_{137}]$; so 0.83 g of HY contains 4.34×10^{19} unit cells. There are eight supercages per unit cell, and therefore 3.47×10^{20} supercages/g of HY available for sorption and also isomerization to take place. Since one mole of hydroxyl group is formed for every mole of Na^+ exchanged by NH_4^+; the number of hydroxyl groups/g of HY, which are responsible for the isomerizations observed can be calculated to be 23.86×10^{20}.

It can be said that the useful catalytic properties of zeolites hinge on three factors: (1) the regular crystalline structure and uniform pore size which allows only molecules below a certain size to react; (2) the presence of strongly acidic hydroxyl groups which can initiate carbonium-ion reactions; and (3) the presence of very large electrostatic fields in the neighbourhood of the cations which can thus induce reactivity in reactant molecules. Catalytic activity therefore depends heavily on the nature of the cation, which also seems to affect the acidity of the hydroxyl groups.

The reaction is believed to proceed via a secondary carbonium-ion, viz:

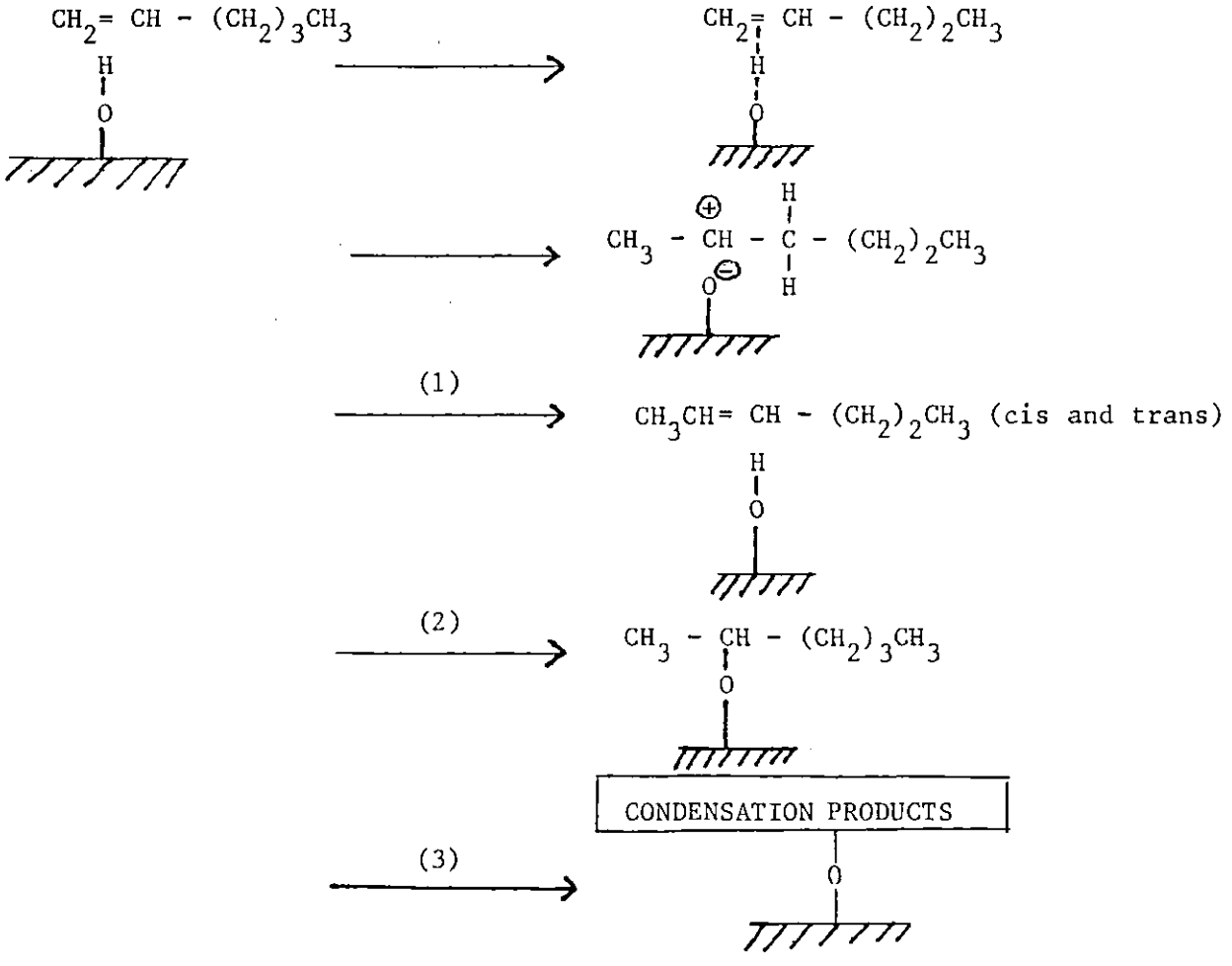

The first step in the reaction is the formation of a strong hydrogen bond between the 1-hexene and protonic centres on the surface. This is followed by proton transfer to the molecule, resulting in the formation of a carbonium-

ion. The carbonium ions rapidly undergo further reactions. They may lose a proton to regenerate the centre and form reaction products (route 1). There is also the possibility of reacting with surface nucleophiles to form surface esters (route 2). The carbonium ions may also react with adsorbed molecules to form complex high-molecular-weight products (route 3). The ratio of the reaction rates of the carbonium ions in these directions depends on the reaction conditions, viz; the temperature, the olefin concentration, and the pore structure of the catalyst. The accumulation of high-molecular-weight products on the surface would result in irreversible deactivation at moderate temperatures.

Additional evidence in support of the mechanism involving the secondary carbonium-ion was obtained from the studies on isomerization of 3,3-Dimethyl-1-butene.

It was found that 3,3-Dimethyl-1-butene is readily isomerized over proton donating catalysts according to the generally adopted scheme:

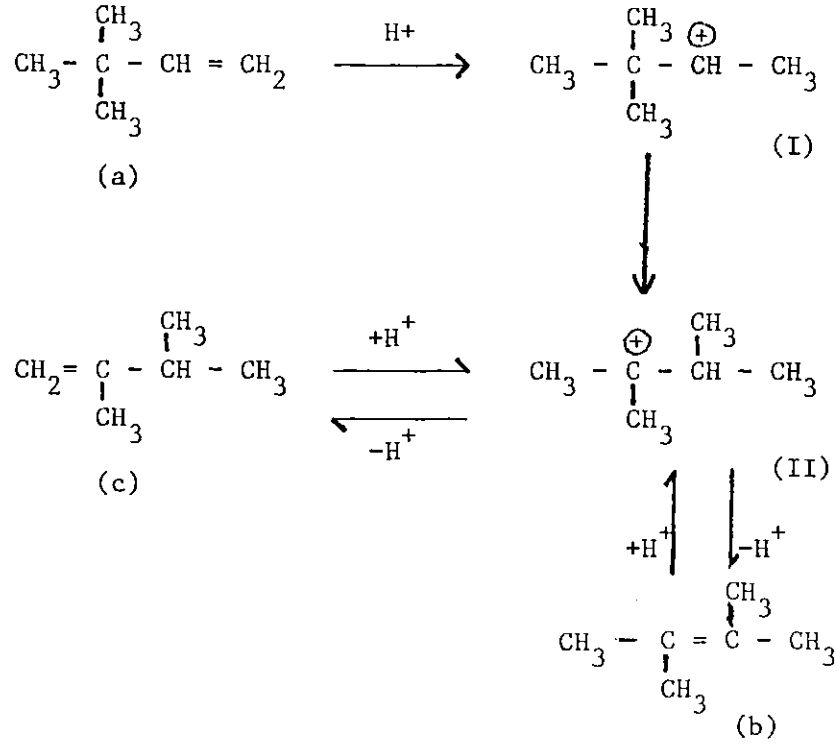

The reaction scheme can also be explained in terms of Whitmore's carbonium-ion theory (106). An alkyl shift in a carbonium-ion is thermodynamically favoured when the new ion is more stable, i.e. more substituted, and the methyl shift from I to II should therefore be easy. The fact that (a) is isomerized to (b) and (c) has to be considered as evidence for the ability of zeolites to display acidic type catalytic activity.

So 3,3,-Dimethyl-1-butene (5 ml) was added to cooled dehydrated zeolites (HY, CaY, CaX, BaY) and left to shake overnight at 25-26^{o}C. The products were analysed by GC and found to isomerize to the more stable 2,3,-Dimethyl-2-butene.

In conclusion to these isomerization studies, there is fair evidence to support the proposed mechanism. Favoured migration of the double bond with respect to cis-trans isomerization, may well be associated with the obstructed rotation of the carbocation in the pores of the zeolite lattice, as has been reported by numerous investigators for zeolite catalysts (109-111).

6.9 DISCUSSION

The present work has shown the potential use of synthetic zeolites (X and Y) for separation of organic molecules from liquid phase solutions. These zeolites have been used by U.O.P. on plant scale to separate chemically similar molecules; using the major commercial sorbex processes, i.e. Olex and Parex. Dyer (75) has reported other similar separations developed by U.O.P. (113) and are summarized below:

Table 6.9.1 Large-scale Application of Zeolite Adsorbents in Sorbex Processing

Component A/Component B	β
p-Xylene/Ethylbenzene	1.6
p-Xylene/o-Xylene	3.8
p-Xylene/m-Xylene	4.0
p-Xylene/Ethylbenzene	2.1
p-Xylene/o-Xylene	2.2
p-Xylene/m-Xylene	2.7
p-Xylene/Ethylbenzene	2.2
o-Xylene/Ethylbenzene	2.9
m-Xylene/Ethylbenzene	3.4
p-Cymene/o-Cymene	2.0
p-Cymene/m-Cymene	3.1

Component A/Component B	β
p-Diethylbenzene/m-Diethylbenzene	2.5
p-Diisopropylbenzene/m-Diisopropylbenzene	4.9
Butene-1/i-Butene	2.2
Butene-1/cis-2-Butene	3.1
Butene-1/trans-2-Butene	3.5
Olefins/Aromatics	< 0.1
Olefins/Paraffins	10
n-Paraffins/i-paraffins	> 1000
p-Cresol/o-Cresol	1.8
p-Cresol/m-Cresol	2.0
p-Cresol/Xylenols	> 5
β-Pinene/α-Pinene	2.6
Fructose/Glucose	7.0
Fructose/Polysaccharides	> 50
Glucose/Fructose	1.7
Glucose/Polysaccharides	> 50

β = Separation factor Component A/Component B

Data suggests that the amount of adsorption of any molecule in the zeolite is influenced by the pore size in the zeolite. For the separation of large molecular diameter molecules, it is essential to use the large pores of zeolite X or zeolite Y.

The amount of adsorption of sorbate is dependent on the ionic radius of the exchanged cation. The smaller the cation the greater the sorption capacity.

In general the selectivity and adsorption capacity of zeolite are influenced by the physical properties of the zeolite and the adsorbed isomer. The following factors have been found to be most influential in isomeric mixture separations:

(1) cation type; (2) the ratio of SiO_2/Al_2O_3 of zeolite; (3) moisture content; (4) solvent used.

Seko et al (117) have measured the acidity of zeolite in order to investigate the selectivity and other physical properties of the cation-exchanged zeolite. The total acidity (sum of Brönsted and Lewis acid sites) is found to have a strong correlation with the ionic radius or valence of exchanged cation. This has been explained by Ward (70), i.e. the smaller the ionic radius or the larger the valencies of the exchanged cation, the stronger is the acidity of the zeolite. On this basis, selectivity can be related in terms of preferential interaction between species of different acidity-basicity. In the case of xylene isomer separation, the lower the acidity of the zeolite, the higher is the selectivity for p-xylene. This is explained by strong affinity between the acidic zeolite and the most basic isomer of m-xylene which has the strongest electron donating characteristics (118). In this the selectivity of the xylene isomer can be predicted by the acidity of the cation exchanged zeolite. It is known that high SiO_2/Al_2O_3 ratio reduces the adsorptive site of AlO_4^- , thereby influencing reduction in the acidity of the zeolite. By varying this ratio, selectivity for each isomer may be effected. The moisture content of zeolite is controlled by calcination time and temperature. The lower the moisture content, the lower the acidity of the zeolite. This is explained by Ward (70), from the fact that the polarized water molecule in the zeolite works as a Brönsted acid. For an effective separation of isomers from the zeolite bed, it is essential to select the desorbent which maintains the stationary elution curve of the isomer adsorption band during the migration through the column. Some important properties required for the desorbent are as follows: (1) the desorbent should not reduce the selectivity and adsorption capacity of zeolite, when it is mixed with isomers; (2) the desorbent should have a suitable desorbing power for the isomers adsorbed in the zeolite; (3) the desorbing power should not be reduced over the wide range of isomer concentration, especially at the boundaries of the band where the concentration of isomer is low; (4) the relative volatility of desorbent to isomer should be large enough so that it is easily removed by distillation; (5) the desorbent should be chemically stable in the operational condition.

Breck (1) lists 165 adsorption processes of which 112 are commercial applications. Many of these are concerned with drying and catalysis; but several hundreds of separations are reported in the literature. It is well known in the separation art that molecular sieves can be employed to separate branched chain hydrocarbons from straight chain hydrocarbons, aromatic hydrocarbons from branched or straight chain hydrocarbons, etc. Separations of olefins from paraffins using selected modified molecular sieves have been reported (119-125), from the vapour phase, the adsorbed components being subsequently desorbed by displacement (using light hydrocarbons) or by pressure swing techniques. Priegnitz (126) has reported the separation of butene-1 from butene mixtures by selective adsorption on Ba^{2+} or K^{+} exchanged zeolites X and Y. In comparing the C_4 mono-olefinic isomers, namely butene-1, cis and trans-2-butene and isobutylene, it is found that butene-1, has the lowest octane rating of the group. It is therefore preferable to remove this component from olefinic mixtures to be used as gasoline fuels. The use of this process allows the separation of butene-1 from the other C_4 mono-olefins and allows a higher octane rating to be obtained.

Peck (127) has reported the separation of olefinic hydrocarbons from saturated hydrocarbons from liquid-phase using molecular sieves. The process was particularly suitable for separating hydrocarbons of three classes. The first class comprises hydrocarbons containing olefinic double bonds which are not isomerized, e.g. an α-olefin of from 4 to 20 carbon atoms or a diolefin. The second class comprises acylic hydrocarbons of from about 10 to about 20 carbon atoms, and the third class comprises hydrocarbons of up to about 20 carbons containing at least one cyclic moiety, i.e. alicyclic compounds and compounds containing an aromatic ring, both of which cannot be readily separated by known processes. The process was performed at room temperature and atmospheric pressure conditions. The mixture to be separated is fed to the top or bottom of the sieve bed and an effluent consisting of olefin-free material recovered. When olefin-breakthrough becomes apparent, or exceed the desired level, the feed to the bed is stopped and the desorption cycle is begun. Instead of stationary beds, moving or fluid beds of molecular sieves can be employed. In addition, several beds may be employed in parallel to provide for a substantially continuous overall operation. Desorption was effected

by draining the bed of unadsorbed hydrocarbons and washing the bed with a highly polar material, such as water, ethers, alcohols and the like. Peck (127) quotes 15 different examples of separating various molecules from the liquid-phase on A and X type zeolites.

Adsorption from the gas phase on many different types of zeolites has been extensively studied by many workers. However, some recent binary gas mixture adsorption on molecular sieves will be discussed. Veyssiere et al (130) studied adsorption of CH_4 + C_2H_6 and CH_4 + CO on molecular sieves (two zeolitic type A and one carbon). Pure gas adsorption isotherms were firstly determined at 298K on all three sieves at pressures up to 30 bar. Adsorption equilibria of the two binary gas mixtures were then studied at 298K. It was found that for the CH_4 + C_2H_6 system; C_2H_6 was adsorbed more than CH_4 in all sieves studied, and this selectivity was enhanced in the case of carbon. Whereas for the CH_4 + CO system, carbon exhibits the opposite selectivity compared with zeolitic sieves i.e. CH_4 was prefered by carbon. This information was ascertained after calculating adsorption phase diagrams of the binary mixture as it is practically impossible to anticipate such a result from considerations restricted to single component adsorption isotherms. Myers and Prausnitz (131) used a simple approach based from single component data to predict binary mixture adsorption equilibria. Ideal Adsorption Solution Theory (I.A.S.T.) was proposed by them; based on the assumption that the sorbed mixture forms an ideal solution at constant spreading pressure. The proposal has been widely used (1, 132, 133) to calculate the total amount adsorbed for a gas mixture from only the pure component data on the same adsorbent at the same temperature.

Vansant and Voets (134) studied adsorption of pure (CO, CO_2 and CH_4) and binary gas mixtures (CO + CO_2, CO_2 + N_2 and CO_2 + CH_4) on ion-exchanged mordenite at three temperatures. No evidence of enhanced sorption of one component over the other was found. Adsorption of gas mixtures on different exchanged mordenites reveals that the separation ability increases with increasing electrostatic field in the adsorption cavities. The effect of the nature of the entering gas molecules on the separation is dependent on the nature of the exchangeable cations. To a first approximation, the difference in isosteric heats of adsorption of the pure components is a measure of the separation possibility. The separation of gas mixtures increases significantly with

decreasing adsorption temperature. This probably is due to the heterogenity of the adsorbed site being more pronounced when the adsorption temperature decreases. This change in heterogenity is probably caused not only by cation - sorbate interaction but also by important different lattice-sorbate and sorbate - sorbate interactions. The best separations of gas mixtures into their pure components was observed at low percentage of CO_2 in the residual gas phase and at high total equilibrium pressures.

Bülow and Kärger (135) have studied the sorption behaviour of heptane - benzene mixture in zeolite NaX. They have shown that by variation of sample, pellet and crystal sizes of zeolite, mixture uptake can be controlled by various processes, different, in general, from intracrystalline diffusion. By contrast, n.m.r. pulsed field gradient technique allowed an unequivocal determination of the self-diffusion behaviour of the single components in the interior of the zeolite crystals. Marutovskii et al (136) have studied intradiffusion kinetics of the adsorption of a binary mixture in microporous zeolite crystals. A theoretical model was derived using adsorption of benzene and heptane on NaX as an example. They found that in the case of the more weakly adsorbing component of the mixture, the kinetic curve for inner diffusion mass exchange does not coincide with the curve of this compound when adsorbed as a pure component. Further adsorption of gas mixtures on solids has been studied by Bülow (137); and sorption kinetics of n-alkanes vapour mixtures on synthetic zeolites by Longaver et al (138).

Recently Harlfinger et al (142) have investigated the adsorption behaviour of a butene gas mixture on potassium modified X and Y molecular sieves. With increasing K^+ content per supercage, an inversion of breakthrough for the single components was observed. The change of breakthrough occurred between cis-2-butene and 1-butene; i.e. cis-2-butene was strongly held by NaX, whilst 1-butene by KX. Adsorption of the three n-butene isomers on zeolites with different degrees of potassium exchange allowed one to postulate the appearance of K^+ cations in the supercage. It was concluded that in the supercage of the dehydrated zeolite, the K^+ cations occupy first the sites II and then sites III. Further work on the effect of cation combinations on the adsorption behaviour of C_4 hydrocarbons has been reported (143).

Benashvili (144) has studied the adsorption separation of isomeric xylenes over Na, H and Ca X type zeolites at 200°C, and found that o- and

m-xylenes are mainly adsorbed on the stated zeolites, while the content of p-xylenes increases in the non-sorbed fraction. Separation efficiency increases in the following order: NaX < HNaX < CaNaX. Guth et al (145) report the influence of thermodynamic factors governing adsorption of p-and m-xylene onto faujasite zeolite containing Na^+ and K^+ cations. Differences in entropy of adsorption obtained from the two ion-exchanged cations was found to be responsible for the selectivity of each isomer. The different interaction energy for a sorbed molecule in a zeolite depends upon the nature and extent of the following interactions: adsorbate-adsorbate, cation-adsorbate and oxygen -adsorbate. The relative extent of these interactions varies with the structure and cations of the zeolite. Dubinin and Astakov (146) suggest that adsorbate-adsorbate interactions are generally weak (147) and only need to be taken into consideration in the case of low-energy interactions. For example, this may occur when the molecules are small in relation to the accessible volume. The molecules occupying the middle of the cavities are not in direct contact with the zeolite, only the dispersion forces need to be considered and these molecules must therefore behave as in the liquid state. The cation-adsorbate interactions are related to the location of the cations (147, 148). These interactions increase as the cations become small, charged, non-screened; in addition, in the case of adsorbed molecules with dipolar, quadrupolar moments, or π-systems, the interactions are enhanced (2, 84). In fact, these strong interactions are able to lock the molecules onto the adsorption sites. The extent of the oxygen-adsorbate interactions increases as the adsorbate draws nearer to the oxygens, and also when it displays $\overset{\alpha}{\wedge}$π-cloud. The repulsion between the π-cloud of the adsorbate and the negative charge of the oxygen results in a strengthening of the intramolecular bonding (145, 147). Finger and Bülow (149) have studied the influence of lattice-sorbate and cation-sorbate interaction on La^{3+} X and Y zeolites. The supercages of these zeolites in contrast to NaX and NaY zeolites are almost completely cation free leaving sorbed benzene molecules to interact with the zeolitic framework, only. El-Akkad et al (166) have studied the correlation of heats of immersion of 3A, 5A and 10A zeolites with their adsorption characteristics in polar and non-polar liquids. The cyclohexane uptake of the 10A zeolites was much greater than that of 3A and 5A zeolites. The large size of the cyclohexane

molecule limits its sorption in the narrow pores. Hence the heats of immersion in cyclohexane were much lower than those in water and were in the order 10A > 5A > 3A and in water 3A > 5A > 10A demonstrating a correlation between pore narrowing and increased energetic interaction in polar wetting liquids.

Bosacek (151) has studied the role of cations in chromatography and adsorption of gases on X-type zeolites. Potassium and calcium ions were used, and measurements of Kr, CH_4, N_2 and CO showed that cations located in the zeolite lattice in positions easily accessible to the adsorption behaviour, in particular of the N_2 and CO molecules, where a strong interaction, either of electrostatic or of specific origin becomes effective. Upto about 40% K^+ exchange; the K^+ preferentially occupy site III positions in the large cavities. On the other hand, at small Ca^{2+} concentrations in the zeolite, the Ca^{2+} cations are in site I positions. So the potassium exchanged zeolite shows preference for molecules capable of either electrostatic or specific interactions whereas with Ca^{2+} exchanged zeolite, these properties are only attained at higher Ca^{2+} concentrations. Extensive research regarding use of zeolites as stationary phases in chromatography has been reported in the literature.

Laperashvili (152) has determined the conditional chromatographic polarity of various zeolites (X, Y, L, O, E and M) and their cation exchanged forms (Li^+, Na^+, K^+, Rb^+, Cs^+, Ag^+, Mg^{2+} etc) using the method of Rorshnaider (153). The adsorbents were used to separate binary mixtures of O_2 and N_2 (both having different quadrupole moment and electronic structures); and the relative polarity of the adsorbents were determined by graphical method (plot of log of the ratio of Retention volumes of two substances on conditional chromatographic polarity of adsorbents). It was found that the polarity of adsorbents depends to a great extent on the type, structure and cation modification of adsorbents. Zeolites with higher $Si/_{Al}$ ratio have larger polarity (e.g. E and M). Zeolite Y shows the following order of relative polarity:

Ag >> Na > Li > K > Rb > Cs > H

Ca > Sr > Ba > Cd > Mg

and zeolite X: Ca > Fe > Ni.

The high polarity of the Ag form is due to the high polarity of the Ag^+ ion. The increase in polarity of divalent forms of X and Y zeolites can be explained by increase in electrostatic energy between the electrical field of the divalent cation and the N_2 atom. Also the potential of the electrical field is greater with divalent cations compared to univalent cations.

The second part of discussion concerns adsorption of organic molecules from liquid phase solutions on zeolites. This aspect has been studied by many workers using many different types of molecules and zeolites; a few are discussed.

Sundstrom and Krautz (159) have studied the adsorption of normal paraffins (heptane, decane, dodecane and tetradecane) from liquid phase on type 5A molecular sieves to determine the effect of molecular size, temperature, and concentration on the equilibrium loadings. Single component loadings were obtained by adding a material with an effective molecular diameter larger than 5A (e.g. $CC\ell_4$ or 1, 1, 2, 2,-tetrachloroethane) with the n-paraffin. Also binary data were obtained by contacting mixtures of known compositions and weight with known quantities of molecular sieves. Preferential adsorption of one of the components resulted in a change of composition of the liquid in contact with the sieves. Their single component adsorption capacities varied irregularly with molecular size and were independent of temperature when loadings were expressed on a volume basis. However, for binary systems, the paraffin with the lower molecular weight was preferentially adsorbed. This was determined mainly by steric factors (49). The shorter chains are better able to satisfy the steric requirements for aligning with and entering the cavities. Temperature had a negligible effect on the composition of adsorbate in equilibrium with a given liquid composition.

Gupta et al (160) have studied liquid phase adsorption of n-paraffins (pentane, hexane, heptane and octane) from benzene (non-adsorbed) on 5A molecular sieve, to determine the effect of temperature and concentration on equilibrium loading. On a mole basis, the adsorption was higher for lower molecular weight paraffins, the reason being that both physicochemical adsorption and steric effects are important. Since type 5A molecular sieves have a pore opening of 0.5 nm and n-paraffins have a critical diameter of 0.49 nm, steric effects will play an important role. In shorter chain compounds (lower molecular weight n-paraffins) steric effects will be less in

comparison to larger chain compounds. The effect of temperature on equilibrium loading decreased with increasing molecular weight. The effect of concentration on equilibrium loading was most significant for n-pentane, decreasing with increase in molecular weight. The time required for the attainment of adsorption equilibrium increased with decreasing temperature; as adsorption is a mass transfer process and increasing the temperature increases the mass transfer coefficient, resulting in the steady state being reached earlier. Adsorption isotherms for individual paraffins in benzene adsorbed on 5A molecular sieve showed that adsorption decreased with increasing temperature over the equilibrium concentration range studied.

Satterfield and Cheng (161) studied liquid sorption equilibria of selected binary hydrocarbon mixtures on large pore zeolites (e.g. Y) of interest in catalysis. Highly selective adsorption from a binary liquid system can occur on molecular sieve zeolites when both components have full access to the entire fine pore structure. The adsorption is caused by the relative affinity or interaction energy of the molecules for the zeolite structure. On NaY aromatic compounds were selectively adsorbed over paraffins and naphthenes. Those aromatic compounds which have the smallest and most compact structure, e.g. benzene and cumene were selectively adsorbed over larger aromatics, e.g. 1,3,5,-triisopropylbenzene. Separation factors on HY between aromatic molecules, paraffins, and naphthenes were less than on NaY due to the lower interaction energy between HY and aromatics. Sorptions of n-paraffins on 5A type zeolite (159) were compared with those on NaY zeolite (162). Whereas steric effects played a dominant part on 5A zeolite, this effect was found to be less pronounced on NaY zeolite. A brief study with cyclooctane showed that it was preferentially adsorbed on NaY from mixtures with n-octane ($K = 3.2 \pm 1.0$). It has been reported (161) that trans and cis decalins were also found to be adsorbed preferentially on NaY from mixtures with n-decane ($K = 13$ and 6.3, respectively). These two observations suggest that a cycloparaffin in general may be the preferentially adsorbed component from a mixture with the n-paraffin of the same carbon number.

Steric effects cannot explain this and the cyclic structure must cause some physico-chemical effect more strongly than that existing with the n-paraffins. The results with the n-paraffin binary systems on NaY suggested that the packing characteristics of the higher molecular weight paraffin rather than physico-chemical properties play a dominant role in the adsorption selectivity on a zeolite. For both molecular sieves (5A and NaY), it was ascertained that dodecane appears to have a relatively more favourable packing in the zeolite cavities than does decane or tetradecane.

Dessau (163) has studied selective sorption properties of intermediate pore size zeolites such as ZSM-5 and ZSM-11. These zeolites have a high silica/alumina ratio and contain two intersecting channel systems composed of 10-membered oxygen rings. The channels in these zeolites are elliptical, with a free cross-section of 5.5 x 5.1 for the linear channels, and a cross-section of 5.6 x 5.4 for the sinusoidal channels in ZSM-5. Both ZSM-5 and ZSM-11 exhibited unusual properties compared to A and Y zeolites in n-paraffin adsorption. Zeolites ZSM-5 and ZSM-11 showed preference for paraffins to aromatics - with the higher molecular weight paraffin preferred over the lower. This difference may be due to the fact that, unlike A and Y zeolites, ZSM-5 contains no large cavities in which n-paraffins can coil around themselves. The coiling of high molecular weight paraffins inside A and Y zeolites results in additional entropy loss upon sorption, thereby reversing the normal order of preferential sorption of the higher molecular weight component. The relatively narrow and uniform channels in ZSM-5 prevent the n-paraffins from coiling about themselves, thereby re-establishing the expected preferential sorption of the higher molecular weight component. Zeolite ZSM-5 also differed considerably from large-pore zeolites mordenite (164) and faujasite (161, 162) in selective separation of n-paraffins relative to branched cyclic hydrocarbons. With ZSM-5, the normal n-paraffin was preferred, in contrast to mordenite and faujasite, where preferential sorption of the cycloparaffin was generally observed.

Becila et al (165) have studied kinetics of simultaneous adsorption of methanol and ethanol from liquid mixtures by type A zeolites with different

ratios of potassium to sodium. They concluded that non-steady-state diffusion occurs in the zeolite pores during adsorption. Adsorption isotherms were described by the Langmuir equation. It was found that adsorption selectivity for methanol increases with increasing amount of potassium exchange and was complete at 45% exchange.

Herden (167) has studied adsorption of tetradec-1-ene/dodecane mixtures on potassium exchanged X and Y zeolites from the liquid phase. Separation factors were determined at 293K. A sharp decrease in separation factor and in limiting adsorption capacity was observed between 20 and 50% exchange of Na^+ by K^+. This indicates that K^+ in site II has an influence on adsorption capacity. Work carried out by Hansjörg et al (168) regarding adsorption of mixtures of alkenes and alkanes of medium chain length on X and Y zeolites show that adsorption and separation depend on the nature and location of the zeolite cations. The excess isotherms were determined on NaX, KX and KY and showed almost a decrease of ~ 30% in limiting adsorption capacity in going from Na^+ to K^+ form. They also report limiting adsorption capacity and separation factors on Ba^{2+} and Ca^{2+} forms of zeolite X, however no mention of isomerization of tetra-dec-1-ene was reported on these zeolites due to the formation of hydroxyl groups. The heats of immersion were also determined and were found to be higher for alkenes than alkanes due to interactions with adsorption centres. Hansjörg (169) studied adsorption of n-hexane/n-olefin binary mixtures of liquid solution on NaX zeolite. The n-olefins used were C_6, C_8, C_{10}, C_{12} and C_{14} and from the excess isotherms it was found that the limiting adsorption capacity of the n-olefins decreased with increasing chain length. A maximum for the system decaline/n-paraffin 5A zeolite (170) was not found. Satterfield and Smeets (162) found that the lower molecular weight paraffins was adsorbed preferentially to the higher molecular weight paraffin, which is opposite to Traube's rule, and a minimum in K occurred with the n-paraffin of intermediate carbon number (e.g., dodecane). The explanation for the minimum was favourable packing of dodecane in the zeolite cavities. Schirmer et al (171) reported separation factors for n-heptane, n-nonane and n-undecane relative to normal paraffins in sorption from the vapour phase. Their results were correlated by the expression: $\ln K = an + b$ where a and

b are constants and n is the carbon number. An analogous behaviour was found by Ali (172) in the system benzene/n-nonane/n-paraffin 5A zeolite in the liquid phase. The results of n-hexane/n-olefin experiments were found to have a linear correlation between the logarithm of the separation factor and the olefin chain length, according to Traube's rule. Such behaviour is typical not only for systems with compounds of the same homologous series but also for mixtures of components with similar chemical properties. The empirical correlation is valuable for estimation of separation factors in practice.

The literature survey regarding sorptions from gas and liquid phase can now be correlated with results from hexene isomers separation studies. It is clear from the survey that the nature and location of cations play a significant role in selective adsorption studies. Results from adsorption of various hexene isomers dissolved in n-heptane on Na^+, K^+ and Cs^+ exchanged X and Y zeolites showed how the significance of various factors, e.g. (1) SiO_2/Al_2O_3 ratio, (2) nature, size and degree of cation exchange, (3) moisture content and (4) the different inter-cation energies between the zeolite and isomer configuration, affected selectivity for the preferred isomer. Selectivity, for the preferred isomer was influenced by the type and moisture content of the zeolite.

Firstly, discussing results from 1-hexene:trans-2-hexene in heptane, for the X case: increasing the cation size and partial dehydration showed a reverse in selectivity i.e. NaX preferred 1-hexene (K = 1.4(4)), CsX (49) preferred trans-2-hexene (K = 0.4(5)). KX showed no essential preference for any isomer. Complete dehydration showed a decrease in separation factor, but preference for 1-hexene was attained i.e., for NaX, KX, and CsX (49), K = 2.0(2), 1.6(2), and 1.0(9) respectively. In the case of Y zeolite, under same conditions, selectivity for trans-2-hexene was indicated, i.e. K = 1.0, 0.6, 0.3(2) and 0.9, 0.3(2) and 0.4(9) for NaY, KY and CsY (61) at partial and complete dehydrations respectively.

For 1-hexene: cis-2-hexene in heptane on the same zeolites and conditions, the X forms showed preference for cis-2-hexene at partial

dehydration; i.e. K = 0.7(1), 0.6(9), and 0.3(5) for Na^+, K^+ and Cs^+ respectively, and K = 1.1(1), 1.6(9), 1.6(1) at complete dehydration; i.e. preference for 1-hexene. For Y forms, they were selective for cis-2-hexene at both dehydration conditions i.e. K = 0.7(1), 0.5(8), 0.3(4) and 0.6(8), 0.4(8), and 0.5(6) for Na^+, K^+, Cs^+ forms respectively the former K values are for the partially dehydrated zeolites.

For 1-hexene: trans-3-hexene in heptane, partial dehydration showed interesting features, viz: K = 0.8(6), 2.0(7) 0.7(1) for NaX, KX and CsX (49); whereas complete dehydration showed a decrease in separation factor, but preference for 1-hexene, i.e. K = 3.3(5), 1.3(2) and 1.7 for Na^+, K^+ and Cs^+ forms respectively. For Y forms, partial dehydration showed K = 1.2(1), 0.4(7), 0.3(5) and complete dehydration K = 1.2(4), 0.1(5), 0.5(1) for Na^+, K^+ and Cs^+ respectively, i.e. increasing cation size influenced preference for the more symmetrical isomer.

These sorption studies suggest that there is competition of the respective isomer for the sorbed sites at the two dehydration conditions, and the isomer that interacts more strongly with the zeolite (dependent on factors mentioned) is adsorbed preferentially. To explain this competition, a knowledge of sorption capacities of these isomers when loaded individually in n-heptane was required. This was carried out for the isomers mentioned on NaX, NaY and KY(sec 6.4). It was found that the Na^+ form of X and Y zeolites showed preference for cis-2-hexene (142) whilst K^+ form of zeolite Y for trans-2 and 3-hexene. So replacing Na^+ by K^+ in zeolite Y, showed an inversion of breakthrough for the individual components. Adsorption of 1-hexene:trans-2-hexene in heptane on partially replaced Na^+ by K^+ at both dehydrating conditions, ascertained a sharp decrease in separation factor between 20 and 50% exchange, i.e. as K^+ exchanges for Na^+ in site II (supercage), preference for trans-2-hexene was indicated (168).

From a knowledge of the sorption capacities of each isomer on a specific zeolite, an explanation for competitive sorption of the respective isomer can be ascertained. This information is useful to predict selectivity

for a particular component in a mixture (130 - 143). Steric factors seem to be most responsible in the present studies which inturn influence packing characteristics of the hexene isomers in the zeolite cavities. An important factor which would influence the packing would be the interaction of π-electrons with the polarity of the cation or SiO_2:Al_2O_3 ratio. High SiO_2:Al_2O_3 ratio zeolites have large polarity; and it has been shown (152) that in zeolite Y, the polarity of univalent ions is as follows: Ag >> Na > Li > K > Rb > H.

Adsorption studies of 1-hexene: trans-2-hexene in methylcyclohexane as solvent at both dehydrating conditions showed the effect of cyclic molecules on adsorption. Only NaX, KX, NaY and KY were used to compare with those obtained from heptane as solvent. For NaX and KX, partial dehydration showed K ≈ 1.0 for both zeolites, whilst complete dehydration showed K = 0.9(1) and 0.4(4) for NaX and KX respectively. For NaY and KY, 1-hexene was preferred by NaY (K = 1.5(9)), whilst trans-2-hexene by KY (K = 0.9(4)) at partial dehydration. Complete dehydration showed preference for 1-hexene; K = 2.5(6) and 1.3(8) for NaY and KY respectively. These results were compared to those when heptane was used as solvent. Differences were in: (1) complete dehydration NaX (K = 2.0(2)), KX (K = 1.6(2)) and (2) partial dehydration; NaY (K = 1.0), KY (K = 0.6); complete dehydration; NaY (K = 0.9), KY (K = 0.3(2)). So a change in shape of solvent has affected selectivity in both forms of X and Y zeolites. This possibly can be attributed to the fact that cyclic molecules are adsorbed much more strongly in the zeolite compared to the linear paraffins. It is unlikely that steric effects are responsibile for this phenomena; but the cyclic structure must cause some physico-chemical effect which is much more stronger than that existing in the linear paraffin (161). As has already been discussed that adsorption in zeolite depends on moisture content. A variation in separation factors for the three isomeric hexene mixtures adsorbed on the same zeolites was observed, when they were calcined (T_c) at the same temperature and length of time in vacuum (i.e. at 350 ± 5°C, ~ 24 hr pressure ~ 10^{-6} torr). They are summarized on the following page:

Zeolite	Air T_c $\frac{K_{1\text{-}C_6H_{12}}}{t\text{-}2\text{-}C_6H_{12}}$	Vacuum T_c $\frac{K_{1\text{-}C_6H_{12}}}{t\text{-}2\text{-}C_6H_{12}}$	Air T_c $\frac{K_{1\text{-}C_6H_{12}}}{c\text{-}2\text{-}C_6H_{12}}$	Vacuum T_c $\frac{K_{1\text{-}C_6H_{12}}}{c\text{-}2\text{-}C_6H_{12}}$	Air T_c $\frac{K_{1\text{-}C_6H_{12}}}{t\text{-}3\text{-}C_6H_{12}}$	Vacuum T_c $\frac{K_{1\text{-}C_6H_{12}}}{t\text{-}3\text{-}C_6H_{12}}$
NaX	2.0(2)	2.4(3)	1.1(1)	1.1	3.3(5)	3.5(3)
KX	1.6(2)	2.1(9)	1.6(9)	2.0(6)	1.3(2)	1.7(2)
CsX(49)	1.0(9)	1.1(1)	1.6(1)	1.4(3)	1.7	1.3(2)
NaY	0.9	0.9(1)	0.6(8)	0.7(9)	1.2(4)	1.5
KY	0.3(2)	0.3(7)	0.4(8)	0.7	0.1(5)	0.1(8)
CsY(61)	0.4(9)	0.6(3)	0.5(6)	0.5(7)	0.5(1)	0.5(9)

1 - C_6H_{12}- 1-hexene

t - 2 - C_6H_{12}-trans-2-hexene

c - 2 - C_6H_{12}-cis-2-hexene

t - 3 - C_6H_{12}-trans-3-hexene

The variation in separation factor for some zeolites tend to suggest that the random distribution and removal of water molecules from supercages and sodalite cages is a function of the method of calcination. The amount of water molecules/unit cell that are left in the zeolite after dehydration from two methods is very unlikely to be similar, and hence the variation.

In another experiment, sec. 6.3 varation of $\frac{K_{1\text{-}C_6H_{12}}}{t\text{-}2\text{-}C_6H_{12}}$ as a function of number of water molecules/unit cell on NaX and NaY was investigated. The zeolites were calcined in vacuum at various temperatures (from 25° to 350°C) for ~ 24 hr at 10^{-6} torr. The separation factor was found to decrease with increasing amount of water left in both zeolites. However, uptake of isomers followed different relationships; exponential for NaX and linear for NaY, indicating the effect of dehydration on various zeolites. So it has been ascertained from this work that water in zeolites plays a very critical part in adsorption.

Adsorption of the more closely related isomers on NaX, KX, NaY and KY revealed the competitive nature of each isomer sec 6.5. Adsorption of cis-2-hexene: trans-2-hexene in heptane on these zeolites calcined in vacuum (T_c = 350°C, 24 hr, 10^{-6} torr pressure) showed the following: NaX preferred cis-2-hexene (K = 1.6(2)), KX preferred trans-2-hexene (K = 0.9(4)), NaY and KY showed preference for trans-2-hexene, (K = 0.9(1) and 0.3(8)) respectively. Adsorption of cis-2-hexene: trans-3-hexene in heptane on the same zeolites showed: NaX and NaY preferred cis-2-hexene (K = 1.6 and 2.1(9)) respectively, whilst KX and KY preferred trans-3-hexene (K = 0.8(5) and 0.2(6)) respectively. So these studies reveal the importance of sorption capacities when determining selective separations. It can be concluded in the present studies that K^+ in X and Y zeolites is selective for trans-2- and -3-hexene; and the effect is much more pronounced in KY then in KX. Separation factor was also found to be dependent on the concentration of each isomer loaded sec 6.6. Studies on NaX adsorbed with various concentrations of 1-hexene: trans-2-hexene in heptane showed that $\frac{K_{1\text{-}C_6H_{12}}}{t\text{-}2\text{-}C_6H_{12}}$ increased with increasing concentration of each isomer (in 1:1 ratio); but decreased as the ratio of the preferentially adsorbed

isomer increased. So separation factor is concentration dependent which agrees very well with work reported in literature.

The generation of weak acid sites on Li^+ exchanged X and Y zeolites has been ascertained from isomerization studies of 2-methyl-1-pentene, sec 6.7. LiX (56), NaX and NaY showed isomerization to 2-methyl-2-pentene, whilst polymerization occurred on LiY (57). The zeolites were calcined at 350°C for 24 hr in air. Isomerization of 1-hexene to trans-2-hexene was found only on LiY (57). Adsorption studies of 1-hexene: cis-2-hexene in heptane and 1-hexene: trans-2-hexene in heptane on Li^+ exchanged zeolites showed that at partial dehydration both zeolites were selective for cis-2-hexene (K = 0.4 and 0.6(9)) and trans-2-hexene (K = 0.5(7) and 0.8) respectively. LiX(56) at complete dehydration showed preference for 1-hexene in both experiments, (K = 1.0(9) and 1.6(1)).

In conclusion to the present work as far as adsorption studies are concerned, there is fair evidence correlating with the literature survey regarding the factors and principles responsible in adsorption. It has been shown how the cation type, size, location, framework structure, SiO_2: Al_2O_3 ratio and moisture content affect selectivity for a particular isomer. Steric considerations remain the top priority in the present studies.

The final part of discussion will be devoted to isomerization reactions over zeolites, with emphasis on adsorption and double bond shifts in olefins.

Several workers have studied isomerization reactions on zeolites, and a few have already been discussed. However, further discussion will be adequate enough to reveal the importance of zeolites as catalysts.

Eberly (173) studied the adsorption of 1-hexene on hydrogen faujasite (HY) and at 93°C, the double-bond character was found to disappear. At 150°C, polymerization and dehydrogenation processes began to occur to form a conjugated polyene type of structure as evidenced by a band at 1600 cm^{-1}. Upon heating to 260°C, cyclization occurred to form a hydrogen-deficient aromatic ring structure characterized by a

band at 1580 cm^{-1}. The main effect of interaction of 1-hexene with other ion-exchanged faujasites was the loss of double bond character in the adsorbed material. The OH groups formed on dehydration of HY zeolite absorb at 3740, 3635 and 3540 cm^{-1}. The groups at 3740 cm^{-1} are almost universally observed on silica-containing materials and are not believed to be necessarily characteristic of HY. The groups at 3635 cm^{-1} are believed to be located inside the adsorption cages near six-membered oxygen rings. The other groups at 3540 cm^{-1} are in inaccessible positions located between two sodalite units. The assignment of the lower frequency to the bridge position is consistent with the possibility of the proton being able to interact with twice as many oxygen anions as its counterpart in the cage position. Also, it explains the preferential interaction of olefins with the 3635 cm^{-1} band.

Adsorption of butenes on NaY and dehydroxylated Y zeolites by i.r. spectroscopy was studied by Datka (174). Butene molecules were found to be bonded to electrophilic acid sites (Na^+ ions or Lewis-acid sites) by their π-electrons. The interaction of butene molecules with Lewis-acid sites resulted in an increase in the extinction coefficient of the band for the anti-symmetric stretching vibration of the CH_3 group thus indicating an increased polarization of the C-H bond. The rates of desorption of the butenes from NaY or dehydroxylated zeolites increased in the sequence 1-butene < cis-2-butene < trans-2-butene. These differences were explained by considering steric factors (i.e. accessbility of π-electrons for interaction with the sorption sites and the effect of CH_3 group on polarization of C-H bonds).

Förster and Seelemann (175) have studied adsorption and isomerization of butenes on A type zeolites containing Zn^{2+}, Ag^+ and Co^{2+} ions at room temperature by i.r. spectroscopy. In the hydrated samples two kinds of water can be distinguished: unspecifically adsorbed water and water specifically interacting with the cations. After complete dehydration no hydroxyl groups were observed in the i.r. spectra. The penetration rate of the butenes was found to follow the sequence trans-2-butene > 1-butene > cis-2-butene and sensitive to SII sites. There

was restricted rotation of the butenes upon adsorption. In addition to the donor bond, there is back-donation from the cations into anti-bonding π*-orbitals of the butenes. While Ag^+ - containing A-type zeolites were catalytically inactive due to the small charge: radius ratio of the cations, on zeolites exchanged with Zn^{2+} ions spontaneous isomerization was observed, which was enhanced on samples containing a non-stoichiometric excess of zinc. Addition of the cocatalyst SO_2 greatly increased the isomerization rate. Isomerization of butenes cocatalysed by SO_2 was also studied on ZnX (176), on which a different reaction pathways for cis/trans-isomerization via adsorption on exposed zinc ions and double-bond shift from 1-butene to 2-butene via carbonium ions, formed on hydroxyl groups, are assumed. Different behaviour for A- and X-type zeolites was also observed by Kladnig and Noller (177) in the dehydrohalogenation of 1- and 2-chlorobutene. Their results were interpreted in terms of an E1 mechanism via carbonium ions on X-type zeolite and in terms of an E2 mechanisms following a concerted reaction on A-type zeolite. On ZnA zeolites, the reaction was first order in both butene and SO_2 and is in accord with the concerted reaction mechanism which has been shown to occur on A-type zeolites exchanged with alkali and alkaline earth ions.

Lombardo et al (110) have studied the catalytic activity and selectivity of group IA-Y zeolites for n-butene isomerization by substituting small amounts of Ca^{2+} for $2Na^+$, by creation of a cation deficiency by hydrolysis, and by major exchange of the original Na^+ by either K^+ or Li^+. Isomerizations were studied with and without added H_2O as a cocatalyst. As the Ca^{2+} content (acidity) was increased, cis-trans isomerization of the 2-butenes was enhanced, relative to double-bond migration. At constant calcium content the activity increased with small additions of H_2O, but reached a constant maximum above $10 H_2O/Ca^{2+}$. Major substitution of either K^+ or Li^+ for Na^+ modified the activity of the sample, but to a lesser extent than by Ca^{2+} substitution.

Hoser and Krzyzanowski (178) studied isomerization of n-butenes and 3,3,-dimethyl-1-butene over cobalt exchanged zeolite X at various degassing and reaction temperatures. The Co^{2+} ions are believed to occupy

positions I', II' and II in the structure where they acquire tetrahedral symmetry by interacting with three lattice oxygen atoms and with the hydroxyl group. The spectrum attributable to the tetrahedral cobalt decreased in intensity as the degassing temperature was raised. This, together with the associated dehydroxylation, were thought to be explicable in terms of migration of the Co^{2+} ions to position I within the hexagonal prisms (to acquire therein octahedral symmetry) and of formation of Co-O-Co groupings. A very small increase in catalytic activity was accompanied by the initial Co^{2+} ions in the zeolite lattice. Only when the degree of exchange had exceeded ~ 28%, catalytic activity increased rapidly, in a nearly direct relation to the degree of exchange. The active centres consisted of hydroxyl groups that arise by residual water molecules being split on the tetrahedral-coordinated Co^{2+} ions. Their relative rate constants on CoX zeolites showed that double-bond shift was strongly favoured compared to cis-trans isomerization. The initial cis: trans ratios for CoX zeolite was equal to or slightly higher than one. In the case of 3,3,-dimethyl-1-butene, isomerization over CoX zeolites, the formation of 2,3,-dimethyl-2-butene was distinctly favoured. The catalysts degassed at 473K were found to be much more active than those having identical cobalt ion contents and degassed at 673K. This was due to the suppression of acidic properties in higher exchanged Co^{2+} zeolites degassed at 673K. A mechanism involving a secondary carbonium-ion intermediate was in good support for the observed isomerizations.

Barthomeuf (179) has reported that some zeolite properties (e.g. acidity), are relevant to collective framework interactions and depending on atoms or ions in the structure (Si, Aℓ, OH, cations). A detailed survey on various aspects of acidity related to catalytic properties has been illustrated by looking at the influence and importance of the framework constituents in view of localized sites and of overall properties. Emphasis are on protonic sites which are more important in carbonium-ion formation.

Venuto (180) has reported synthesis, reactions and interactions of olefins, aromatics and alcohols in molecular sieve catalyst systems.

At low temperatures, hydrogen bonding of the π-electron systems of simple olefins with the protons in hydrogen zeolites has been observed. At higher severities, however, proton transfer and isotopic exchange can occur. Pore mouth catalysis and reverse molecular size selectivity ("the faujasite trap") have been observed in the reactions of low molecular weight olefins at relatively low temperatures.

Zhavoronkov at al (181) have studied isomerization of 1-hexene using the following cations: HY, CaY, LaY and YY and amorphous aluminosilicate at 100-200°C. It was found that 1-hexene was converted to cis/trans-2-hexene and 3-hexene at the same time by parallel routes. The ratio of the rate constants of the formation of cis-2-hexene and trans-2-hexene and 3-hexene and 2-hexene showed that with the rare-earth form of zeolite Y, increasing the percentage exchange of Na^+ resulted in a decrease in activity of isomerization of zeolite. At high percentage exchange of Na^+ the isomerization activity changed according to the following order: CaNaY-84 > LaNaY-96 > YNaY-94 (i.e. inversely proportional to the polarization activity ($e/_r$) of the multivalent cations). In all catalysts the formation of 3-hexene is slower than 2-hexene. The ratio of rate constants of the formation of cis and trans-2-hexene on all catalysts was nearly one except LaNaY-67 and YNaY-63 where it was 0.7 and 0.6 respectively. This meant that isomerization of 1-hexene on amorphous aluminosilicate was processed through the formation of carbonium ion. For LaNaY-67 and YNaY-63 the low ratio of cis: trans-2-hexene formation may mean that the multivalent cations have taken part in isomerization. The observed variations suggest that isomerization of 1-hexene was processed on weak-acid centres. The rate determining step of the isomerization was the abstraction of proton from the carbonium ion and the desorption of the products, but not the intermolecular transferring of the hydride ion. At this rate determining stage the isomerization proceeds with the most weak centres of adsorption, i.e. the most weak acid sites. An increase in isomerization activity of amorphous aluminosilicate and HNaY-81 compared to other catalysts was due to the presence of a large amount of weaker acid sites on their surface.

Tonyvesa et al (182) studied isomerization of 1-hexene on alkali forms (Li^+, Na^+ and K^+) of Y type faujasites; and also the effect of SiO_2/Al_2O_3 ratio (2.8, 5.1, 7.6 and 13) on isomerization. The effect of the alkali metal cations revealed that the catalyst activity decreased with increasing cation size. LiY and NaY were the most active catalysts between 210-250°C. Products of isomerization of 1-hexene on all catalysts were double-bond shift and cis-trans isomerization. The content of cis-2-hexene in all conditions reached equilibrium very quickly and the amount of 3-hexene increased linearly with contact time. At any contact time, it was found that the amount of trans-2-hexene was always larger than cis-2-hexene. So the alkali metal forms behaved quite similar, mechanism of isomerization was the same; but catalytic activity are quite different. So the type of cation that is present in the zeolite framework influences catalytic activity. The ratio of SiO_2/Al_2O_3 on conversion of 1-hexene showed, the larger the ratio, the more active the catalyst and the lower the temperature range required for complete conversion. The activity is related to the increase of electrostatic field of the cation which intensifies the effectiveness of the catalytic centre. In summing up, the study revealed how these catalysts exhibit high catalytic activity, stability and selectivity in the transformation of double-bond and cis-trans isomerization of 1-hexene. Also, acidity of catalysts increases as the radius of the cation decreases, and as the SiO_2/Al_2O_3 ratio in the zeolite framework increases.

Irving, et al (184) studied the comparison of catalytic properties of zeolites with various SiO_2/Al_2O_3 ratios i.e. HZSM-5 (60:1), HFu-1 (22:1) and amorphous Silica-Alumina (10:1). HFu-1 has been discovered by I.C.I. (185) and is probably closely related to ferrierite whilst the ability of ZSM-5 is well known to convert methanol directly into a liquid-phase product usable as a motor gasoline (186). Isomerization of 1-butene was carried out to probe the nature of the active sites on the surface of catalysts. The ratio of cis- to trans-2-butene produced is governed mainly by the mechanisms of the isomerization, although superimposed upon this are the geometric constraints which arise because of the differing sizes of cis- and trans-2-butene when catalysts, such as zeolites, with molecular-

sieving properties are investigated. Isomerization of 1-butene to cis- and trans-2-butene on the catalysts activated at 673 K for 15 h was found to proceed according to first order reversible kinetics. The initial rates of reaction were found to be independent of the pressure of 1-butene to which the catalysts were exposed. Pumping at reaction temperature subsequent to an experiment and admission of a fresh sample of 1-butene yielded rates which were much lower than those for first experiment, the ratios being 0.24, 0.28 and 0.52 for HFu-1, HZSM-5, and SiO_2- Al_2O_3 respectively. Values for the cis: trans product ratios at 241K were 1.65, 0.86 and 0.78 for HFu-1, HZSM-5, and silica-alumina respectively, although they varied with temperature; cis: trans ratios for second runs on catalysts which had been evacuated at reaction temperatures were found to be lower than those for first experiments in the case of zeolites but unaltered for silica-alumina. This implies that the surface deposits formed on evacuation modify the active centres on the zeolites but not those of the SiO_2-Al_2O_3. The results on all three catalysts were consistent with a carbonium-ion mechanism for the isomerization and after a fast initial uptake of the butene by the catalyst, disappearance of 1-butene by two parallel routes to form (i) cis-and trans-2 butene and (ii) surface oligomers. It was suggested that both these reactions occurred on acidic centres. Isomerization of 1-butene on the same catalysts as a function of pretreatment temperature was also examined at various reaction temperatures. Activation energies were essentially constant for all three catalysts. However, the rate of isomerization was found to decrease with increase in temperature of activation beyond 600K for HFu-1 and SiO_2-Al_2O_3; this was attributed to the involvement of Brönstead acidity in the catalysis of 1-butene isomerization. Lewis acid sites are relatively inactive. However, activation energies suggest that the reaction sites are of the same type on all three catalysts. On HZSM-5 the activity did not fall at pretreatment temperatures above 600K. This was attributed to the higher stability of the hydroxyl groups (187) on HZSM-5. Isomerization on Lewis acid sites generated by condensation of hydroxyl groups at high temperatures is less likely.

Vedrine et al (188) have reported conversion of Brönstead into Lewis sites on HZSM-5 at 673 K. It is well known that the stability of hydroxyl groups correlates with the SiO_2: Al_2O_3 ratio, since a high ratio can on geometrical grounds be associated with a lower probability of dehydroxylation. Vedrine et al used a 22.5:1 ratio HZSM-5 sample and it is relevant that the pretreatment temperature corresponding to the maximum concentration of hydroxyl-groups used by them was similar to that of the maximum rate of reaction on HFu-1 used by Irving et al i.e. both having the same SiO_2: Al_2O_3 ratio. The initial cis- to trans-2-butene ratios reported by Irving et al showed that those in the range 1-2:1 found for most runs were further evidence of catalysis by Brönstead acid sites. High cis- to trans-2-butene ratios resulted from a Lewis acid catalysed 1-butene isomerization. Irving et al have concluded that the constant cis: trans ratios obtained over HZSM-5 provide further evidence of the lack of involvement of Lewis acid centres with the zeolite.

Isomerization studies as discussed by various workers suggest that Brönstead acid sites are the active centres for reactions; and can be ascertained readily by the values of initial cis: trans product ratios. Even though, isomerization kinetics revealed differences from gas and liquid phase, the cis:trans product ratios were in good agreement (~ 1.5:1 from liquid phase) to ascertain the importance of Brönstead acid sites. Isomerization studies of 3,3,-dimethyl-1-butene on CoX exchanged zeolites from the gas phase (178) agreed very well from liquid phase over HY, to ascertain the mechanism of isomerization and for the ability of zeolites to display acidic type catalytic activity. Experimental conditions of isomerization over these catalysts seem to be the most important factor regarding the relative rates of double-bond shift or cis-trans isomerization and in determining which isomerization step, the catalyst is particularly active for.

6.10 CONCLUSIONS

The present study has provided useful information in assessing the importance of zeolites to separate chemically similar molecules from liquid phase solutions. The extent of various factors that were thought to be responsible for selective separation have been revealed in this work. Steric factors seem to overrule other factors in the present investigation, but the potential value of the latter must not be underestimated. For example, in separation of xylene, cresols, etc., isomers, one isomer (the meta form) is more basic than others, and can hence be readily separated on zeolites containing acidic cations (e.g. Li^+) i.e. preferential interactions between species of different acidity-basicity.

It is recommended, that further separation studies with hexene isomers be carried out using long chain solvents, e.g. C_7- C_{14} paraffins and also cyclic molecules with the same carbon number as the paraffins. In the light of this study, it can be ascertained what type of solvent is best suited for a particular isomeric separation. Also the polarity of solvent is important in determining the selectivity for a particular adsorbate in solution. This factor is important when designing a continuous, countercurrent fluid-solid process. It is recommended, therefore, to look at the effect of solvent polarity on the adsorption isotherms. The separations of isomers from various solvents can be compared by studying adsorptions on various types of zeolites with different SiO_2:Al_2O_3 ratios, cation type, structure of the channel systems and pore diameters, e.g. erionite, ferrierite, chabazite, mordenite and ZSM5. It is also important to consider separations from solvents which cannot enter pores of the zeolite. A competitive survey can be established by studying adsorptions on synthetic and naturally occurring zeolites. Clinoptilolite, for example, may be the first natural zeolite to be of commercial value as a molecular sieve because large, relatively pure deposits are now being worked in Japan and the United States.

It will also be interesting to study isomerization reactions over various zeolites both from gas and liquid phase, to ascertain the activity of a particular zeolite for double-bond shift or cis-trans isomerization.

The use of molecular sieves as selective sorbent in high-pressure liquid chromatography seems promising (190) and their use in TLC (191) is possible. It will be most interesting to compare the predicted separations from equilibrium studies with experimental separations in a HPLC system. These uses are not so limited, as catalysis by the zeolite is less likely to occur under the prevailing experimental conditions.

The work described herein, together with that recommended for further investigation will demonstrate the value of competitive sorption tests in characterizing the physical and catalytic properties of various zeolites. A knowledge of relative adsorptivities under both kinetic- and thermodynamic-controlled conditions is essential for interpreting and predicting catalytic reaction phenomena.

REFERENCES

1. D.W. Breck, "Zeolite Molecular Sieves", Wiley, N.Y.(1974).

2. Y.A. Elketov, and A.V. Kiselev, "Molecular Sieves", p. 267, Society of the Chemical Industry, London,(1968).

3. D.B. Broughton, Chem. Eng. Progr., 49 (1977).

4. H.C. Ries, "n-paraffins", Process Economics Program, Report No. 55, 1969, Stanford Research Institute, Menlo Park, Calif.

5. D.B. Broughton, et al., Chem. Eng. Progr. 66, 70 (1970).

6. R.S. Atkins, Hydrocarbon Proc., 49, 132 (1970).

7. R.W. Neuzil; U.S. Patent, 3,558,732 (Jan 26, 1971).

8. R.W. Neuzil; U.S. Patent, 3,626,020 (Dec 9, 1971).

9. R.W. Neuzil; U.S. Patent, 3,663,638 (May 16, 1972).

10. N.Y. Chen, S.J. Lucki; U.S. Patent, 3,668,266 (June 6, 1972).

11. R. Bearden, R.J. DeFeo; U.S. Patent, 3,686,343 (Aug. 22, 1972).

12. R.W. Neuzil, A.J. de Rosset; South African Patent, 692,327 (April 5, 1968).

13. R.W. Neuzil, A.J. de Rosset; British Patent, 1,236, 691 (June 23, 1971).

14. A.A. Yeo, et al., World Petrol. Congr., 6th, Sect IV 45, 209 (1965).

15. A.A. Yeo, C.L. Hicks; British Patents 898,058 and 898,059 (June 1962).

16. R.N. Lacey, et al; U.S. Patent 3,201,490 (Aug 17, 1965).

17. W.J. Asher, et al; U.S. Patent 3,070,542 (Dec 25, 1962).

18. H.A. Richards, et al; U.S. Patent, 2,988,502 (June 13, 1961).

19. W.F. Avery, M.N.Y. Lee, Oil Gas J. 60, 121 (1962)

20. G.J. Griesmer, et al., Hydrocarbon Proc. 44, 147 (1965).

21. E. Guiccione, Chem. Eng. 72, 104 (April 26, 1965).

22. W.R. Franz, et al., Petrol Refiner, 38, 125 (1959).

23. D.E. Cooper, et al., Chem. Eng. Progr., 62, 69 (1966).

24. Shell Internationale, British Patent, 1,059,879 (Feb 22, 1967).

25. K. Wehner, et al., British Patents, 1,135,801 and 1,135,802. (Dec 4, 1968).

26. J.W. McBain, The Sorption of Gases and Vapours by Solids, Rutledge, London(1932).

27. R.M. Barrer, J. Soc. Chem. Ind., 64, 130, (1945).

28. R.M. Barrer, Chem. Abs., 49, 3617, (1955).

29. R.M. Barrer, Nature, 176, 1188, (1955).

30. R.L. Hay, "Zeolites and Zeolitic Reactions in Sedmimentary Rocks", Spec. Paper No. 85, Geological Society of America, N.Y.(1966).

31. R.A. Sheppard, Molecular Sieve Zeolites, Advan. Chem. Ser., 101, American Chemical Society, Washington, D.C.,(1971).

32. W. Lowenstein, Amer. Mineralogist, 39, 92 (1954).

33. J.V. Smith, "Molecular Sieve Zeolites - I", Adv. Chem. Ser., Amer. Chem. Soc., p. 171, (1971).

34. D.H. Olson, J. Phys Chem., 74, 2758 (1970).

35. W.J. Mortier, H.J. Bosmans, J. Phys Chem., 75, 3327 (1971).

36. H.S. Sherry, J. Phys Chem., 70, 1158 (1966).

37. N.G. Parsonage, "Molecular Sieve Zeolites - I", Adv. Chem. Ser., 101, 198.

38. E. Dempsey, D.H. Olson, J. Phys Chem., 74, 2305, (1970).

39. R.M. Barrer, H. Villiger, J. Chem. Soc., D 659 (1969).

40. L.V.C. Rees, P.P. Lai, J.C.S. Farad. I., 72, 1809 (1976).

41. Ibid., p. 1818.

42. Ibid., p. 1827.

43. E. Dempsey, J. Phys Chem., 73, 3660 (1969).

44. J.A. Rabo, et al., Discussions of the Farad. Society, 41, 328 (1966).

45. P. Ducros, Bull. Soc. Fr. Mineral Christallogr., 83, 85, (1960).

46. S.P. Gabuda, G.M. Mikhavlov, Zh. Strukt; Khim., 4, 446, (1963).

47. K. Tsutsumi, H. Takashi, Bull. Chem. Soc. Japan, 45, 2332, (1972).

48. G.R. Eulenberger, et al., J. Phys Chem., 71, 1812 (1967).

49. D.W. Breck, J. Chem. Educ., 41, 678 (1964).

50. L. Broussard, P. Shoemaker, J. Amer. Chem. Soc., 82, 1041, (1960).

51. W. J. Mortier,"Compilation of Extra Framework Sites in Zeolites". Published by Butterworth Scientific Limited on behalf of the structure Commission of the International Zeolite Association, 1982.

52. H.S. Thompson, J. Roy. Agr. Soc. Engl., 11, 68 (1850).

53. J.T. Way, Ibid., 11, 313, (1850).

54. F. Harm, A. Rümpler, 5th Int. Congr. Pure Appl. Chem., 59 (1903).

55. H.S. Sherry, "Molecular Sieves Zeolites - I", Adv. Chem. Ser., Amer. Chem. Soc., 350 (1971).

56. R.M. Barrer, L.V.C. Rees, J.A. Davies, J. Inorg. Nucl. Chem., 30, 3333 (1968).

57. Ibid., 28, 629 (1966).

58. Ibid., 31, 2599 (1969).

59. H.S. Sherry, Molecular Sieves, 2nd Int. Conf. Worcester,(1970).

60. B.K.G. Theng, E. Vasant and J.B. Uytterhoeven, Trans Farad. Soc., 64, 3370 (1968).

61. R.M. Barrer, W. Bauser and W.F. Grutter, Helv. Chim. Acta., 29, 518 (1956).

62. P.P. Lai, L.V.C. Rees, J. Chem. Soc. Farad. Trans I, 72, 1809 (1976).

63. H.S. Sherry, J. Phys Chem., 71, 780 (1967).

64. H.S. Sherry, J. Coll. Int. Sci, 28, 288 (1968).

65. H.S. Sherry, J. Phys Chem., 72, 4086 (1968).

66. A. Maes, A. Cremer, Molecular Sieves, 3rd Int. Conf., Zurich, Switzerland (1973).

67. H.S. Harned, B.B. Owen, "The Physical Chemistry of Electrolyte Solutions", Reinhold, N.Y.

68. J. Kielland, J. Soc. Chem. Ind., 54, 232 (1935).

69. C.L. Angell, P.C. Schaffer, J. Phys Chem. 69, 3463 (1965).

70. J.W. Ward, J. Catal., 10, 34, (1968).

71. P.B. Venuto, L.A. Hamilton and P.S. Landis, J. Catal., 5, 484 (1966).

72. J.A. Rabo, C.L. Angell, P.H. Kasai and V. Schomaker, Disc Farad. Soc. 41, 328 (1966).

73. W.K. Hall, Chem. Eng. Progr. Symp. Ser. 63 (No. 73), 68 (1967).

74. D.H. Olson, E. Dempsey, J. Catal., 13, 221 (1969).

75. A. Dyer, Separation Science and Technology, 13 (6), 501, 1978.

76. R.M. Barrer, D.A. Lanley, J. Chem. Soc., 3804 (1958).

77. H. Bremer, W. Mörke, R. Schodel and F. Vogt., Molecular Sieves, 3rd Int. Conf. Zurich, Switzerland(1973).

78. D.H. Olson, G.T. Kokokailo, and J.F. Charnell, J. Coll. Int. Sci., 28, 305, 1968.

79. N.H. Ray, J. Appl. Chem., 4, 21, 82 (1954).

80. E. Kovats, Helv. Chim. Acta 41, 1915 (1958).

81. J.F. Smith, M.B. Evans, J. Chromatog. 5 ,300 (1961).

82. J. Rohrschneider, J. Chromatog. 22, 6-22 (1966).

83. L.S. Ettre, Chromatographia, 6, (11),(Nov 1973); ibid, 7, (1),(Jan 1974);ibid, 7, (5),(May 1974).

84. A.V. Kiselev, A.A. Lopatkin, "Zeolite Molecular Sieves", p. 252, Society of the Chemical Industry, London(1968).

85. S.P. Zhdanov, A.V. Kiselev, and L.F. Pavlova, Kinetics and Catalysis (U.S.S.R.), 3, 391, (1962).

86. I. Langmuir, J. Am. Chem. Soc. 38, 2267 (1916).

87. S. Brunauer, P.H. Emmett and E. Teller, J. Am. Chem. Soc. 60, 309 (1938).

88. S. Brunauer, L.S. Derring, E.W. Derring and E. Teller, J. Am. Chem. Soc. 62, 1723 (1940)

89. S. Brunauer, "The Adsorption of Gases and Vapours", Oxford University Press, London (1944).

90. J.J. Kipling, "Adsorption from Solutions of Non-Electrolytes", Academic Press, London (1965).

91. D.H. Everett, Trans. Farad. Soc. 60, 1803 (1964).

92. M. Siskova, E. Erdös, Collect. Czech. Chem. Commun. 25, 1729 (1960).

93. G. Foti, L.G. Nagy and G. Schay, Acta. Chim. Acad. Sci. Hung., 80, 25 (1974).

94. G.A.H. Elton, J. Chem. Soc., 3813 (1954).

95. A. Schuchowitzsky, Acta. Physicochim., 19, 176, 508 (1944).

96. J.W. Belton, M.G. Evans, Trans. Farad. Soc., 1, 41 (1945).

97. D. Patterson, G. Delmas, J. Physic. Chem., 64, 1827 (1960).

98. D.H. Everett, Trans Farad. Soc. 46, 942, (1950).

99. C.E. Brown, D.H. Everett, "Colloid Science", Vol II, p. 52, (1975).

100. D.H. Everett, "Colloid Science", Vol I, p. 49, (1973).

101. W.M. Meier, J.B. Uytterhoeven, Advances in Chemical Series, 121 (1973).

102. R.M. Barrer, "Zeolites and Clay Minerals as Sorbents and Molecular Sieves", Academic Press (1978).

103. J.A. Rabo, "Zeolite Chemistry and Catalysis", Amer. Chem. Soc., Washington, D.C.(1976).

104. L.V.C. Rees, "Proceedings of the 5th International Conference on Zeolites", Naples, Italy, June(1980).

105. J.V. Smith, in "Zeolite Chemistry and Catalysis" (J.A. Rabo, Ed.), ACS Monograph 171, pp 38-41, American Chemical Society, Washington, (1976).

106. F.C. Whitmore, Chem. Eng. News, 26, 668 (1947).

107. C. Dimitrov, N.F. Leach, J. Catal., 14, 336 (1969).

108. D.M. Browuer, J. Catal., 1, 22 (1962).

109. E.A. Lombardo, W.K. Hall, AIChEJ 14, 1229 (1971).

110. E.A. Lombardo, et al., J. Catal. 22, 54 (1971).

111. E.A. Lombardo, W.K. Hall, Int. Cong. Catal., 5th, 1972, 2, 1365, (1973).

112. J.J. Collins, Chem. Eng. Prog., Vol 64, No. 8, 66 (1968).

113. H.J. Bieser, Proceedings of the Fourth Conference on Molecular Sieve Zeolite, Chicago,(1976).

114. K.T. No, et al., J. Phys Chem 85, 2065 (1981).

115. S. Beran, et al., J. Phys Chem. 85, 1951 (1981).

116. D.A. Whan, Chemistry in Britain, p. 532 (1981).

117. M. Seko, T. Miyake and K. Inada, Ind. Eng. Chem. Res. Dev., 18, (4), 263 (1979).

118. M. Kilpatrick, F.E. Luborsky, J. Am. Chem. Soc., 75, 577 (1953).

119. R.W. Neuzil, et al; U.S. Patent, 3,510,423 (May 5, 1970).

120. G.F. Feldbauer, Jr., et al., U.S. Patent, 2,920,038, (Jan 5, 1980).

121. W.P. Ballard, et al; U.S. Patent, 2,818,455, (Dec 31, 1957).

122. C.N. Kimberlin, Jr., et al. U.S. Patent, 2,971,993, (Feb 14, 1961).

123. R.M. Milton; U.S. Patent, 3,078,636, (Feb 26, 1963).

124. R.M. Milton; U.S. Patent, 3,078,644, (Feb 26, 1963).

125. H.G. Naylor; British Patent, 1,255,775 (Jan 23, 1968).

126. J.W. Priegnitz; U.S. Patent, 3,723,561 (Mar 27, 1973).

127. D.W. Peck, et al., U.S. Patent, 3,265,750 (Aug 9, 1966).

128. R.L. Mays and P.E. Pickert, "Molecular Sieves", p. 112, Society of the Chemical Industry, London,(1968).

129. R.M. Milton; Ibid, p. 199.

130. M.C. Veyssiere, et al., J. Chem. Soc., Farad. Trans 1, 77, 1417 (1981).

131. A.L. Myers and J.M. Prausnitz, AIChEJ, 11, 121 (1965).

132. A.J. Glessner and A.L. Myers, Chem. Eng. Prog. Symp. Ser., 65, 73, (1969).

133. C. Clavaud, et al., Rapport D.G.R.S.T., 1980 (D.G.R.S.T.), 35, Rue Saint Dominique, 75700 Paris.

134. E.F. Vansant and R. Voets, J. Chem. Soc., Farad. Trans, 1, 77, 1371 (1981).

135. V.M. Bülow and J. Kärger, Z. Phys Chemie, Leipzig 262, 145 (1981).

136. R.M. Marutovskii, et al., Zh. Fiz. Khim., 55 (12),3049 (1981).

137. M. Bülow, et al., J. Coll. Int. Sci., 85 (2), 457 (1982).

138. I. Longaver, et al., Chem. Zvesti., 35 (6), 721 (1981).

139. H. Herden, et al., Chem. Tech (Leipzig), 34 (4), 189 (1982).

140. D. Ganguli, et al., Trans. Indian. Ceram. Soc., 39 (2), 57, (1980).

141. M. Mangel, Chem-Tech (Heidelberg), 10 (11), 1135 (1981).

142. R. Harlfinger, et al., Z. Phys Chemie, Leipzig 4, 657 (1981).

143. R. Harlfinger, et al., Chem Tech. (Leipzig) 33 (8), 424 (1981).

144. E.M. Benashvili, et al., Soobshch. Akad. Nauk. Gruz. S.S.R., 103 (2), 329 (1981).

145. J. Guth, et al., J. Coll. Int. Sci., 76 (2), 298 (1980).

146. M.M. Dubinin and L.A. Astakhov, Adv. Chem. Ser. 102, 69 (1981).

147. R.J. Neddenriep, J. Coll. Int. Sci. 28, 293 (1968).

148. P.A. Jacobs, et al., J. Chem. Soc. Trans Farad. Soc. I., 69, 1056 (1973).

149. G. Finger and M. Bülow, Z. Phys Chemie. Leipzig, 4, 732 (1981).

150. G.V. Tsitsishvili, et al., Russ. J. Phys Chem., 43, 524 (1969).

151. V. Bosacek, "Molecular Sieves", p. 164, Soc. of Chem. Ind. Lond.(1968).

152. L. Ya Leperashvili, Izvestia Ackademiia. Navk. Gruzincko, C.C.P., 7 (1), 41 (1981).

153. L. Rorshnaider, Anal. Chem. 170, 256 (1959).

154. O.A. Sinitsyna, et al., Kinetika i Kataliz., 21 (3), 728, May-June (1980).

155. N.F. Foster, R.J. Cvetanovic, J. Am. Chem. Soc., 82, 4272 (1960).

156. Kk. M. Minachev, et al., Uspekhi Khimii 12, 2151 (1966).

157. E.A. Paukshtis, et al., Kinetika i Kataliz, 21 (2), 455, March-April (1980).

158. L.V. Malysheva et al., Kinet. Katal., 21, 536 (1980).

159. D.W. Sundstrom and F.G. Krautz, J. Chem. Eng. Data, 13 (2), 223 (1968).

160. R.K. Gupta et al., J. Chem. Eng. Data, 25, 14 (1980).

161. C.N. Satterfield and C.S. Cheng, AIChE Journal 18 (4), 720 (1972).

162. C.N. Satterfield and J.K. Smeets, Ibid, 20, 618 (1974).

163. R.M. Dessau, "Second Chemical Congress of the North American Continent", San Francisco, Aug 1980. Paper on selective sorption properties of zeolites.

164. A. Voorhies and W.J. Hatcher, Ind. Eng. Chem., Prod. Res. Develop., 8, 361 (1969).

165. R. Becila, J. Jose and J.M. Vergnaud, J. Chim. Phys. Phys Chim. Biol., 78 (6), 531 (Fr), (1981).

166. T.M. El-Akkad, et al., Surf. Technol. 14 (2), 283 (1981).

167. H. Herden, Z. Chem., 22 (1), 33 (1982).

168. H. Herden, et al., Math-Naturwiss R. 30 (4), 411 (1981).

169. H. Herden., et al., J. Coll. Int. Sci., 79 (1), 280 (1981).

170. N.N. Grazev et al., Dokl. Akad. Nauk. U.S.S.R. 169, 375 (1966).

171. W. Schirmer, et al., Z. Chem. 10, 198 (1970).

172. H. Ali, thesis, Cornell University, Ithaca, N.Y.(1975).

173. P.E. Eberly, Jr., J. Phys Chem. 71 (6), 1717 (1967).

174. J. Datka, J. Chem. Soc., Farad. Trans 1, 77, 1309 (1981).

175. H. Förster and R. Seelemann, J. Chem. Soc., Farad. Trans 1, 77, 1359 (1981).

176. K. Otsuka, et al., J. Catal., 50, 379 (1977).

177. W. Kladnig and H. Noller, Ibid., 29, 385 (1973).

178. H. Hoser and S. Krzyzanowski, J. Catal., 38, 366 (1975).

179. D. Barthomeuf, Catalysis by Zeolites. 55 (1980).

180. P.B. Venuto, Ibid., p. 1.

181. M.N. Zhavoronkov et al., Prevrashchen. Uglevodorodov. Kislotno. Osnovn. Geterogennykh. Katal. Tezisy. Dokladov. Konf. 182 (1977).

182. K.B. Tonyvesa et al., Neftekhimiya, 17, 226 (1977).

183. A.L. IIpockyphuh, et al., Ibid., 20, 46 (1980).

184. J.D.N. Irving, et al., J. Chem. Res. (S) 66,(1982)(3) and 108,(1982)(4).

185. T.V. Whittam, U.S. Patent, 4, 209, 498 (1980).

186. W.O. Haag and H. Pines, J. Am. Chem. Soc., 82, 387 (1960).

187. S.C. Eastwood, et al., Proceedings of the Eighth World Petroleum Congress, p. 245, (1971).

188. J.C. Vedrine, et a., J. Catal., 59, 248 (1979).

189. G.R. Landolt and G.T. Kerr, Sep. Prif. Methods, 2, 283 (1973).

190. H.M. McNair and C.D. Chandler, Anal. Chem., 45, 1117 (1973).

191. R.W.A. Oliver and Z. Zumbe, unpubished results.